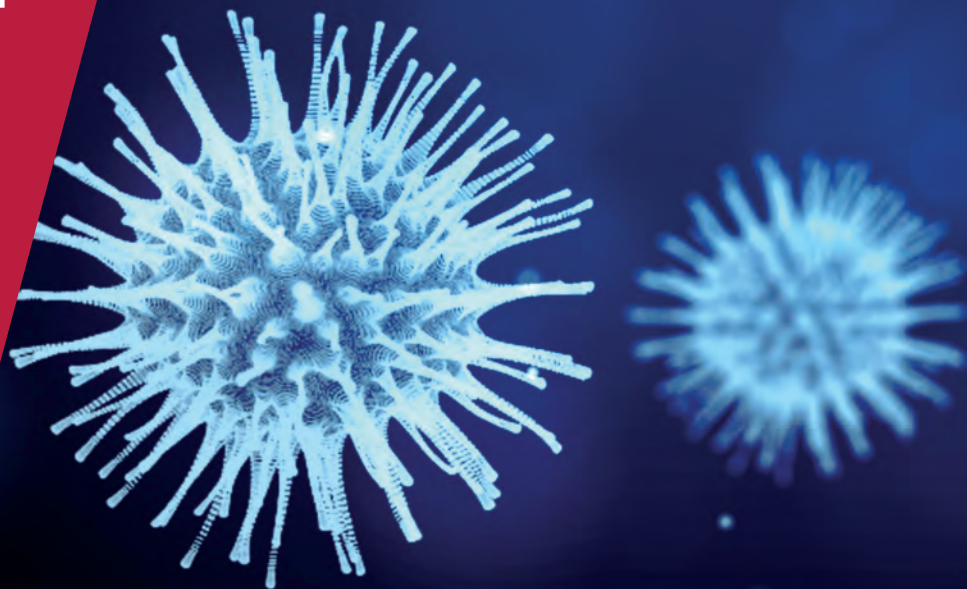


**CENTRE FOR
ECONOMIC
POLICY
RESEARCH**

CEPR PRESS



COVID ECONOMICS
VETTED AND REAL-TIME PAPERS

ISSUE 10
27 APRIL 2020

**THE GREAT INFLUENZA IN
ITALY**

Mario Carillo and Tullio Jappelli

**A SIMPLE NON-RECURSIVE
MODEL**

Ernst-Ludwig von Thadden

FALLEN ANGELS IN THE US

Viral Acharya and Sascha Steffen

**CONSUMPTION RESPONSES
TO CARES**

Christopher Carroll, Edmund Crawley,
Jiri Slacalek and Matthew White

**OLG AS AN ALTERNATIVE
TO SIR**

Michael Beenstock and Xieer Dai

SEVEN SCENARIOS

Warwick McKibbin
and Roshen Fernando

Covid Economics

Vetted and Real-Time Papers

Covid Economics, Vetted and Real-Time Papers, from CEPR, brings together formal investigations on the economic issues emanating from the Covid outbreak, based on explicit theory and/or empirical evidence, to improve the knowledge base.

Founder: Beatrice Weder di Mauro, President of CEPR

Editor: Charles Wyplosz, Graduate Institute Geneva and CEPR

Contact: Submissions should be made at <https://portal.cepr.org/call-papers-covid-economics-real-time-journal-cej>. Other queries should be sent to covidecon@cepr.org.

© CEPR Press, 2020

The Centre for Economic Policy Research (CEPR)

The Centre for Economic Policy Research (CEPR) is a network of over 1,500 research economists based mostly in European universities. The Centre's goal is twofold: to promote world-class research, and to get the policy-relevant results into the hands of key decision-makers. CEPR's guiding principle is 'Research excellence with policy relevance'. A registered charity since it was founded in 1983, CEPR is independent of all public and private interest groups. It takes no institutional stand on economic policy matters and its core funding comes from its Institutional Members and sales of publications. Because it draws on such a large network of researchers, its output reflects a broad spectrum of individual viewpoints as well as perspectives drawn from civil society. CEPR research may include views on policy, but the Trustees of the Centre do not give prior review to its publications. The opinions expressed in this report are those of the authors and not those of CEPR.

Chair of the Board

Sir Charlie Bean

Founder and Honorary President

Richard Portes

President

Beatrice Weder di Mauro

Vice Presidents

Maristella Botticini

Ugo Panizza

Philippe Martin

Hélène Rey

Chief Executive Officer

Tessa Ogden

Editorial Board

Beatrice Weder di Mauro, CEPR
Charles Wyplosz, Graduate Institute
Geneva and CEPR

Viral V. Acharya, Stern School of
Business, NYU and CEPR

Abi Adams-Prassl, University of
Oxford and CEPR

Guido Alfani, Bocconi University and
CEPR

Franklin Allen, Imperial College
Business School and CEPR

Oriana Bandiera, London School of
Economics and CEPR

David Bloom, Harvard T.H. Chan
School of Public Health

Tito Boeri, Bocconi University and
CEPR

Markus K Brunnermeier, Princeton
University and CEPR

Michael C Burda, Humboldt
Universitaet zu Berlin and CEPR

Paola Conconi, ECARES, Universite
Libre de Bruxelles and CEPR

Giancarlo Corsetti, University of
Cambridge and CEPR

Fiorella De Fiore, Bank for
International Settlements and CEPR

Mathias Dewatripont, ECARES,
Universite Libre de Bruxelles and
CEPR

Barry Eichengreen, University of
California, Berkeley and CEPR

Simon J Evenett, University of St
Gallen and CEPR

Antonio Fatás, INSEAD Singapore
and CEPR

Francesco Giavazzi, Bocconi
University and CEPR

Christian Gollier, Toulouse School of
Economics and CEPR

Rachel Griffith, IFS, University of
Manchester and CEPR

Timothy J. Hatton, University of
Essex and CEPR

Ethan Ilzetzki, London School of
Economics and CEPR

Beata Javorcik, EBRD and CEPR

Sebnem Kalemli-Ozcan, University
of Maryland and CEPR Rik Frehen

Tom Kompas, University of
Melbourne and CEBRA

Per Krusell, Stockholm University
and CEPR

Philippe Martin, Sciences Po and
CEPR

Warwick McKibbin, ANU College of
Asia and the Pacific

Kevin Hjortshøj O'Rourke, NYU
Abu Dhabi and CEPR

Evi Pappa, European University
Institute and CEPR

Barbara Petrongolo, Queen Mary
University, London, LSE and CEPR

Richard Portes, London Business
School and CEPR

Carol Propper, Imperial College
London and CEPR

Lucrezia Reichlin, London Business
School and CEPR

Ricardo Reis, London School of
Economics and CEPR

Hélène Rey, London Business School
and CEPR

Dominic Rohner, University of
Lausanne and CEPR

Moritz Schularick, University of
Bonn and CEPR

Paul Seabright, Toulouse School of
Economics and CEPR

Christoph Trebesch, Christian-
Albrechts-Universitaet zu Kiel and
CEPR

Thierry Verdier, Paris School of
Economics and CEPR

Jan C. van Ours, Erasmus University
Rotterdam and CEPR

Karen-Helene Ulltveit-Moe,
University of Oslo and CEPR

Ethics

Covid Economics will publish high quality analyses of economic aspects of the health crisis. However, the pandemic also raises a number of complex ethical issues. Economists tend to think about trade-offs, in this case lives vs. costs, patient selection at a time of scarcity, and more. In the spirit of academic freedom, neither the Editors of *Covid Economics* nor CEPR take a stand on these issues and therefore do not bear any responsibility for views expressed in the journal's articles.

Covid Economics

Vetted and Real-Time Papers

Issue 10, 27 April 2020

Contents

Pandemic and local economic growth: Evidence from the Great Influenza in Italy <i>Mario F. Carillo and Tullio Jappelli</i>	1
A generalized SEIR model of Covid-19 with applications to health policy <i>Ernst-Ludwig von Thadden</i>	24
The risk of being a fallen angel and the corporate dash for cash in the midst of COVID <i>Viral V. Acharya and Sascha Steffen</i>	49
Modeling the consumption response to the CARES Act <i>Christopher D. Carroll, Edmund Crawley, Jiri Slacalek and Matthew N. White</i>	67
The natural and unnatural histories of Covid-19 contagion <i>Michael Beenstock and Xieer Dai</i>	92
The global macroeconomic impacts of COVID-19: Seven scenarios <i>Warwick McKibbin and Roshen Fernando</i>	121

Pandemic and local economic growth: Evidence from the Great Influenza in Italy¹

Mario F. Carillo² and Tullio Jappelli³

Date submitted: 21 April 2020; Date accepted: 23 April 2020

We investigate the link between the Great Influenza Pandemic of 1918 and regional economic growth in Italy. The pandemic caused 600,000 deaths in Italy, a death rate of about 1.2%. We find that going from regions with the lowest mortality to the ones with the highest mortality is associated with a decline in GDP per capita growth of about 6.5%, an effect that dissipated within three years. We find limited evidence of mechanisms that may uncover long-term effects of the pandemic, such as human capital accumulation and industrialization. The severity of the pandemic in the less developed regions of the country, along with the limited implementation or largely ineffective measures of central and local interventions by public authorities, point to our estimates as indicative of an upper bound of the transitory adverse effect of pandemics on local economic growth.

1 We thank Luigi Guiso for useful comments and MIUR for financial support (PRIN Grant N. 2017RHFXX4).

2 Postdoctoral Research Fellow, University of Naples Federico II.

3 Professor of Economics, University of Naples Federico II and CEPR Research Fellow.

1 Introduction

The COVID-19 pandemic induces policymakers to take urgent decisions on policy interventions to contain contagion and its adverse economic consequences. Such choices involve important trade-offs between the adverse economic effects of pandemic *vis-à-vis* those of the intervention. Yet, the economic consequences of pandemics are not fully clear, mostly because historically they have been typically attenuated by government interventions. We shed light on this issue by studying the effects of a pandemic on local economic activity by exploring the regional exposure to the 1918 Great Influenza Epidemic in Italy. The limited policy interventions undertaken over the Italian peninsula to contain the pandemic, along its heterogeneous exposure across the diverse regions of the country, provide a unique opportunity to estimate an upper bound of the potentially adverse effect of pandemic mortality on local economic growth.

The 1918 influenza caused about 600,000 deaths in Italy, mostly concentrated between the end of September and the end of October. Mortality varied substantially across regions, ranging from less than 1% in Veneto to over 1.5% in Sicily and Calabria. This variability provides the ground for our identification of the effect of the health shock on subsequent GDP growth. To assess the GDP impact of the influenza we follow an approach similar to Barro et al. (2020), regressing regional GDP growth on flu mortality for various sample periods, ranging from 1900 to 1930, and controlling for other potential covariates, like war mortality, initial GDP and proxies for human capital. We find that the influenza contributed substantially to the difference performance of the Italian regions during the 1919-21 recession. Regions with the highest mortality rates experienced an excess GDP decline of about 6.5% relative to the lowest mortality regions. Using a distributed lag specification, we also find that the impact of the influenza was highest immediately after the pandemics, and that the effect vanished within 4 years. In the longer run (ten years and beyond), the statistical analysis does not reveal an economic effect of the influenza on manufacturing employment, and measures of human capital. These findings are qualitatively consistent with recent cross-country evidence by Barro et al. (2020), and country evidence for the US (Correia et al., 2020) and Denmark (Moller Dahl et al., 2020).

From an economic point of view, they are consistent with a standard Solow growth model, where a reduction in the labor force leads to a recession. The historical accounts of the influenza reveal that the response of the health care system was inadequate in essentially all regions, and that lockdown measures were mild and ineffective. The results are therefore more helpful to understand the potential impact of an epidemic in a developing country with poor health infrastructure and limited ability to impose and enforce lockdown measures.

The paper is organized as follows. In Section 2, we describe the developments of the influenza in Italy and the recession of 1919-21. Section 3 reviews the possible economic mechanisms linking the pandemics and economic growth, and the empirical literature. Section 4 presents our data. Section 5 presents descriptive evidence. Section 6 presents regressions results for GDP growth, and Section 7 explores the potential long-run consequences of the influenza. Section 8 concludes.

2 The 1918 Influenza in Italy

The 1918 influenza killed around 40 million people worldwide, corresponding to 2.0 percent of the world's population at the time. Italy was one the most affected countries. Current estimates suggest that it killed about 0.6 million people out of 36 million, about the same death rate as in WWI, with a mortality rate estimated at 1.2%, below the world average (2%), but substantially above the mortality of other developed countries (Barro et al., 2020). For instance, in Germany the estimated mortality was 0.8%, in the US and in the UK 0.5%, and in France 0.7%. So, the combined effect of influenza and war mortality was to reduce a population of 36 million the population of about 1.2 million people between 1915 and 1919.

There were three waves of influenza in Italy, between May 1918 and early 1919. The first wave, in the Spring of 1918, was relatively mild, while the second one was by far the most severe. The first cases were reported in late August, but by mid-September the influenza spread in all parts of Italy, reaching a peak in early or mid-October, and ending in early November. With very few days of difference, the influenza hit every part of Italy. Tognotti (2015) provides a thorough investigation of the pandemics, and reports that deaths peaked in mid-October, with about only ten days difference between the different parts of the country.¹

Several factors contributed to the spread of the disease and the high mortality rate. First of all, the period the spread of the influence coincided with the end of WWI, and the Italian final attack against the Austro-Hungarians in late October, and the final victory of November 4, 1918. The movements of troops, sick soldiers and refugees in both South and Northern Italy most likely contributed to the rapid spread of the disease. While in many countries measures of social distance and quarantine were implemented, in Italy due to lack of coordination, and poor organization the measures were implemented when it was too late to stop the pandemic and were largely ineffective.

¹ Daily deaths peaked on October 7 in Naples (256 cases), October 16 in Milan (127), October 18-19 in Turin (119 deaths), and October 19 in Rome (226 deaths).

The material conditions of the population were another aggravating factor. Cohabitation of entire families in the same room, overcrowding, lack of running water, electricity, toilets and sewers were the rule rather than the exception in many parts of Italy, with most people living in precarious conditions. Even though there are no systematic accounts of measures of social distancing that can be exploited in the empirical analysis of the economic impact of the pandemics, Tognotti (2015) reports that these measures were introduced only when the pandemics was out of control and were in practice ineffective and not feasible.²

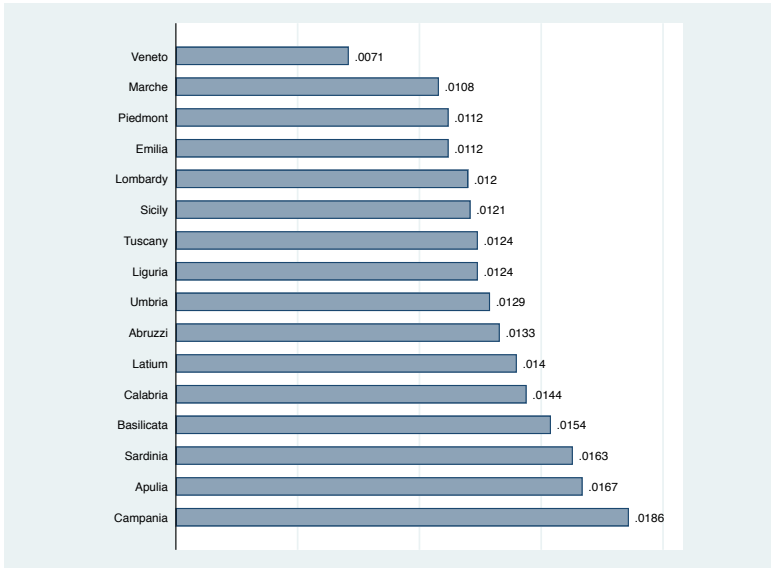
Healthcare was quite problematic as well, because most doctors and medical personnel was used in support of the military, hospitals were concentrated in large cities and absent in smaller towns and rural areas. Finally, information through the press was limited due to censorship, at least initially, which was in place in order not to give information to the enemies on the real proportion of the epidemics.

As in other countries, mortality was highest among the young (20 to 40 years old). A peculiar characteristic of the Italian case is the excess mortality of young women. Pinnelli and Mancini (1998) advance a tentative explanation. Since contagion depends on frequency of contact, girls were more exposed to the flu, as their activities were mainly at home and often had to take care of the elderly and sick, themselves fell ill more easily. Mortality varied considerable across regions as well, with mortality exceeding 1.5% in some regions such as Campania and Calabria, and others such as Veneto where mortality was substantially less than 1% (see Figure 1 and Appendix Table B.1.). To some extent, these differences are likely to reflect a gap in resources, human capital and infrastructure between the North and the South. Therefore, in assessing the economic consequences of the epidemics it will be important to take into account pre-existing differences in initial conditions.

We base our analysis on recorded statistics of influenza mortality. As noted by Johnson and Mueller (2002), these data have potential limitations, given non-registration, missing records, misdiagnosis, and non-medical certification, and may also vary between locations. Indeed, Johnson and Mueller (2002) report country-level statistics of the 1918 influenza mortality showing that in many countries reported mortality rates severely underestimate the mortality rate recalculated considering revisiting official records and calculating "excess" deaths from recorded mortality for influenza, respiratory causes, or all causes. While we cannot exclude that reported mortality rates exhibit greater variability at the regional level, for Italy the reported mortality rate (1.1%) is actually quite close to the recalculated death rate (1.07%) (Johnson and Mueller, 2002, p. 113, Table 4), which is reassuring for our empirical analysis.

² There are also reports showing that even at the end of September and early October of 1918, when the epidemics was near its peak, there were large gatherings for religious or political reasons.

Figure 1: Influenza Mortality by Region



The pandemics hit the Italian economy in the last year of WWI, which was a period of significant economic expansion, particularly of firms involved in war production stimulated by large government expenditures. The war was followed by the 1919-21 recession, with a strong recession in 1919 (-19%), and a cumulative decline in GDP per capita of approximately 30% over three years. In assessing the economic history of Italy, Malanima and Zamagni (2010) write that “public spending rose dramatically and was mostly financed with debt; particularly foreign debt. Social relations after the war became violently conflicting and political stability was lost, with the rise of new movements and parties that destabilized the formation of long lasting-governments. Italian democracy was incapable of meeting these challenges and, in October 1922, Benito Mussolini became prime minister. At the end of 1925 he turned his government into a dictatorship.” A feature of the fascist period is that it widened dramatically the North-South divide. In the 50 years between 1861 and 1911 the ratio between per capita GDP of the South and the North declined by 13 points (from 93% to 80%), while during the fascist period it declined by further 21 points (to 59%).

The economic differences across regions before 1918 and the significant macroeconomic and political shocks that characterized the period of study may induce concerns that areas with higher exposure to the pandemic may simultaneously be more exposed to other adverse economic shocks, given their low levels of health and education. Even though we take into account initial conditions, the lack of regional convergence in economic growth between Northern and Southern regions implies that our estimates

should be interpreted with caution as they plausibly indicate the upper bound of the potential adverse effect of pandemics on regional growth trajectories.

3 Review of the Literature

In reviewing the literature on the on the economic consequences of the 1918 pandemics, it is useful to distinguish between short-run effects, long-run effects due to reduced productivity and human capital, and very long-run effects.³ To evaluate the impact of pandemics, we consider a standard Solow growth model where the pandemics destroys part of the labor force, and that there is limited or no labor mobility across regions and countries. After the pandemics the labor force shrinks, particularly in the working age groups, so the capital-labor ratio increases. The scarcity of labor induces an increase in the wage rate and a reduction in the return to capital, slowing down investment and capital accumulation. The demand for investment falls, and the economy enters into a recession, with negative growth in income per capita. In the medium and long run, the capital-labor ratio returns to its level, wages fall, and the economy converges back to the initial steady state.

This recessionary effect might be reinforced if the pandemics affect also the saving rate through an income effect, due to the loss in income of those exposed to the pandemics, and loss of confidence. Furthermore, as we see today, individual and social measures to reduce disease spread can seriously disrupt economic activity, reducing output, income and saving in the short run.

The recession might have long run consequences also because human capital (in both the form of health and education) falls after the pandemics, reducing the productivity of labor, especially in more human capital-intensive sectors (manufacturing). If there are externalities in human capital, this might affect also the productivity of other household members, and of the economy at large. The reduction in savings can lead to lower investment in human capital, for instance in the education of children.

Most economic arguments lead to the presumption that pandemics have recessionary effects, the empirical findings report different estimates on the size and duration of the effect. The approach of the empirical studies is essentially the same. They exploit country, region or city variations in flu mortality rates and trace the effect of the pandemics on various outcomes (GDP or GDP components, wages, poverty rates, and levels of human capital) in the years (or decades in some studies) after 1918.

In assessing the literature on the economic effects of the 1918 pandemics in the U.S.,

³ See Weil (2014) for an overview of the literature on health and economic growth.

Garrett (2008) concludes that most of the evidence indicates that the effects were short term, hitting differentially firms and households. According to Garrett (2009), the most noticeable effect of the pandemics was to decrease manufacturing labor supply, and to increase wage growth in U.S. states and cities by 2 to 3 percentage points for a 10 percent change in per capita mortality.

Brainerd and Siegler (2003) find that the epidemic is actually positively correlated with subsequent economic growth in the United States. In particular, one more death per thousand resulted in an average annual increase in the rate of growth of real per capita income over the next ten years of 0.15% per year. The authors argue that states with higher influenza mortality rates had a greater increase in capital per worker and thus also income per worker after the pandemic.

More recently, Correia et al. (2020) use geographic variation in mortality during the 1918 influenza in the U.S., and find that more exposed areas experienced a sharp and persistent decline in economic activity. In particular, they find that the influenza led to an 18% reduction in state manufacturing output for a state at the mean level of exposure. They also use variation in the degree and intensity of non-pharmaceutical interventions (lockdown) and find that cities that intervened earlier and more aggressively do not perform worse and, if anything, grow faster after.⁴

The Swedish and Danish cases are interesting, because Sweden and Denmark did not take part in World War I, reducing the risk of confounding effects of the pandemic with disturbances related to the war. Both countries however suffered the indirect effect of the war on international trade. Karlsson et al. (2014) find that in Sweden the pandemic had a strong negative impact on capital income: the highest quartile (with respect to influenza mortality) experienced a drop of 5% during the pandemic and an additional 6% afterwards. The pandemics also increased the poverty rate (defined as the share of the population living in public poorhouses), but no effect on earnings. Moller Dahl et al. (2020) find that more severely affected municipalities experienced short-run declines in income (5 percent on from 1917 to 1918), suggesting that the epidemic led to a V-shaped recession, with relatively moderate, negative effects and a full recovery after 2-3 years. They also report that unemployment rates were high during the epidemic, but decreased only a couple of months after it receded. It should also be noted that, overall, Denmark experienced one of the lowest mortality rates worldwide (Barro et al., 2020), 0.3% against a world average of 2%.

⁴ Not all economic historians agree with the fact that the 1918 flu had a large impact on the economy. According to Barry Eichengreen (interviewed by John Cassidy for the new Yorker on March 18, 2020), the economic impact of the 1918 pandemics in the U.S. was relatively mild. "The pandemic had a big negative impact on retail sales, but, according to the available statistics, the over-all economy didn't fall into a recession. There was eventually a slump, in 1920-21, but Eichengreen and other economic historians have typically attributed it to the Federal Reserve raising interest rates to head off inflation"

Barro et al. (2020) provide an overall assessment of the effect of epidemics in a cross-country comparative study. They regress the annual growth rate of per capita GDP between 1901 and 1929 against the current and lagged values of the flu death rate and the war death rate in a panel of 42 countries. They find a coefficient of -3.0 on the flu death rate meaning that, at the cumulative aggregate death rate of 0.020 for 1918-1921, the epidemic is estimated to have reduced real per capita GDP by 6.0 percent in the typical country.⁵

Some studies focus on the long-run consequence of the influenza pandemic. Almond (2006) finds that the US cohorts born during the pandemic display reduced educational attainment, increased rates of physical disability, and lower income compared with other birth cohorts. Percoco (2016) finds that the Italian cohorts born in 1918-20 experience an average reduction of 0.3-0.4 years of schooling relative to other cohorts. Guimbeau et al. (2020) find that in the Brazilian state of Sao Paulo the pandemics had significant effects on infant mortality, sex ratios at birth, fertility and marriage patterns in the short-run, as well as persisting impacts on health, educational attainment and productivity (as measured by the primary sector's output per employee and per establishment) in the long-run. Using information about attitudes of respondents to the General Social Survey (GSS), Le Moglie et al. (2020) find that experiencing the influenza had permanent consequences on individual behavior in terms of lower social trust. In particular, the paper finds that lower social trust was passed on to the descendants of the survivors of the influenza pandemic who migrated to the US.

Furthermore, there is an important tradition of studies looking at the economic consequences of pandemics for Italy. For instance, Alfani (2013) emphasizes that plagues in seventeenth-century Europe, by affecting more severely Italy and the south of Europe, hindered the economic performance of Italy relative to northern European countries. Alfani and Percoco (2019) explores the effects of plague across Italian cities in pre-industrial times. They find that the 1629-30 plague was linked to persistently lower economic growth in cities more exposed. Malanima (2018) points to the effect of the severe and frequent plagues that affected the Italian peninsula in the age of Renaissance (1350-1550) and shows that they were associated with an increase in resources per worker, ultimately improving standard, which eventually converged back to their low pre-Renaissance levels. Our study contributes to these works by exploring the Great Influenza Epidemic, which affected the Italian economy in more recent historical periods, and focusing on aggregate regional economic growth.

⁵ They also estimate the effect of death rates on consumption and asset prices. The effect on consumption growth rate are of the same sign as GDP, and somewhat larger magnitude. The effect of the flu death rate on realized real returns on equity and short-term government bills are both negative, but only statistically different from zero for government bills.

4 Data

We explore yearly data on real Gross Domestic Product per capita by (Daniele et al., 2007) across the 16 Italian regions as of 1918. We link GDP data with information on mortality for the year 1918, which we digitized from the Mortality Statistics Volume for 1918 (*Statistica delle Cause di Morte 1918*) by the Ministry of the National Economy (see Appendix Table B.1). These data provide information on the number of deaths for the year 1918 for influenza and pneumonia. We follow the literature and measure deaths due to the Great Influenza by summing the deaths for these two diseases (specifically we sum *influenza*, *broncopolmonite*, and *polmonite*). We construct the mortality variable by dividing the number of regional deaths from these diseases in 1918 over population from the Italian Statistical Office Population Census, which was taken in 1911. We do not employ data on the 1919 wave as it was predominantly an outcome of the 1918 wave and of local economic conditions.

We have digitized the number of deaths due to World War I from the *Albo d'Oro* archive of the *Institute for History and Resistance and Contemporary Society* (Istoreco). The year of death is not always certain and often military deaths occur with significant lags. Thus, our variable for WWI death rates takes value zero for the years before 1915 (the year in which Italy joined the war) and after 1918. Over the war years the variable equals the total number of military deaths due to WWI over population as of 1911. We also use as an outcome the share of labor force employed in manufacturing from Daniele and Malanima (2014). Additional outcomes of regional indicators of human capital (health and education) are from Felice (2007).

5 Descriptive Evidence

To introduce the regression analysis, it is useful to report the correlations of flu mortality, GDP and human capital indicators in the pre-war period. Table 1 reports two-by-two regressions of flu mortality and per capita GDP in 1913, GDP growth in 1907-1911, the share of manufacturing employment in 1911, the WWI death rate, 1911 literacy and the 1911 Human Development Indicator. There is some mild evidence that flu mortality was higher in regions which before the war exhibited lower income and lower growth per capita. However, the standard errors reported in square brackets in Table 1 indicate that the correlations are not statistically different from zero.

On the other hand, Table 1 and Figure 2 indicate that flu mortality was lower in regions with high WW death rate (the regression coefficient is -0.33 and statistically different from zero at the 5 percent level). For instance, the central regions of Emilia,

Figure 2: Influenza and World War I Mortality

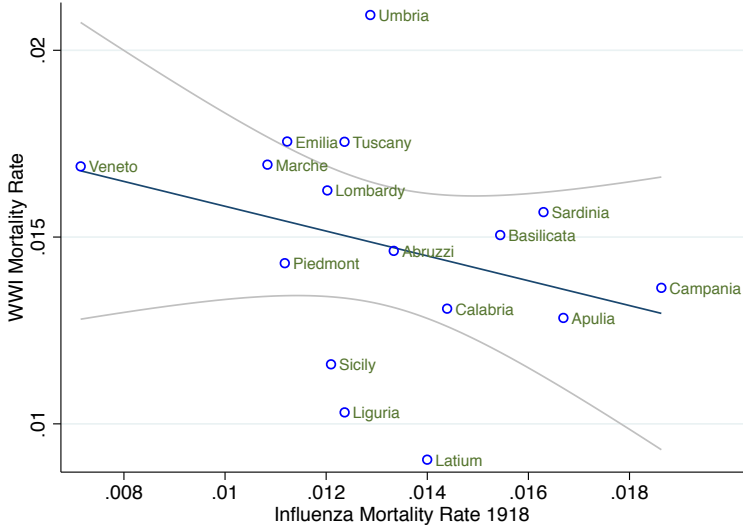


Table 1: Influenza and Pre-1918 Characteristics

VARIABLES	Dependent Variables:						
	(1)	(2)	(3)	(4)	(5)	(6)	(7)
	Ln GDP pc 1918	Ln GDP pc 1913	GDPpc Growth 1907-11	% Manuf. L.F. 1911	WWI Death Rate	Literacy 1911	HDI 1911
Influenza 1918	-23.331 [22.573]	-16.680 [15.983]	-0.938 [0.582]	-4.069 [4.177]	-0.332** [0.119]	-40.349*** [10.701]	-36.143*** [8.647]
Observations	16	16	16	16	16	16	16
R-squared	0.048	0.051	0.098	0.030	0.091	0.336	0.382

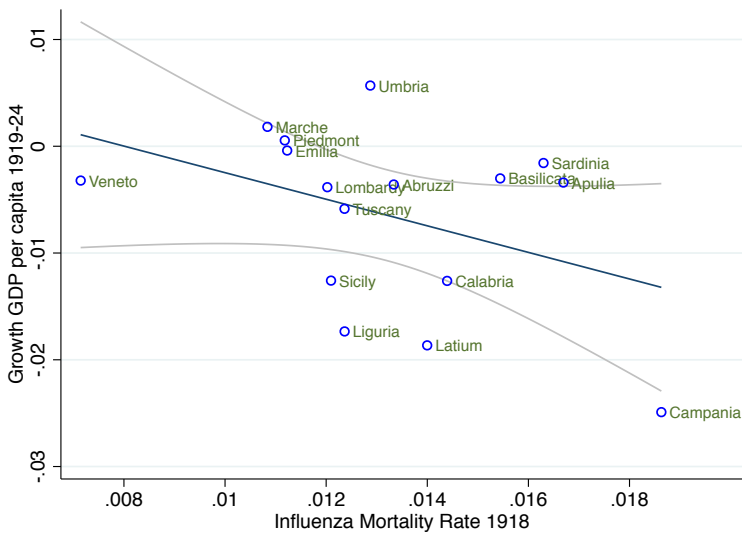
Notes: Observations are at the region-year level. Robust standard errors clustered at the regional level are reported in brackets.

*** indicates significance at the 1%-level, ** indicates significance at the 5%-level, * indicates significance at the 10%-level.

Marche and Tuscany exhibit relatively high war death rates, but below average flu mortality. For our regression analysis the negative correlation between the two mortality rates helps in identifying the separate effects of war and flu mortality on subsequent GDP growth. Table 1 also shows that flu mortality is negatively correlated with human capital indicators, as also suggested by the historical account of the pandemics provided by Tognotti (2015). Controlling for health conditions and education will therefore be important in the empirical analysis.

To introduce the regression analysis, in Figure 2 we plot the flu death rate against the GDP growth rate in 1919-24. In the period, the average growth rate is negative, reflecting the recession of 1919-21. However, regions with above average flu mortality (such as Calabria, Campania and Latium) exhibit lower than average growth, while regions with more limited mortality (Veneto and Marche) exhibit also milder recessions. For instance, doubling the flu death rate (from 0.8 to 1.6%) is associated with a reduction of subsequent annual growth of 1%.

Figure 3: Economic Growth and Influenza Mortality



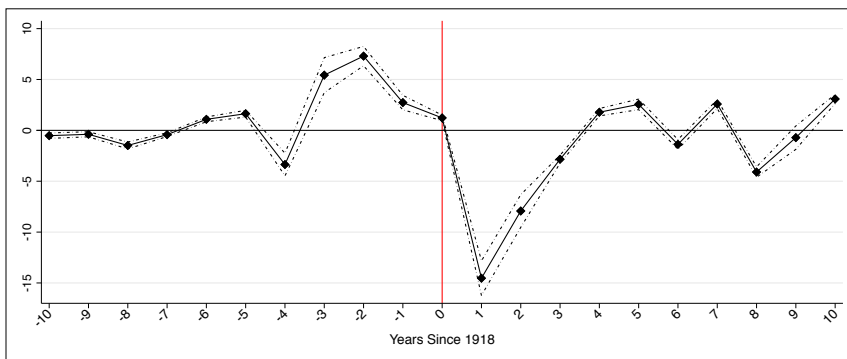
6 Regression Analysis

In this section, we explore empirically the link between influenza mortality rate and GDP per capita growth across Italian regions. As described in Section 2, mortality due to the influenza pandemic took place predominantly in 1918, in particular towards

the end of the year. Therefore, our variable of interest takes value zero in the years before and after 1918. We first explore the link between flu mortality and economic growth by regressing GDP per capita on flu mortality in 1918 with 10 years of lags and 10 years of leads. This approach allows us to check the presence of pre-treatment trends in regional GDP growth as well as potential lags in the estimated relationship between mortality and growth. Figure 4 depicts the series of estimated coefficients ordered by their distance to 1918, the year of the pandemic outbreak, with negative coefficients representing the leads.

Three main elements are evident from the figure. First, the estimated coefficients for the 10th to the 5th year leads (from 1908 to 1913) do not reveal differential trends. However, from the 4th-year lead (1914) until 1918, the period World War I, we observe significant swings around zero. Such finding points to the importance of taking into account potential differential exposures of regional growth rate to the war. Second, in line with the historical timing of the pandemic outbreak in Italy in late 1918, the negative link between flu mortality and economic growth emerges with one-year lag (thus in 1919). This result points to the importance of exploring these lags in the empirical specification. Finally, the estimated coefficients of the lags converge back towards zero after four years from the pandemic, so that by 1922 the effect seems to vanish. Such a pattern suggests that the link between influenza and economic growth may have lasted about three years, pointing to the potential transitory nature of the adverse effect of the pandemic on local economic growth.

Figure 4: Influenza ad Economic Growth: Leads-Lags Analysis



Notes: The figure shows the estimated coefficients from a regression of growth in real GDP per capita on influenza mortality in 1918 with 10 years of lags and 10 years of leads, along with 95% confidence intervals based on robust standard errors clustered at the regional level. The figure shows that the estimated link between influenza mortality and economic growth dissipated within four years from the event. Oscillations in the estimated coefficients for the years before the event coincide with WWI.

In Table 2 we restrict the sample of real per capita GDP growth to the years from 1919 to 1924 so as to explore the short-run effects of the pandemic and minimize concerns on the difficulties in interpreting World War I data on living standards. Our variable

of interest is influenza mortality in 1918 lagged by one year. As demonstrated by the empirical analysis graphically depicted in Figure 4, such an approach is ideal in the Italian setting given that the pandemic affected the Italian peninsula only at the end of 1918, in turn potentially having an effect on living standards which could be observed only in 1919. Later in the analysis, we will explore both contemporary and lagged effects. We correct inference by clustering standards errors at the level of regions so as to allow any arbitrary serial correlation of the error terms across periods.⁶

Table 2: Influenza Mortality and Growth in GDP per capita 1919-1924

	(1)	(2)	(3)	(4)
Dependent Variable: Growth GDP per capita 1919-24				
Influenza 1918 - 1 year lag	-12.927*** [0.740]	-9.692*** [2.798]	-9.675*** [2.644]	-10.677*** [2.948]
Influenza 1918 - 2 years lag				-7.502** [2.608]
Influenza 1918 - 3 years lag				-1.644** [0.636]
Influenza 1918 - 4 years lag				-0.552 [0.520]
WWI Death Rate		-3.072 [2.430]	-3.112 [2.314]	-3.224*** [0.721]
Observations	96	96	96	96
R-squared	0.604	0.609	0.615	0.885
Initial GDP pc	No	No	Yes	Yes
WWI Death Rate Lags	No	No	No	Yes

Notes: Observations are at the region-year level. Robust standard errors clustered at the regional level are reported in brackets.

*** indicates significance at the 1%-level, ** indicates significance at the 5%-level, * indicates significance at the 10%-level.

In column 1, we regress growth in GDP per capita on influenza mortality. The coefficient is -12.9 and statistically different from zero at the 1 percent level, which suggests that an increase in the influenza mortality equal to the 1918 average (0.132) is associated with an average reduction of 13% growth in real GDP per capita, almost half of the overall GDP decline in 1919-22. Another way to interpret our results is to compare regions with relatively high and low mortality rates. For instance, going from Calabria or Basilicata, which features mortality rates of about 1.5%, to Marche or Piedmont, which feature rates of about 1%, is associated with a reduction in GDP growth of 6.5

These effects are broadly comparable in magnitude with the one estimated by

⁶ In the Appendix Table A.1, we experiment several specifications and show that two-way clustered standards errors over regions and years provide very similar results.

Barro et al. (2020) in a cross-country setting, which is about 6%. Our coefficient is larger, possibly because policy interventions by central and local authorities to limit the spread of the pandemics were weak or largely ineffective. In column 2, we also control directly for WWI mortality. The variable is the total number of military deaths during WWI over population in 1911. The variable is lagged by one year and takes value zero for the years after 1918. The estimated coefficient for WWI mortality is negative, but not statistically different from zero. The coefficient of flu mortality remains negative, statistically significant, and almost unchanged with respect to the regression reported in column 1.

To take into account pre-existing differences in the level of economic activity, in column 3 we control for real per capita GDP in 1919, which is the initial year of the sample employed. Remarkably, this additional control has almost no effect on our coefficient of interest, which remains almost unchanged in magnitude and statistical significance. Since the effect of the 1918 influenza and economic growth may have lasted for more than a year, in column 4, we introduce four lags of influenza mortality. As a control, we also introduce four lags for WWI mortality (coefficients not reported). Interestingly, the coefficients of the lagged influenza variables are negative and significant up to the third lag, implying that the adverse effect of the pandemic on economic growth lasted for three years. This finding suggests that the effect of the Italian pandemic on regional economic growth is transitory, which is consistent with recent findings for the 1918 influenza across Danish municipalities (Moller Dahl et al., 2020).

In Table 3, we extend forward the sample until 1929. We do not go beyond 1929 so as to prevent the 1930s Great Depression to confound the estimates. As evident from the table, the estimated coefficients are very similar in magnitudes and significance to the ones reported in Table 2. Such a result further supports the conclusion that the adverse effects of the influenza pandemic on local economic growth has been transitory.

In Table 4, we extend the sample backward so as to include the years from 1901 to 1929. We can now include contemporary influenza mortality, as well as its lags up to the fourth year. The estimated coefficient for the contemporary effect in column 1 is actually positive and precisely estimated, yet very small in magnitude. The coefficient refers to 1918, the last year of the war, which may potentially confound the estimates. In the following specification we control for WWI casualties to take into account this effect. The coefficients for the lagged influenza mortality are negative and highly significant up to the third lag, which is consistent with our previous findings. The coefficient for the fourth lag is positive and significant. This finding is consistent with the influenza having a transitory adverse effect also on the levels of economic activity (Barro et al., 2020). However, our estimates of this coefficient are not robust across specifications, thus we cannot reject the hypothesis that the influenza had a permanent effect on the

Table 3: Influenza Mortality and Growth in GDP per capita 1919-1929

	(1)	(2)	(3)	(4)
Dependent Variable: Growth GDP per capita 1919-29				
Influenza 1918 - 1 year lag	-13.3303*** [0.789]	-9.8888*** [2.838]	-9.8819*** [2.778]	-10.2513*** [2.906]
Influenza 1918 - 2 years lag				-7.0770** [2.619]
Influenza 1918 - 3 years lag				-1.2183** [0.449]
Influenza 1918 - 4 years lag				-0.1271 [0.404]
WWI Death Rate		-3.2517 [2.447]	-3.2667 [2.401]	-3.2245*** [0.704]
Observations	176	176	176	176
R-squared	0.502	0.506	0.507	0.699
Initial GDP pc	No	No	Yes	Yes
WWI Death Rate Lags	No	No	No	Yes

Notes: Observations are at the region-year level. Robust standard errors clustered at the regional level are reported in brackets.

*** indicates significance at the 1%-level, ** indicates significance at the 5%-level, * indicates significance at the 10%-level.

levels of economic activity.

In column 2, we control for contemporary WWI death rates, as well as its lags up to four years. In line with the historical evidence, the contemporary effect is now indistinguishable from zero, in turn suggesting that the potential confounding effect of WWI exposure may induce a bias which is opposite in sign to the coefficient of influenza mortality. The estimated coefficients for the lags are negative and significant up to the third lag. In column 3, we control for per capita GDP in 1901, the first year of our sample. Controlling for initial conditions makes the one-year lag slightly more negative and the two-years lag slightly less negative. Albeit minor, such changes are potentially due to initial GDP per capita absorbing part of the differential exposure to the epidemic across regions. In column 4, we take into account potential common trends by controlling for a time polynomial of order two. The introduction of these controls implies minor changes in the estimated coefficients, in turn reducing concerns on the potentially confounding effect of a common trend across regions.

In column 5, we test the robustness of our specification to the introduction of regional fixed effects (our geographical unit of analysis) so as to completely control for heterogeneity in initial conditions.⁷ While this is not our preferred specification for

⁷ In the Appendix Table A.1, we extend this specification and incorporate additional controls, exclude potential outliers, and correct inference with two-way clustering.

Table 4: Influenza Mortality and Growth in GDP per capita 1901-1929

	(1)	(2)	(3)	(4)	(5)
Dependent Variable: Growth GDP per capita 1901-29					
Influenza 1918	0.667*** [0.124]	0.420 [0.537]	0.432 [0.575]	0.505 [0.594]	0.446 [0.800]
Influenza 1918 - 1 year lag	-15.087*** [0.953]	-12.161*** [1.744]	-12.138*** [1.794]	-12.192*** [1.831]	-12.299*** [2.238]
Influenza 1918 - 2 years lag	-8.482*** [0.913]	-4.164** [1.913]	-4.141* [1.994]	-4.097* [2.029]	-4.205* [2.384]
Influenza 1918 - 3 years lag	-3.395*** [0.203]	-2.988** [1.225]	-2.965** [1.243]	-2.816** [1.254]	-2.924* [1.659]
Influenza 1918 - 4 years lag	1.225*** [0.202]	-0.216 [0.933]	-0.204 [0.961]	-0.002 [0.938]	-0.062 [1.140]
Observations	464	464	464	464	464
R-squared	0.559	0.712	0.715	0.723	0.724
WWI Death Rate	No	Yes	Yes	Yes	Yes
Initial GDP pc	No	No	Yes	Yes	-
Time Trend	No	No	No	Yes	Yes
Region FE	No	No	No	No	Yes

Notes: Observations are at the region-year level. Robust standard errors clustered at the regional level are reported in brackets.

*** indicates significance at the 1%-level, ** indicates significance at the 5%-level, * indicates significance at the 10%-level.

interpreting the magnitudes of the estimated coefficients, it is important to observe that the estimates are robust to implementing this specification, which also takes into account pre-existing specialization patterns across regions that may not be captured by initial GDP. For instance, any differences between the North-West, specialized in heavy industry, and the South, specialized in agriculture, would be differenced out. Overall, our result points to a strong and negative association between the influenza mortality rate and economic growth in 1919, which was then absorbed in the subsequent three years.

7 Influenza, Human Capital, and Industrialization

Having explored the short-run nature of the link between influenza pandemic and GDP growth, we now turn to investigating mechanisms that may uncover long-term effects of the pandemic. To do so, we have assembled a regional data set with indicators of human capital (health and education) and manufacturing employment (see Section 4 for sources). Unfortunately, these data are only available in the years of the census (approximately every decade), and thus they are unsuitable to investigate short-term dynamics. In this setting, mortality varies only across regions and not over time. Results are shown in Table 5.

Table 5: Influenza, Human Capital, and Industrialization

VARIABLES	(1)	(2)	(3)	(4)
	Manuf. L.F. 1911-1921	Human Dev. Index 1911-1938	I. Human Dev. Index 1911-1938	Ln Population 1911-1931
Influenza 1918	-0.838 [0.658]	-0.628 [1.885]	-2.328 [2.988]	-8.424 [6.810]
Observations	32	32	32	48
R-squared	0.967	0.929	0.937	0.992
Initial level	Yes	Yes	Yes	Yes
WWI Death Rate	Yes	Yes	Yes	Yes
Linear Trend	Yes	Yes	Yes	Yes

Notes: Observations are at the region-year level. All the columns control for the level of the outcome variable measured in 1911 and for WWI total mortality rate. Robust standard errors clustered at the regional level are reported in brackets.

*** indicates significance at the 1%-level, ** indicates significance at the 5%-level, * indicates significance at the 10%-level.

After WWI, Italy was a predominantly rural society, with more than half of the labor force employed in agriculture. Recent studies have shown that over the 1920s and

1930s human capital accumulation and industrialization were important to understand long-run development patterns across areas of the country (Carillo, 2018). It is then possible that the influenza pandemic affected the transition of the labor force towards the manufacturing sector, in turn influencing long-term economic development. In column 1, we investigate this hypothesis by employing as an outcome the share of the labor force employed in manufacturing and controlling for its level in 1911 and for a linear trend. The estimated coefficient is statistically indistinguishable from zero, pointing to the potentially limited long-run effects of the pandemic.

In columns 2 and 3, we use as outcomes two indexes of human capital and living standards, the *Human Development Index* (HDI) and its *improved* version (IHDI), respectively. These indexes are based on three indicators of living standards: education, life expectancy, and income per capita. The differences between the HDI and the IHDI is the methodology used to aggregate the underlying three variables (see Felice (2007)). We explore the link between the influenza epidemic and these indexes and find limited evidence of a significant relationship, pointing to the potentially limited persistent effect of the pandemic on human capital and living standards across regions. The absence of an effect on indicators that include life expectancy might be due to the fact that mortality was higher among people with low socioeconomic conditions, which were typically characterized by low life expectancy and human capital. Thus, the overall effect on life expectancy and human capital of the surviving population is ambiguous.

We also explore whether mortality associated with the pandemic has persistently reduced population in the areas more exposed, potentially preventing population from returning to its initial trajectory. In the last column, we relate influenza mortality to the log of population. The estimated coefficient is negative but not statistically different from zero, thus non supporting the hypothesis of a persistent effect of the influenza on the regional composition of the population.

8 Concluding Remarks

In this paper, we investigate empirically the link between pandemics and local economic growth. We explore the case of the Great Influenza Pandemic of 1918 in Italy and study its link with regional growth in GDP per capita. Our estimates show that going from regions with the lowest mortality to the ones with the highest mortality is associated with negative GDP per capita growth of about 6.5%. Our estimates are comparable with recent findings on the cross country effect of the Influenza on economic growth (Barro et al., 2020), yet larger in magnitude. One possible explanation is the limited and largely ineffective interventions to contain the influenza pandemic in

Italy. We also find that the link between influenza and growth dissipates three years after the shock, a finding in line with recent studies of the influenza pandemic across localities in other countries.

The limited interventions to contain the pandemic, along with the poor health infrastructures that characterized many parts of the country after WWI, make the Italian historical experience of the Great Influenza an important case to cast light on the economic consequences of pandemics in societies in which lockdown policies cannot be implemented, or where the health care system is unable to protect citizens. The Italian case may provide also policy guidance to compare the recessionary effects of pandemics in the absence of interventions with the adverse effects of the interventions aimed at containing it. Given that exposure to the influenza was linked to pre-existing living standards, our findings should be interpreted cautiously and possibly as an upper bound of the effects of the influenza on local economic growth. We hope that our study will stimulate future research to explore further this important link and shed novel light on the heterogeneous effects of pandemics across localities and individuals.

References

- Alfani, G. (2013). Plague in seventeenth-century Europe and the decline of Italy: an epidemiological hypothesis. *European Review of Economic History*, 17(4):408–430.
- Alfani, G. and Percoco, M. (2019). Plague and long-term development: the lasting effects of the 1629–30 epidemic on the Italian cities. *The Economic History Review*, 72(4):1175–1201.
- Almond, D. (2006). Is the 1918 influenza pandemic over? Long-term effects of in utero influenza exposure in the post-1940 US population. *Journal of political Economy*, 114(4):672–712.
- Barro, R. J., Ursua, J. F., and Weng, J. (2020). The Coronavirus and the Great influenza Epidemic—Lessons from the “Spanish Flu” for the Coronavirus’s Potential Effects on Mortality and Economic Activity.
- Brainerd, E. and Siegler, M. V. (2003). The economic effects of the 1918 influenza epidemic. *CEPR Discussion Paper*.
- Carillo, M. F. (2018). Agricultural policy and long-run development: evidence from Mussolini’s Battle for Grain. Technical report, University Library of Munich, Germany.
- Correia, S., Luck, S., and Verner, E. (2020). Pandemics depress the economy, public health interventions do not: Evidence from the 1918 flu. *Public Health Interventions Do Not: Evidence from the*.
- Daniele, V. and Malanima, P. (2014). Falling disparities and persisting dualism: Regional development and industrialisation in Italy, 1891–2001. *Investigaciones de Historia Económica-Economic History Research*, 10(3):165–176.
- Daniele, V., Malanima, P., et al. (2007). Il prodotto delle regioni e il divario Nord-Sud in Italia (1861-2004). *Rivista di politica economica*, 97(2):267–316.
- Felice, E. (2007). I divari regionali in Italia sulla base degli indicatori sociali (1871-2001). *Rivista di politica economica*, 97(3/4):359.
- Garrett, T. A. (2008). Pandemic economics: The 1918 influenza and its modern-day implications. *Federal Reserve Bank of St. Louis Review*, 90(March/April 2008).
- Garrett, T. A. (2009). War and pestilence as labor market shocks: US manufacturing wage growth 1914–1919. *Economic Inquiry*, 47(4):711–725.

- Guimbeau, A., Menon, N., and Musacchio, A. (2020). The Brazilian bombshell? the long-term impact of the 1918 influenza pandemic the south American way. Technical report, National Bureau of Economic Research.
- Johnson, N. P. and Mueller, J. (2002). Updating the accounts: global mortality of the 1918-1920 "Spanish" influenza pandemic. *Bulletin of the History of Medicine*, pages 105–115.
- Karlsson, M., Nilsson, T., and Pichler, S. (2014). The impact of the 1918 Spanish flu epidemic on economic performance in Sweden: An investigation into the consequences of an extraordinary mortality shock. *Journal of Health Economics*, 36:1–19.
- Le Moglie, M., Gandolfi, F., Alfani, G., and Aassve, A. (2020). Epidemics and Trust: The Case of the Spanish Flu. Technical report, IGIER Working Paper.
- Malanima, P. (2018). Italy in the renaissance: a leading economy in the European context, 1350–1550. *The Economic History Review*, 71(1):3–30.
- Malanima, P. and Zamagni, V. (2010). 150 years of the Italian economy, 1861–2010. *Journal of Modern Italian Studies*, 15(1):1–20.
- Moller Dahl, C., Hansen, C. W., and Jensen, P. S. (2020). The 1918 Epidemic and a V-shaped Recession: Evidence from Municipal income Data. *CEPR's Covid Economics Review No. 6*.
- Percoco, M. (2016). Health shocks and human capital accumulation: the case of Spanish flu in Italian regions. *Regional Studies*, 50(9):1496–1508.
- Pinnelli, A. and Mancini, P. (1998). Mortality peaks in Italy in the late 19th and early 20th centuries: trends by age and sex. *European Journal of Population/Revue européenne de Démographie*, 14(4):333–365.
- Tognotti, E. (2015). *La "spagnola" in Italia. Storia dell'influenza che fece temere la fine del mondo (1918-1919): Storia dell'influenza che fece temere la fine del mondo (1918-1919)*. FrancoAngeli.
- Weil, D. N. (2014). Health and economic growth. In *Handbook of economic growth*, volume 2, pages 623–682. Elsevier.

Appendices

A Robustness

Table A.1: Robustness to Alternative Specifications

VARIABLES	Dependent Variable: Growth GDP per capita 1901-29					
	(1)	(2)	(3)	(4)	(5)	(6)
		Excluding Campania	Excluding Veneto			
Influenza 1918	0.446 [0.800]	0.572 [0.995]	0.019 [0.857]	-1.434 [0.934]	-1.324 [0.813]	-1.324 [1.920]
Influenza 1918 - 1 year lag	-12.299*** [2.238]	-12.429*** [2.792]	-13.381*** [2.343]	-15.018*** [3.661]	-14.852*** [3.757]	-14.852*** [3.447]
Influenza 1918 - 2 years lag	-4.205* [2.384]	-3.796 [2.954]	-5.342** [2.430]	-3.405 [2.377]	-3.291 [2.421]	-3.291 [2.185]
Influenza 1918 - 3 years lag	-2.924* [1.659]	-2.905 [2.090]	-4.069** [1.638]	0.941 [0.616]	0.789 [0.618]	0.789 [1.649]
Influenza 1918 - 4 years lag	-0.062 [1.140]	0.147 [1.410]	-0.853 [1.071]	5.187*** [0.882]	4.505*** [1.000]	4.505** [2.047]
Observations	464	435	435	464	464	464
R-squared	0.724	0.715	0.724	0.820	0.823	0.824
WWI Death Rate	Yes	Yes	Yes	Yes	Yes	Yes
Time Trend	Yes	Yes	Yes	Yes	Yes	Yes
Region FE	Yes	Yes	Yes	Yes	Yes	Yes
National GDPpc	No	No	No	Yes	Yes	Yes
War Years FE	No	No	No	No	Yes	Yes
Two-Way Clustering SE	No	No	No	No	No	Yes

Notes: Observations are at the region-year level. Column 1 is the same as the last column of Table 4 for comparison. Column 2 excludes the region with the maximum level of mortality (Campania). Column 3 excludes the region with the minimum level of mortality (Veneto). WWI Death Rate is a set of five control variables including WWI death rates contemporary and lagged up to four years. Time trends are linear and quadratic terms of the year variable. National GDP per capita controls include linear, quadratic and cubic terms of real national GDP per capita. War Years fixed effect is a dummy taking value one over the years in which Italy was in war (from 1915 to 1918). Robust standard errors clustered at the regional level are reported in brackets, with the exclusion of column 6 in which we employ two-way clustering over regions and years.

*** indicates significance at the 1%-level, ** indicates significance at the 5%-level, * indicates significance at the 10%-level.

B Data Description

Table B.1: Mortality for Influenza and World War I across Italian Regions

Region	Influenza Mortality	WWI Mortality	Population (000) Year 1911
Abruzzi	20165	22121	1512
Apulia	36639	28173	2195
Basilicata	7505	7316	486
Calabria	21963	19965	1526
Campania	57789	42315	3102
Emilia	31587	49391	2813
Latium	24791	16012	1771
Liguria	14924	12440	1207
Lombardy	58780	79437	4889
Marche	12410	19395	1145
Piedmont	39078	49982	3495
Sardinia	14147	13600	868
Sicily	46111	44197	3812
Tuscany	33009	46860	2670
Umbria	7904	12860	614
Veneto	26699	63124	3737

Notes: The table reports mortality for the Great Influenza and World War I across Italian regions. Column 1 reports the name of the region. Column 2 reports the number of deaths in 1918 for influenza and pneumonia. Column 3 reports the number of military deaths in World War I. Column 4, reports the population in each region as of 1911 (in thousands). For data sources, see Section 4.

A generalized SEIR model of Covid-19 with applications to health policy¹

Ernst-Ludwig von Thadden²

Date submitted: 19 April 2020; Date accepted: 21 April 2020; Date revised: June 2020

This paper generalizes the standard epidemiological SEIR model of the spread of diseases such as Covid-19 in two respects. First, it considers the structure of the infectious population in more detail and introduces the concept of the "cohort composition kernel" that generalizes the aggregate transmission function in the infected population. Second, it shows how policy measures such as testing and quarantine rules can affect this kernel and how this can provide estimates for the impact and lag of non-pharmaceutical policy interventions. On the technical side, the paper shows how to dispense with the standard assumption of exponential transition dynamics and to work with general transition processes consistent with observed duration frequencies, by using the convolution of densities.

- 1 An early version of this paper was called "A simple, non-recursive model of the spread of Covid-19 with applications to policy". I am grateful to Toni Stocker and Carsten Trenkler for advice, to Michèle Tertilt and Harald Uhlig for comments, and to Lukas Mevissen and Tobi Palmowski for great research assistance. Financial support by the German Research Foundation through Grant CRC TR224, TP C03, is gratefully acknowledged.
- 2 Professor of Economics, Universität Mannheim and CEPR Research Fellow.

Covid-19 “might be a one-in-a-century evidence fiasco”
(J. Ioannidis, STATnews 17/3/20)

1 Introduction

Much of the rapidly developing economic literature on the spread of the Covid-19 pandemic builds on the classic SIR-model of contagion and its different compartmental versions such as the SEIR model.¹ The simplest version of this model derives the dynamics of transmission in a recursive framework, in which the number of newly infected individuals in a population (ΔI or $\frac{d}{dt}I$) depends on the number of non-infected individuals (S) who are susceptible to an infection and on the number of currently infected individuals in a reduced-form model of personal encounters.² In its simplest form, the increase takes the form $n_t = \beta S_{t-1} I_{t-1}$, where I_t denotes the number of infectious individuals and β the net transmission rate (per period), and is mitigated by the outflow $-\gamma I_{t-1}$. At the early stage of the epidemic where we are currently, the modulating effect of having increasing numbers of individuals removed (R) from the susceptible group through immunization or death can be neglected. Hence, we approximately have $n_t = (\beta - \gamma) I_{t-1}$, simple exponential growth.

While the model is a useful basis for longer-run macroeconomic analyses,³ Covid-19 presents (at least) two problems that make an application of the basic exponential model difficult for short- and medium-run policy. First, transmission does not simply depend on the number of infectious individuals, but on the composition of this group, which is directly influenced by policy measures such as testing. And second, the data at our disposal are quite inadequate to observe this composition. In fact, in most countries we do not even know the number of infected, not even their magnitude, let alone that of infectious individuals. This state is very unsatisfactory, as it is difficult to evaluate the effectiveness of policy with insufficient data. In the basic SIR model, the number of infectious individuals depends on the inflow rate β and the outflow rate γ and therefore in principle on two dimensions of intervention: one ex-ante, restricting interaction through hygiene and social distancing rules, which affecting the transmission parameter β , and one ex post, through testing or quarantining, thus intervening after possible infections and affecting γ .

¹The SIR-model goes back to Kermack and McKendrick (1927). Useful reviews are Brauer (2008) and Allen (2017) and, just in time, Stock (April 5, 2020). A classic description is in Braun (1978, Ch. 4).

²Sometimes the acronym is interpreted as “susceptible-infected-recovered”. This is too narrow, and the original model (e.g., in Braun, 1978) divides the population more generally in susceptible, infectious, and removed agents. Removal may be recovery, but it is much broader, as it also includes quarantine and other policy measures. On the other hand, infectious is narrower than infected, which is a key problem with Covid-19 and one of the aspects of the model developed in this paper.

³Such as Atkeson (2020), Brotherhood et. al (2020), and Eichenbaum, Rebelo, Trabant (2020). This literature grows like $n_t = \beta I_{t-1}$.

This paper presents a simple model that addresses both the modelling and the policy problem by looking in more detail into the structure of the “ex-post part” of the transmission process and how it is influenced by policies. It is therefore related to the so-called “compartmental models” of epidemiology (see, e.g., Brauer, 2008, and Blackwood and Childs, 2018), but it differs from them by abandoning the usual exponentially distributed duration framework. Modelling the transition from one health status to another by an exponential duration is mathematically convenient, but imposes a rigid structure on the dynamics, which cannot incorporate more complex insights from the medical literature on actual observed durations.

The model identifies the variables which we need to understand and measure better, establishes relations between them that can be used to make efficient use of the data that we can observe, and points to several mechanisms by which policy influences these variables. The model essentially generalizes the SIR-relation $n_t = \beta_t S_{t-1} I_{t-1}$ in two respects. First, it considers the structure of the infectious population in more detail and introduces the concept of the “cohort composition kernel” that describes transitions between health compartments and thus generalizes the aggregate transmission model and makes it non-recursive. Second, it shows how policy measures such as mass testing or quarantine rules affect this kernel directly and how this can improve our estimates for the impact and lag of non-pharmaceutical policy interventions.

By modelling the exit process from the infectious group in more detail, the present model may also help with the identification of the key parameters of the SIR-model in applied policy work such as Dehning et al. (2020). As noted initially, in the early phases of the pandemic where infections and recoveries are small relative to the population size, the SIR-model boils down to an essentially exponential growth model with effective growth parameter $\beta - \gamma$. In Bayesian inference models over short horizons, such as in Dehning et al. (2020), it is therefore difficult to identify β and γ separately. Adding prior information about γ , by modelling the composition of I_t more precisely, thus alleviates the identification problem for β .⁴

The research presented here is preliminary and uses findings from the medical literature until May. My emphasis is on policy and, of course, I am most familiar with the German data and policy. But the structural problem is the same everywhere.⁵

⁴In fact, in their parameter estimation of the early German lockdown, Dehning et al. (2020) mostly focus on estimating the spread parameter β and keep γ constant, although also it is likely that also γ changed as a result of policy in March/April.

⁵There is a rapidly growing body of clinical evidence, mostly evaluating small sample experiences from China in January and February 2020; and not being an expert, I am much indebted to the summaries provided by the websites of the Centers for Disease Control and Prevention, its German counterpart, the Robert-Koch Institute, or public discussions by virologists, such as Christian Drosten of the Charité at Humboldt University. These are, respectively, <https://www.cdc.gov/coronavirus/2019-ncov/hcp/clinical-guidance-management-patients.html>, https://www.rki.de/DE/Content/InfAZ/N/Neuartiges_Coronavirus/Steckbrief.html, and the remarkable podcast <https://www.ndr.de/nachrichten/info/Corona-Podcast-Alle-Folgen-in-der-Uebersicht.podcastcoronavirus134.html>.

The model presented here is at the same time much simpler than the influential model by Ferguson, Cummings et al. (2005) that is the basis for the simulations recently conducted by Ferguson et al. (March 16, 2020, the “Imperial Study”), and more detailed in some respects, as it works with more general distributions and explicitly considers the impact of parameters on them that can be used for policy. It thus tries to bridge the gap between the mathematical theories of dynamical systems, the clinical evidence, and the reduced form models used by economists to evaluate the economic consequences of the health crisis.

2 The Disease

At the individual level, the disease and its consequences evolve in stages after the infection. Time is discrete, $t = \dots, -1, 0, 1, \dots$, and measured in days. Suppose infection is at time $t = 0$. The different stages of the disease are then given by the following random times T , measured in days after infection:

- T^c (contagious): first day of being contagious
- $T^o = T^c + \tau^o$ (outbreak): day of first symptoms (if at all) or undetected outbreak for mild or asymptomatic cases
- $T^s = T^o + \tau^s$ (severe): first day of severe symptoms if any
- $T^e = T^o + \tau^e$ (end of infectivity): first day of being no longer contagious if no severe symptoms
- $T^{ex} = T^s + \tau^{ex}$ (exit): first day of being healthy after severe symptoms
- $T^d = T^s + \tau^d$ (death): day of death after severe symptoms

The above events refer to the evolution of the disease only, not to any interventions. T^c and the incremental times τ are random variables taking values in \mathbb{N}_0 . In case of no clear symptoms or no symptoms at all, T^o is an imputed date to make the subsequent timing comparable.⁶

We denote the distributions and their densities (probability mass functions) of event days T^x by p^x , letting $p^x = (p_0^x, p_1^x, \dots)$. Densities of incremental times between two event days T^{x_1} and T^{x_2} , conditional on event x_1 having occurred, are denoted by $\pi^{x_1 x_2}$ where

$$\pi_k^{x_1 x_2} = \Pr(T^{x_2} = T^{x_1} + k), k \geq 0 \tag{1}$$

denotes the probability that event x_2 occurs k days after event x_1 . Note that $\pi_k^{x_1 x_2}$ is independent of the realization of T^{x_1} . This simplification can easily

⁶The extent of asymptomatic cases is still debated. Completely asymptomatic cases seem to be rare, though. Upon careful investigation, most patients seem to be able to identify at least some very mild signs that can be used to trace the infection back to its original source (as in the “Munich study” by Böhmer et al. (2020) or the “Vo’ study” by Lavezzo et al. (2020)).

be generalized.⁷ For further simplicity and in line with much of the mathematical epidemiological literature, we assume that all these random variables are independent.⁸

The diagnoses at the time of outbreak are grouped into three types:

- a : asymptomatic (resp., unnoticed by patient)
- m : mild, but clear symptoms (fever, cough, etc.)
- s : severe, potentially life-threatening (acute respiratory distress (ARD), pneumonia, lung failure, etc.)

Since the focus of this paper is on transmission, we simplify the presentation by not distinguishing between patients with severe symptoms and critically ill patients. In functioning medical environments the former is usually associated with hospitalization,⁹ the latter with progression to ICUs. The outbreak at time T^o produces the outcomes a , m , and s with probabilities θ_a , θ_m , and θ_s , respectively, where $\sum_o \theta_o = 1$.

One important feature of Covid-19 is the fact that severe symptoms may still materialize some time after an initial incubation with no or only mild symptoms.¹⁰ In order to capture this possibility, we assume that after an initial draw of a or m , there is a conditional probability θ_{sl} of getting severe symptoms late. If the individual outbreak immediately produces severe symptoms, we have $\tau^s = 0$, i.e. $T^s = T^o$. Initially asymptomatic and mild cases develop severe symptoms after $\tau^s > 0$ days with probability θ_{sl} , or recover after $\tau^e > 0$ days with no deterioration with probability $1 - \theta_{sl}$.¹¹

This paper is only concerned with transmission and in particular its start and end times. Here, I make the twin assumption that severely ill patients are hospitalized and that they cease to transmit once in hospital. Both assumptions are largely satisfied in countries with functioning public health systems, albeit imperfectly. Infected patients therefore stop transmitting the virus on day

$$\tau^n = \begin{cases} \tau^s & \text{with prob. } \theta_{sl} \\ \tau^e & \text{with prob. } 1 - \theta_{sl} \end{cases} \quad (2)$$

⁷For example, the distribution of the time from incubation to the end of infectivity (τ^e) may depend on the day of incubation (T^o). I am not aware of any empirical evidence on this matter.

⁸See, e.g., Brauer (2008), Ferguson et al. (2005).

⁹This was different during the early spread of the disease in Wuhan in January, where hospitalization was also used as an isolation device, or in Lombardy in March/April, when hospitals were overloaded.

¹⁰As of June 1, 2020, the website of the CDC simply notes "Clinicians should be aware of the potential for some patients to rapidly deteriorate one week after illness onset". There is significant evidence from Wuhan for the clinical progression of Covid-19 during hospitalization. This is informative also for the non-clinical progression because in the early phase of the outbreak in Hubei many patients with relatively mild symptoms were hospitalized. An interesting example is Zhou, Yu, Du et al. (2020).

¹¹This means that the conditional probability θ_{sl} is realized early and together with it the distribution of the resulting delay τ^n , given by (2).

Alternatively one can assume that uncertainty persists longer and is only resolved at time $T^o + \tau^n$, where $\tau^n = \min(\tau^s, \tau^e)$. The analysis is the same under both assumptions, only the way the distribution of τ^n is obtained from those of τ^s and τ^e differs.

after incubation.¹²

Figure 1 provides an illustration of the evolution of the infection starting from the onset of infectivity on day T^c .

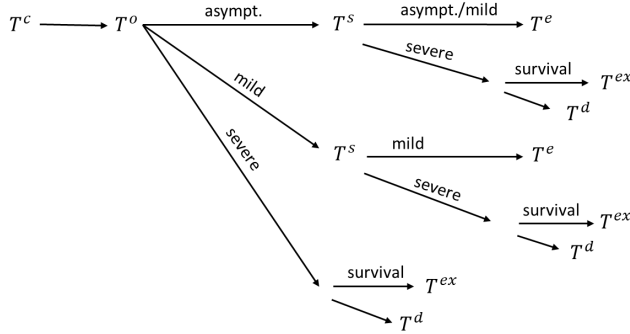


Figure 1: The Evolution of the Disease

The probabilities θ_a , θ_m , θ_s , and θ_{sl} are highly group-specific, and therefore general estimates vary strongly and are not very informative. Furthermore, only repeated testing can distinguish between pre-symptomatic and asymptomatic cases.¹³

Given the experience of the first few months of 2020,¹⁴ the probabilities are probably in the following ranges:

$$\theta_a \in [0.2, 0.5] \tag{3}$$

$$\theta_m \in [0.4 - 0.7] \tag{4}$$

$$\theta_s \in [0.01, 0.03] \tag{5}$$

¹²The superscript n stands for “no longer transmitting.”

¹³The broad meta-analysis by Koh, Naing et al. (2020), based on 66 original studies, reports a fairly wide range of estimates, with an average of 25.9% of all cases asymptomatic at diagnosis, but only 8.4% asymptomatic throughout the observation period. In another review, Byambasuren et al. (2020) put the proportion of truly asymptomatic cases at 15%.

Some important large-scale studies such as the Vo¹-Study by Lavezzo et al. (2020) report a proportion of asymptomatic cases of above 40%. (it is not clear from the manuscript whether these cases stayed asymptomatic between the two test dates).

Findings also differ across subgroups. An interesting early example from a comprehensive test in an old-age home in King County, Washington, found that 57% of all tested positive had no symptoms on the day of testing, but that only 10% still had no symptoms 7 days later (Kimball et al. 2020).

¹⁴See, e.g., Robert-Koch Institut (2020) and a burgeoning medical literature reviewed, in particular, by the U.S. CDC and the European ECDC.

The conditional probability of progressing to severe symptoms from initially no or mild symptoms, θ_{sl} , is not systematically documented it seems.¹⁵ Given estimated overall probabilities of developing severe symptoms eventually, this probability probably is in the range of

$$\theta_{sl} \in [0.05 - 0.1] \quad (6)$$

Together with (5), (6) is consistent with an interval for the overall probability of severe symptoms conditional on infection of $\theta = \theta_s + (1 - \theta_s)\theta_{sl} \in [0.03, 0.08]$.¹⁶

There seems to be even less evidence about the actual distributions of the event days T^x . Most studies report means or medians and information about the support, but little about the overall shape of the distributions.

A widely accepted estimate for the median incubation date T^o seems to be around 5 days, with most of the mass on the interval $[3, 10]$.¹⁷ For patients with mild symptoms at outbreak, severe symptoms are observed, if at all, 5 to 10 days after incubation.¹⁸ For severe cases, mortality rates and time to death depend on the clinical environment and can therefore not be pinned down universally and without reference to specific policy. Since the focus of this paper is on transmission these data are of little concern here. Of great concern, in this paper and in practice, however, is to know when infected patients are contagious. One of the most striking features of COVID-19 is that the virus can be transmitted before an outbreak is noticed. The time span over which transmission can occur is usually stated with reference to the outbreak date T^o , which is the interval $[T^o - \tau^o, T^o + \tau^e]$ if there are no severe symptoms. Current estimates for the onset of contagiousness, T^c , suggest values $\tau^o \in [0, 2]$.¹⁹ For the end date of untreated cases, $T^o + \tau^e$, there seems to be a window of $\tau^e \in [6, 12]$ days after the outbreak, with even longer times possible for children.²⁰ For example, evidence from the Munich group of early German infections by Woelfel et al.

¹⁵Some good case studies exist, though. For example, in a detailed progression study of a large group of hospitalized cases in Shenzhen (China), Wang et al. (2020) report that 21.7% of all mild/moderate cases progressed to the severe/critical stage within a median of 5 days after hospitalization. Given the missing observations on all asymptomatic and some mild cases, this is consistent with θ_{sl} being between 5 - 10%.

¹⁶See Robert-Koch Institut (2020) and many other similar institutions.

A word of caution: These are percentages of all infections, not just confirmed infections.

Ferguson et al. (2020), building on Verity et al. (2020), give an estimate of 4.4% for θ , arguing that their original data from China are likely to be biased. On the cruise ship "Diamond Princess" 52 of the 697 infected cases developed critically severe symptoms. These 7.5% are high compared to what one can expect for the general population, as the overall group on the ship was relatively high risk (and by far most infections occurred in the over-60 age group). Data from Russel et al. (2020), with some preliminary background.

¹⁷An early study is Lauer et al. (2020).

¹⁸Relevant data seem to be mostly from Hubei, summarized by Wu et al. (2020). Early cases in Wuhan were documented by Huang, et al. (2020). See also Wang et al. (2020).

¹⁹Ferguson et al. (2020), assumes a point estimate of $\tau^o = 0.5$, which implies a larger upper bound for the actual distribution of τ^c , consistent with other findings. Larger field studies such as Lavezzo et al. (2020) suggest slightly higher values.

²⁰See <https://www.cdc.gov/coronavirus/2019-ncov/hcp/clinical-guidance-management-patients.html>, https://flexikon.doccheck.com/de/SARS-CoV-2#cite_note-50 and the references therein. An interesting small sample result is in Wölfel et al. (2020).

(2020) indicate that the viral load in the throat - an important determinant of individual infectivity - decreases from the time of the outbreak on and that the virus actively replicates in the throat until date $T^o + 5$, but not much thereafter. The Guangdong study by He et al. (2020) confirm that the viral load peaks before day T^o , and even finds that approx. 44% of all infections may take place before T^o (the transmission probability is highly left-skewed).²¹

This implies that, in the absence of mass testing, the vast majority of infections occur when the transmitter either is completely unaware of her disposition or has mild symptoms for which she has not been tested. Combined with the evidence for T^o , this yields an overall broad time interval of [2, 23] days after infection, during which (at least some) individuals can be contagious, with substantial left-skewness and little or no mass in the far right tail.

The following tools from probability theory are useful to put these distributions to work. Central is the concept of the convolution of two distributions. Proofs are straightforward calculations.

1. Subsequent event times: Let p^{x_1} be the distribution of event time T^{x_1} and $\pi^{x_1x_2}$ the distribution of days from event time T^{x_1} to T^{x_2} . Then the distribution of event time T^{x_2} is given by the probability mass function over days k

$$p_k^{x_2} = \sum_{m=0}^k p_m^{x_1} \pi_{k-m}^{x_1x_2} \tag{7}$$

2. Time intervals: Let p^{x_1} be the distribution of event time T^{x_1} and $\pi^{x_1x_2}$ the distribution of days from event time T^{x_1} to T^{x_2} . Then the probability that on day k after infection event x_1 has happened, but event x_2 has not yet happened is

$$p_k^{x_1x_2} = \Pr(T^{x_1} \leq k < T^{x_2}) = \sum_{n=k+1}^{\infty} \sum_{m=0}^k p_m^{x_1} \pi_{n-m}^{x_1x_2} \tag{8}$$

Note that the $p_k^{x_1x_2}$ do not define a probability distribution. They are probabilities, but do not sum to 1 because of double-counting.

The following example illustrates these ideas and will be continued in Section 5. Suppose that the onset of infectivity, T^c , occurs according to the following distribution

$k :$	0	1	2	3	4	5	6	7	8
$\bar{p}_k^c :$	0	0	0.2	0.2	0.2	0.2	0.1	0.1	0

(9)

with $\bar{p}_k^c = 0$ for $k \geq 8$. Hence, on average individuals start being contagious

²¹The evidence on individual infectivity as measured by viral loads is increasing. An interesting observational study on 23 patients in Hong Kong is To et al. (2020). For more evidence, see <https://www.cdc.gov/coronavirus/2019-ncov/hcp/clinical-guidance-management-patients.html#Asymptomatic> and the studies cited there, and (as usual) the Drosten Podcast (e.g., no. 20, 24/3/2020).

4.1 days after infection, and infectivity begins one week after infection at the latest. This is in line with the evidence discussed above. Suppose further that the distribution of days between the onset of infectivity (on day T^c) and the onset of symptoms, if any, (on day T^o) is given by

$$\frac{k :}{\bar{\pi}_k^{co} :} \begin{array}{|c|c|c|c|} \hline 0 & 1 & 2 & 3 \\ \hline 0.4 & 0.3 & 0.3 & 0 \\ \hline \end{array} \tag{10}$$

with $\bar{\pi}_k^{co} = 0$ for $k \geq 3$. Hence, infectivity starts on the day of the outbreak or up to 2 days prior to it, which again is consistent with the empirical evidence mentioned above.

Figure 4 (in the Appendix) shows the distribution \bar{p}^o of the outbreak day T^o generated by these two distributions by applying (7). By construction, the distribution has support $\{2, \dots, 9\}$. Its mean and median is 5.0, and the distribution is left skewed, which is consistent with the above noted estimates of the early medical literature. Furthermore, using (8), Figure 5 plots the probabilities p_k^{co} that for any day k the individual is contagious (i.e. on or past event day T^c), but yet without (possibly imputed) symptoms (i.e. before day T^o). This is the case of being pre-symptomatic but infectious that is of particular concern for Covid-19. As the figure shows, in our simple parametrization, although on average individuals remain only 0.9 days in that state, its overall incidence is spread over 7 days with a peak on days 3 - 5 after infection.

3 The Population

The model developed above divides the course of the individual infection into different stages ("compartments" in the epidemiological literature²²). We now turn to the description of the aggregate evolution. Capital letters denote stocks (numbers measured at the end of the day) of current cases, lower case letters denote flows (during day t). Script letters denote subgroups of individuals in the population.

Consider a given population \mathcal{P} (which may be a specific sub-population of another population). A key group of interest in the population is the group of all currently infected individuals, called \mathcal{X}_t , of which there are (at the end of day t) X_t . The increment during day t is $\Delta X_t = X_t - X_{t-1}$. The size of the inflow into \mathcal{X}_t (the new infections on day t) is n_t . Note that, despite the common use of language in the media or politics, neither X_t nor ΔX_t nor n_t are observable or appear in any of the official statistics.

In order to define the subgroups of \mathcal{X}_t that are relevant for policy, we consider two types of policy variables, testing and enforcement. With respect to the former, it is assumed that the population can be tested for the virus and that tests are correct.²³ Furthermore, to simplify the exposition and, in fact, as is

²²See Brauer (2008) or Allen (2017) for broader reviews.

²³In particular, in a situation in which only few people are infected (such as is currently the case with Covid-19), the test's specificity is a concern in general (false positives). Since the present model currently only considers infected individuals, this is less of a concern here.

the case in all somewhat functioning health systems, I assume that all severe cases are automatically tested and hospitalized, and that people only die from Covid-19 in hospital.²⁴

One of the most important policy variables for Covid-19 is testing. In line with the above model structure, we introduce this variable as the intensity with which patients with mild symptoms are tested. Figure 2 therefore generalizes the event tree of Figure 1 to include the outcomes “mild - no test” and “mild - test” after the outbreak date T^o , where the probability of testing, conditional on m , is the policy variable $\lambda \in [0, 1]$. This variable aggregates several components of a country’s testing policy, such as whether tests are mandatory for certain groups, for what groups (if any) they are covered by social insurance, the availability of testing stations and laboratories, etc. The higher λ , the more expensive is the testing policy. If an individual is not tested, she follows the branch leading to event T^s as discussed in the previous section. If tested, by construction she will be positive and will be put into quarantine.

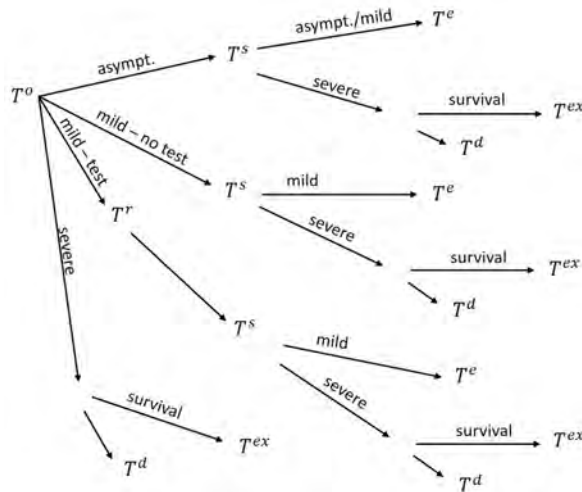


Figure 2: Evolution with testing

In the present model, testing and the resulting quarantine are inefficient along two dimensions. First, the test is carried out and its results are commu-

²⁴This assumption only simplifies the presentation. Under extreme stress, such as in Lombardy in March 2020, it is probably systematically violated, but deaths may occur in private homes in normal times. The assumption does not mean that all hospitalized cases receive the same treatment. In fact, the experience of spring 2020 has shown that the mortality rate in hospitals depends on the hospitalization rate and hospital capacity.

nicated and implemented with a time lag. This yields a new event in the event tree following the outbreak date T^o :

- $T^r = T^o + \tau^r$ (result): time until result communicated and implemented if tested.

In the first wave of the European pandemic in March to May 2020, testing capacity was quite restricted and τ^r largely exogenous. It had several additive components: (i) time until individual realizes that the symptoms are potentially problematic,²⁵ (ii) time until appointment with GP, (iii) time until tested,²⁶ (iv) time until test result. During the first wave, the delay can probably be described as random with most mass on

$$\tau^r \in [2, 5]. \tag{11}$$

The second inefficiency in the testing-quarantine policy is the degree to which it is being followed in the population. Once infected, there is little private benefit for egotistical individuals to obey quarantine orders or recommendations. Hence, incentives are unlikely to work in this case, which is a classical externality (see Garibaldi et al. 2020 for a broader analysis). We denote by $\nu \in [0, 1]$ the fraction of individuals who comply with quarantine. ν partially depends on the stringency, clarity and consistency of government health policy at all levels (this is to some extent costless, but requires good policy), and partly depends on resources invested in enforcement, which ranges from the staffing and equipment of local health offices to the amount of police deployed for enforcement. Again, higher ν comes at a higher cost.

The subgroups of \mathcal{X}_t of interest now are:

	Definition	Size	Increment
\mathcal{N}_t	newly infected on day t	n_t	
\mathcal{E}_t	early infections: not yet contagious	E_t	ΔE_t
\mathcal{Y}_t	contagious and not in quarantine or hospitalized	Y_t	ΔY_t
\mathcal{Q}_t	confirmed positive and in quarantine at home	Q_t	ΔQ_t
\mathcal{H}_t	confirmed positive and hospitalized	H_t	ΔH_t
	exits from \mathcal{Y}_t as no longer contagious		$\ell_t^{\mathcal{Y}}$
	exits from \mathcal{H}_t as no longer contagious		$\ell_t^{\mathcal{H}}$
	exits from \mathcal{Q}_t as no longer contagious		$\ell_t^{\mathcal{Q}}$
\mathcal{A}_t	confirmed currently infected	A_t	ΔA_t
	new confirmed infected	o_t	

Table 1: Sub-groups of \mathcal{X}_t

²⁵This time span was probably substantial in the early phases of the Corona wave and may even have exceeded τ^s in some cases. This has probably changed now. I therefore assume that $\tau^r \leq \tau^s$.

²⁶In Germany, during the first wave tests have been administered only after referral by the GP. This was different in other countries, without necessarily speeding up procedures.

These subgroups correspond to some of the “compartments”, into which infected individuals in epidemiological SEIR models are classified. In particular, \mathcal{E}_t corresponds to the “exposed” group E in SEIR. Unfortunately, in the context of Covid-19, most of these groups are not documented in official statistics. This includes the numbers of healed exits ℓ_t^H and ℓ_t^Q (from hospital or from home-quarantine), which are not officially documented in most countries.²⁷ The exits from undetected outbreaks, ℓ_t^Y , are of course unobservable. Hence, even the number of confirmed currently infected cases (A_t) and its daily change is not observable. That is very unfortunate, in particular as the number is sometimes publicly reported.²⁸

In addition to the above partition of \mathcal{X}_t two further sub-groups of the initial population are of interest: \mathcal{D}_t , the set of all dead, D_t in number, and \mathcal{C}_t , the set of all cured (recovered) individuals, numbering C_t . We have (suppressing time indices for convenience)

$$\Delta C_t = \ell^Y + \ell^Q + \ell^H$$

since \mathcal{C}_t is an absorbing set, which only has inflows.²⁹ For each transitory subgroup \mathcal{G} the net increment at date t is the difference between inflow i_t^G and outflow. If a group has several inflows then we let $i^{\mathcal{M}\mathcal{N}}$ denote the inflow from \mathcal{M} into \mathcal{N} . The flow accounting is as follows (where we suppress the time indices):

- $\Delta E = n - i^Y$
- $\Delta Y = i^Y - i^{YH} - i^{YQ} - \ell^Y$
- $\Delta Q = i^{YQ} - i^{QH} - \ell^Q$
- $\Delta H = i^{YH} + i^{QH} - \ell^H - \Delta D$

The outflows i^{YH} and i^{YQ} are in principle observable, but they don't seem to have been collected separately in most countries.³⁰ Publicly available (and widely reported) is the official number

$$o_t = i_t^{YH} + i_t^{YQ} \tag{12}$$

Summing the above 4 flow equations yields the total net flow equation

$$\begin{aligned} \Delta E + \Delta Y + \Delta Q + \Delta H &= n - \Delta D - \ell^Q - \ell^H - \ell^Y & (13) \\ &= n - \Delta D - \Delta C & (14) \end{aligned}$$

²⁷For Germany, see the official website of the Robert-Koch Institut on 25 March 25, at https://www.rki.de/DE/Content/InfAZ/N/Neuartiges_Coronavirus/Situationsberichte/2020-03-25-en.pdf?__blob=publicationFile.

The RKI has begun reporting estimates of recovered cases in early April, see https://www.rki.de/DE/Content/InfAZ/N/Neuartiges_Coronavirus/Situationsberichte/2020-04-08-en.pdf?__blob=publicationFile

There are many other estimates, and it is not clear how reliable they are for scientific work.

²⁸E.g., on <https://www.worldometers.info/coronavirus/#countries>

²⁹Or so we hope.

³⁰But unfortunately, simply aggregating total hospital admissions with positive test results is not sufficient. One needs days of first symptoms.

We have the following fundamental counting relations for total infections (using (13)):

$$X_t = E_t + Y_t + H_t + Q_t \quad (15)$$

$$\Delta X_t = n_t - \Delta D_t - \Delta C_t \quad (16)$$

Hence, if (16) is positive, the number of infected increases ($\Delta X_t > 0$); if it is negative it decreases. Unfortunately, except for ΔD_t , none of these variables is observed, either because of intrinsic difficulties or because of administrative overload.

4 Transmission Dynamics

If there are no nosocomial infections, new infections depend on the uncontrolled contagious population \mathcal{Y}_t and the transmission rate(s). Under standard assumptions,³¹ the basic SEIR model of epidemiology predicts transmission to occur according to the following system of difference equations:

$$S_t = S_{t-1} - \beta S_{t-1} I_{t-1} \quad (17)$$

$$E_t = E_{t-1} + \beta S_{t-1} I_{t-1} - \rho E_{t-1} \quad (18)$$

$$I_t = I_{t-1} + \rho E_{t-1} - \gamma I_{t-1} \quad (19)$$

$$R_t = R_{t-1} + \gamma I_{t-1} \quad (20)$$

where S_t is the number of all susceptible, I_t that of all infectious, R_t the number of all removed individuals, $\beta > 0$ is the disease transmission rate, $\rho > 0$ the transition rate from the exposed to the infectious state, and $\gamma > 0$ that from the infectious to the removed state ("removed" includes the cured C_t and the dead D_t - from the perspective of disease dynamics all that matters is that they are removed from the transmission activity).

This model and its many refinements are the standard workhorse for the analysis of disease dynamics, but it is not ideal for the analysis of health policy towards Covid-19 for at least three reasons. First, even if one assumes that the population mixes homogeneously, transmission depends on the composition of the infectious group, which we have called \mathcal{Y}_t , because it is more intricate than the simple " I_t " of the standard model. Second, the size of the sub-populations of \mathcal{Y}_t is affected directly by policy intervention, such as testing and quarantining, and this can and should be modelled. And third, as discussed in Section 2, the transition between the different health "compartments" \mathcal{E}_t , \mathcal{Y}_t , etc. almost certainly does not follow the geometric distribution assumed in (17) - (20). The most important impediment for effective health policy is, of course, that the

³¹These include: perfect mixing of the population, no demographic changes (no births and exogenous deaths), no aggregate uncertainty, immunity after recovery, and so-called mass incidence (which seems to be a better description of Covid-19 than the so-called standard incidence that is more relevant for sexually transmitted diseases). See, e.g., Brauer (2008) or Allen (2017).

group of infectious but not isolated cases (\mathcal{Y}_t) is unobservable. Hence, the two basic pillars in the fight against Covid-19, which are (ex-post) testing and (ex-ante) social distancing. As discussed in the introduction, this paper concentrates on the ex-post dimension.

We therefore take the transmission rate as exogenous and simply let $\beta(k)$ denote the average daily transmission rate per active person on day $k \geq 0$ after infection.³² It is likely that the transmission rate is age-specific. Furthermore, Ferguson et al. (2020) assume that it differs between asymptomatic and symptomatic cases.³³ This could easily be incorporated into this model by distinguishing between β^a and β^m . In line with the basic structure of the SEIR model discussed above, the current empirical evidence reviewed in Section 2 suggests that $\beta(k) = 0$ for k small.

Overall, it seems difficult to estimate transmission rates from population data, because neither n_t nor Y_t , let alone its composition, are observable. Even observations from natural experiments, such as the cruise ship *Diamond Princess*, are difficult to interpret, as transmission onboard was massively interrupted from the early days of the outbreak on because (i) all confirmed infected cases were continuously evacuated and (ii) passengers (not crew members) were quarantined (but not fully isolated).³⁴

However, focussing on the ex-post dimension of the dynamics, while taking β as given, one can make predictions about the inflow of new infections, n_t . Conceptually, n_t is a random variable with a probability distribution $f_t | \mathcal{Y}_{t-1}$ on \mathbb{N}_0 . If we limit our attention to average new infections, the associated transmission dynamics is governed by

$$E [n_t | \mathcal{Y}_{t-1}] = S_{t-1} \sum_{k=1}^t \beta(k) |\mathcal{N}_{t-k} \cap \mathcal{Y}_{t-1}| \tag{21}$$

where $|\mathcal{Z}|$ denotes the size (number of elements) of a set \mathcal{Z} . (21) states that at the end of day $t - 1$, the expected number of new infections on day t is equal to the sum, over all previous days $t - k$, of the number of infections caused by the members that were infected in $t - k$ and are still infectious and not hospitalized or home-isolated at the end of day $t - 1$. Note that (21) is a generalization of (18)-(19) to the case where not only the size but also the composition of \mathcal{Y}_{t-1} matters. In fact, (21) describes an expectation of day t conditional on the full state of infections in $t - 1$. In this sense (21) would in principle be useful for

³²Potentially, there are at least two ingredients going into the construction of the individual transmission rate. First, the degree of biological individual infectivity (i.e., the viral load spread per day), which has a distribution over the time interval $[T^c, T^n]$, as described previously. Second, transmission depends on individual behavior, which in turn depends on personal traits, incentives, policy, and social rules (see, e.g., Blackwood and Childs (2018), Brotherhood et al. (2020), and Garibaldi et al. (2020)). $\beta(k)$ compounds these two dimensions into one single number, describing the average infectivity per cohort member k days after infection.

³³The assumption being that symptomatic cases are 50 % more infectious than asymptomatic ones. For evidence, see, e.g., Lavezzo et al. (2020).

³⁴See Government of Japan, Ministry of Health, Labour and Welfare, at <https://www.niid.go.jp/niid/en/2019-ncov-e/9407-covid-dp-fe-01.html>

daily forecasting, if the information about \mathcal{Y}_{t-1} were known in $t - 1$ (which it is not).

If we want to derive an ex ante law of motion similar to (17) - (20), we must use the expected composition of \mathcal{Y}_{t-1} . Given the structure described in Section 3, for each cohort \mathcal{N}_t the duration in \mathcal{Y} is of different length for the different branches of the event tree in Figure 2:

sub-group	path	cond. probability at T_o	end time
\mathcal{Y}^c	between T^c and T^o		T^o
\mathcal{Y}^{am}	a , then a/m	$\theta_a(1 - \theta_{sl})$	T^e
\mathcal{Y}^{as}	a , then s	$\theta_a\theta_{sl}$	T^s
\mathcal{Y}^{mNQm}	m , not in quarantine, then m	$(1 - \lambda\nu)\theta_m(1 - \theta_{sl})$	T^e
\mathcal{Y}^{mNQs}	m , not in quarantine, then s	$(1 - \lambda\nu)\theta_m\theta_{sl}$	T^s
\mathcal{Y}^{mQ}	m , tested, in quarantine	$\lambda\nu\theta_m$	T^r

Table 2: Sub-groups of \mathcal{Y}_t

Here, sub-groups \mathcal{Y}^{mNQm} and \mathcal{Y}^{mNQs} consist of individuals with initially mild symptoms who are either not tested or tested and do not obey quarantine rules. Sub-group \mathcal{Y}^{mQ} consists of individuals who are tested upon mild symptoms and stay quarantined. These latter individuals do not transmit after T^r anymore because regardless of whether they develop severe symptoms later or not, they remain isolated.

By construction,

$$\mathcal{Y} = \bigcup_{j \in \{c, am, as, mNQm, mNQs, mQ\}} \mathcal{Y}^j$$

Using the distributions of the evolution of single cohorts introduced in Section 2, the transmission equation (21) becomes

$$E[n_t | \mathcal{Y}_{t-1}] = S_{t-1} \sum_{k=1}^t \beta(k) w(k) n_{t-k} \tag{22}$$

where the ‘‘cohort composition kernel’’ is given by

$$w(k) = \Pr(T^c \leq k - 1 < T^o) \tag{23}$$

$$+ \lambda\nu\theta_m \Pr(T^o \leq k - 1 < T^r) \tag{24}$$

$$+ [\theta_a + (1 - \lambda\nu)\theta_m]\theta_{sl} \Pr(T^o \leq k - 1 < T^s) \tag{25}$$

$$+ [\theta_a + (1 - \lambda\nu)\theta_m](1 - \theta_{sl}) \Pr(T^o \leq k - 1 < T^e) \tag{26}$$

Here the first term of the sum gives the fraction of cohort n_{t-k} that at the end of day $k - 1$ is contagious without having developed symptoms yet (the ‘‘pre-symptomatic transmitters’’), the second term the fraction of mildly

symptomatic cases that are tested and will be follow home-quarantine once the test result is available, the third the fraction with no or mild symptoms that have not been tested or have been tested but do not self-quarantine, and develop severe symptoms later (the “short-term stealth transmitters”), and the fourth the fraction with no or mild symptoms that have not been tested or have been tested but do not self-quarantine, and that do not develop severe symptoms (the “long-term stealth transmitters”).

Note that the $w(k)$ do not sum to 1. They describe the size of subgroups of cohorts that are not necessarily distinct as they evolve over time; being fractions, they are bounded by 1 for each k and not more. They depend on the interaction of policy and the different durations in (23)-(26). This latter fact is different from the basic recursive SIR model, in which the $w(k)$ simply decrease exponentially, driven by the uniform removal rate from the infectious population, and from its compartmental generalization (17) - (20), where two such exponential decreases are folded into each other.

The cohort composition kernel describes how the group of currently infectious individuals can be constructed from the infections of previous cohorts. In particular, it describes how past policy interventions, such as a change in testing intensity or test evaluation speed, affect the currently infected population, and thus, by (22), current infections. The analysis shows that the two ex-post policy tools of testing and quarantining are complements: the higher the level of one of these variables, the more effective is an increase of the other. For the calibration presented in the following section we therefore only need to consider their product, $\lambda\nu$.

5 A Simple Calibration

To illustrate the dynamics derived above, this section extends the simple parametric calibration of Section 2. The basic assumptions are in lign with the preliminary medical evidence presented in Section 2 and so are the derived distributions, as far as this can be judged from this evidence. But the calibration is not statistically optimized and the example meant to be illustrative rather than descriptive.

Continuing the description of Section 2, the building blocks of the model are the distributions

- p^c for the onset of contagiousness T^c ,
- π^{co} for the time τ^o between T^c and the time of first symptoms T^o
- π^{or} for the time τ^r between T^o and the start of quarantine on day T^r , if any
- π^{os} for the time τ^s between T^o and onset of severe symptoms on day T^s , if any

- π^{oe} for the time τ^e between T^o and the end of infectivity on day T^e , if no severe symptoms

The cohort composition kernel w takes the following form:

$$w(k) = p_{k-1}^{co} + \lambda\nu\theta_m p_{k-1}^{or} + [\theta_a + (1-\lambda\nu)\theta_m](1-\theta_{sl})p_{k-1}^{oe} + [\theta_a + (1-\lambda\nu)\theta_m]\theta_{sl}p_{k-1}^{os} \tag{27}$$

where

	Time	Group	Status
p_k^{co}	$= \Pr(T^c \leq k < T^o)$	\mathcal{Y}^c	pre-symptomatic stealth transmitters
p_k^{or}	$= \Pr(T^o \leq k < T^r)$	\mathcal{Y}^{mQ}	tested after mild symptoms, but not quarantined yet
p_k^{oe}	$= \Pr(T^o \leq k < T^e)$	$\mathcal{Y}^{am}, \mathcal{Y}^{mNQm}$	long-term stealth transmitters
p_k^{os}	$= \Pr(T^o \leq k < T^s)$	$\mathcal{Y}^{as}, \mathcal{Y}^{mNQs}$	short-term stealth transmitters

Remember that these probabilities do not sum to 1 because of double counting.

Continuing with the example of Section 2, the distributions of T^c and τ^o have been defined in (9) and (10), respectively. For π^{or} we assume that it takes 3 days for the test to be taken, the result to be established and quarantine to begin. Hence, the delay τ^r has a point distribution with mass $\bar{\pi}_3^{or} = 1$ and $\bar{\pi}_k^{or} = 0$ for all $k \neq 3$.³⁵ Concerning π^{os} , the available evidence seems to be summarized adequately by the following probability mass function for the distribution of τ^s :

$k :$	0	1	2	3	4	5	6	7	8	9	10
$\bar{\pi}_k^{os} :$	0	0	0	0.1	0.1	0.1	0.2	0.2	0.1	0.1	0.1

(28)

Hence, on average patients with initially no or mild symptoms develop severe symptoms 6.5 days after incubation with a symmetric distribution around this mean. Finally, we assume that the infectivity of the "long-term stealth transmitters" is distributed as follows:

$k :$	0	1	2	3	4	5	6	7	8	9	10
$\bar{\pi}_k^{oe} :$	0	0	0	0	0	0.1	0.2	0.2	0.2	0.2	0.1

(29)

Hence, this group stops being infectious between day 5 to 10 after the outbreak with mean and median at day 7.5, but with no discernible time structure between days 6 and 9. Again, this is consistent with the evidence discussed in Section 2.

In order to calculate the cohort composition kernel w in (27), we have already calculated the distribution of the length of the incubation period T^o from (7) and plotted it in Figure 4. The figure shows that in the example, more than 80 per cent of all outbreaks occur 3 - 7 days after infection.³⁶

³⁵On average, this is consistent with media coverage in Europe in March to May when testing capacity was scarce, practices not yet established, and patients not used to preventive self-quarantine.

³⁶Again: remember that T^o is imputed if a case is completely asymptomatic. Hence, the date T^o is defined for each cohort member.

Now an application of (8) yields the first term of the cohort composition kernel. It is plotted in Figure 5. Turning to the second term, the cohort fractions p_k^{or} are plotted in Figure 6. The shares (ex-ante probabilities) of long-term and short-term "stealth transmitters" are shown in Figures 7 and 8, respectively. Clearly, these shares are very high (above 60%) between 5 and 11 days after the infection for the long-term stealth transmitters and between 5 and 10 days for the short-term ones.

To illustrate the impact of the composition of \mathcal{Y}_{t-1} on En_t given by (22) in our example, let us assume that the average individual transmission rate $\beta(k)$ is constant over the course of the individual infection, just as in the basic SEIR model. As noted in Section 4, this is quite certainly not correct, but it helps to make the point.

Consider the following baseline scenario:

$$\begin{aligned}\theta_m &= 0.7, \theta_s = 0.01, \theta_{sl} = 0.06 \\ \lambda\nu &= 0.1\end{aligned}$$

In this scenario, 70 per cent of all infected cases develop mild symptoms at the time of the (potentially unobserved) outbreak, 29 per cent are asymptomatic, and the conditional probability of developing severe symptoms after initially no or mild symptoms is 6 per cent. More than 10 per cent of all mild cases are tested, depending on how strictly self-quarantining rules are observed (under perfect self-quarantining, $\lambda = 0.1$). Given the lack of data on the evolution of \mathcal{Y}_t , it is difficult to translate these percentages into observables, but at least the values of θ_a and θ_m are consistent with what we seem to know from the natural experiments and large-scale surveys discussed above.³⁷ Since testing in the present model refers to all mild Covid-19 infections and their number is unobservable, the test rate λ is not documented in official statistics and must be estimated by Bayes' Law from imperfect existing data.³⁸ By back-of-the-envelope estimates, 10 per cent is in the ball park for λ during the first wave of the pandemic in Europe.

The time structure of the cohort composition kernel w for this scenario is given by the grey bars in Figure 3. Almost 90 per cent of the total mass lies between days 5 and 12, and less than 1 per cent after day 15. Hence, policies affecting new infections will show very little effect in the first 5 days, and one will have to wait for almost 2 weeks after infection to see most of the impact. This is very different from the case of exponential growth in which much more mass is concentrated on the early days.³⁹

³⁷Remember that our analysis refers to all infections, not just the detected ones reported officially.

³⁸See Peracchi and Terlizze (2020) for a careful attempt at disentangling Italian data this way.

³⁹However, different from some current very conservative scenarios, one would need to self-quarantine for less than 2 weeks after incubation to reduce transmission risks below 1 per cent.

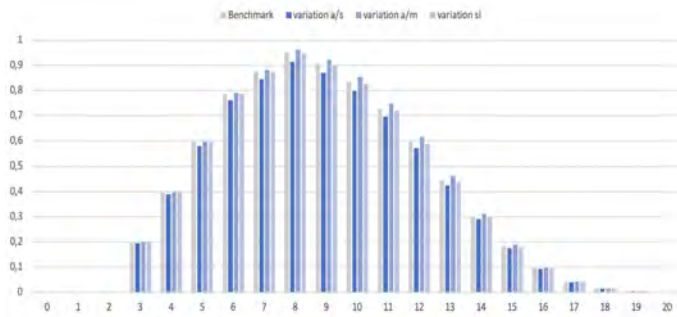


Figure 3: The Cohort Composition Kernel

This picture changes little for alternative scenarios, where we vary the crucial infection parameters quite substantially and keep $\lambda\nu$ unchanged:

variation a/s:	$\theta_m = 0.7$	$\theta_s = 0.05$	$\theta_{sl} = 0.06$
variation a/m:	$\theta_m = 0.4$	$\theta_s = 0.01$	$\theta_{sl} = 0.06$
variation sl:	$\theta_m = 0.7$	$\theta_s = 0.01$	$\theta_{sl} = 0.06$

The finding that all four scenarios differ only little is interesting because the fraction of asymptomatic patients, θ_a , and of mildly symptomatic patients is difficult to estimate and not yet well understood.

Another set of scenarios varies the testing/compliance parameters from $\lambda\nu = 0.1$ to values of 0.05, 0.2, and 0.3. As documented in Figure 9 in the appendix, these variations change the picture by 10 to 20 per cent if one expands testing dramatically (to $\lambda\nu = 0.3$). More importantly, the analytical expression for the cohort composition kernel w in (27) makes it possible to quantify this effect. This is important because the gain in lives and treatment costs brought about by the mitigation of the transmission activity can now be compared to the considerable monetary and non-monetary costs of expanding the testing capacity.

In a next step, the improved transmission dynamic (22) can be integrated in dynamic economic models. We need better data and a more granular model to do these estimates reliably, but first simulations already suggest that these modified SEIR dynamics react non-trivially to policy interventions in the cohort composition kernel.

6 Conclusions

We currently know far too little about the epidemic. While the empirical evidence on small samples of patients or from unplanned natural experiments is rising rapidly, aggregate data are very problematic. Hardly any of the basic

numbers in the fundamental counting relation (15) is known. The model of this paper is one step in understanding and using the available data better by focussing on the composition of the group of unobserved infectious individuals, which is driving the current pandemic. Better data can be obtained from large-scale public testing, but will also require the intelligent use of selective random tests. To organize and interpret such data collection, it is important to understand the underlying structure of the population and its dynamics. The research described in this paper may help on both these fronts: understanding the available data and organizing the collection of new data. And even without new data, new statistics of the transmission process such as the cohort composition kernel introduced in this paper are able to help with more precise forecasts, e.g., for quarantine times, as shown in Section 5.

Testing is important, but the question is what testing. In the early stage of an epidemic, mass testing is likely to be very expensive and relatively uninformative, since outbreaks are random and so are observed clusters. But controlled mass testing of specific populations can be very useful to identify key theoretical parameters, such as the θ_z in the above model. As the model has shown, such tests must control carefully for the timing of interventions, for example to be able to distinguish asymptomatic cases from pre-symptomatic ones. Given the great uncertainty and the different needs and views with respect to policy, it is now the time for controlled experiments.

7 References

- Allen, L.J.S. (2017), "A primer on stochastic epidemic models: Formulation, numerical simulation, and analysis," *Infectious Disease Modeling* 2 (2), 128-142.
- Atkeson, A. (2020), "What will be the economic impact of COVID-19 in the US? Rough estimates of disease scenarios," NBER Working Paper 26867, March 2020.
- Blackwood, J. and L. Childs (2018), "An introduction to compartmental modeling for the budding infectious disease modeler," *Letters in Biomathematics* 5, 195-221.
- Böhmer, M., U. Buchholz et al. (2020), "Outbreak of COVID-19 in Germany resulting from a single, travel-associated primary case," SSRN preprint 31/3/2020.
- Brotherhood, L., Ph. Kircher, C. Santos, M. Tertilt (2020), "An economic model of the Covid-19 epidemic: The importance of testing and age-specific policies", Working Paper, University of Mannheim.
- Brauer, F. (2008), "Compartmental models in epidemiology," in F. Brauer, P. van den Driessche, J. Wu (eds.), *Mathematical Epidemiology*, Springer Mathematical Biosciences 1945, Heidelberg 2008, 19-79.

- Braun, M. (1978), *Differential equations and their applications*, 2nd ed., Springer.
- Byambasuren, O. (2020), "Estimating the extent of true asymptomatic COVID-19 and its potential for community transmission: systematic review and meta-analysis," medRxiv. June 04, 2020: 2020.05.21.20108746.
- Dehning, J. et al. (2020), "Inferring change points in the spread of Covid-19 reveals the effectiveness of interventions," *Science* 369, DOI: 10.1126/science.abb9789, published online May 15, 2020.
- Eichenbaum, M., S. Rebelo, and M. Trabant (2020), "The macroeconomics of epidemics," NBER Working Paper 26882, March 2020.
- Ferguson N., D. Cummings, et al. (2005), "Strategies for mitigating an emerging influenza pandemic in Southeast Asia," *Nature* 437(7056), 209-214.
- Ferguson, N. et al. (2020), "Impact of non-pharmaceutical interventions (NPIs) to reduce COVID-19 mortality and healthcare demand," manuscript, Imperial College, March 16, 2020.
- Giagheddu, M. A. Papetti (2020), "The Macroeconomics of Age-Varying Epidemics", SSRN at https://papers.ssrn.com/sol3/papers.cfm?abstract_id=3651251.
- He, X., E. Lau, G. Leung et al. (2020), "Temporal dynamics in viral shedding and transmissibility of COVID-19," *Nature Medicine* forthcoming, MedRxiv, 18/3/2020.
- Huang, C., Y. Wang, X. Li et al. (2020), "Clinical features of patients infected with 2019 novel coronavirus in Wuhan, China," *Lancet*, published online 24/1/2020.
- Kermack, W. and A. McKendrick (1927), "Contributions to the mathematical theory of epidemics," *Proceedings Roy. Stat. Soc.*, A 115, 700-721.
- Kimball, A., et al. (2020), "Asymptomatic and Presymptomatic SARS-CoV-2 Infections in Residents of a Long-Term Care Skilled Nursing Facility — King County, Washington," MMWR Morbidity and mortality weekly report 2020; ePub: 27 March 2020.
- Koh, W. C., L. Naing, et al. (2020), "What do we know about SARS-CoV-2 transmission? A systematic review and meta-analysis of the secondary attack rate, serial interval, and asymptomatic infection," medRxiv 2020:2020.05.21.20108746, May 23, 2020.
- Lauer, S.A., et al (2020), "The Incubation Period of Coronavirus Disease 2019 (COVID-19) from Publicly Reported Confirmed Cases: Estimation and Application," *Annals of Internal Medicine*, 5 May 2020, <https://www.acpjournals.org/doi/10.7326/M20-0504>.
- Lavezzo, E. et al. (2020), "Suppression of COVID-19 outbreak in the municipality of Vo', Italy," medRxiv doi.org./10.1101/2020.04.17.20053157, 18/4/2020.
- Peracchi, F. and D. Terlizze (2020), "Estimating the prevalence of the Covid-19 infection, with an application to Italy," *Covid Economics* 43, 19-41.

- Robert Koch Institut (2020), *Epidemiologisches Bulletin*, Various Issues, at <https://www.rki.de/DE/Content/Infekt/EpidBull/Archiv/2020/>
- T.W. Russel et al. (2020), "Estimating the infection and case fatality ratio for COVID-19 using age-adjusted data from the outbreak on the Diamond Princess cruise ship," *MedRxiv* 05/03/2020.
- Stock, J.H. (2020), "Data gaps and the policy response to the novel coronavirus", *Covid Economics* 3, 10/4/2020.
- To, K., O. Tsang, W. Leung et al. (2020), "Temporal profiles of viral load in posterior oropharyngeal saliva samples and serum antibody responses during infection by SARS-CoV-2: an observational cohort study", *Lancet Infect Dis*, published online March 23, 2020.
- Verity, R., Okell, L. Dorigatti, I. et al. (2020), "Estimates of the severity of coronavirus disease 2019: a model-based analysis," *Lancet Infect Dis*, published online March 30, 2020 (MedArxiv, 09/03/2020).
- Wang, F. et al. (2020), "The timeline and risk factors of clinical progression of COVID-19 in Shenzhen, China," *Journal of Translational Medicine* (2020) 18:270
- Wölfel, R., V. Corman, W. Guggemos et al. (2020), "Clinical presentation and virological assessment of hospitalized cases of coronavirus disease 2019 in a travel-associated transmission cluster", *MedRxiv* 8/3/20, *Nature*, forthcoming.
- Wu, Z., J. McGoogan (2020), "Characteristics of and Important Lessons From the Coronavirus Disease 2019 (COVID-19) Outbreak in China", *Journal of the American Medical Association*, 24/2/2020.
- Zhou, F., T. Yu, R. Du et al. (2020), "Clinical course and risk factors for mortality of adult inpatients with COVID-19 in Wuhan, China: a retrospective cohort study," *Lancet* 28/03/2020.

Appendix: Graphs

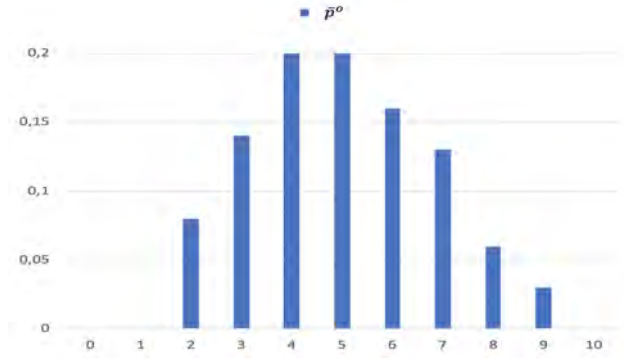


Figure 4: The distribution of T^o

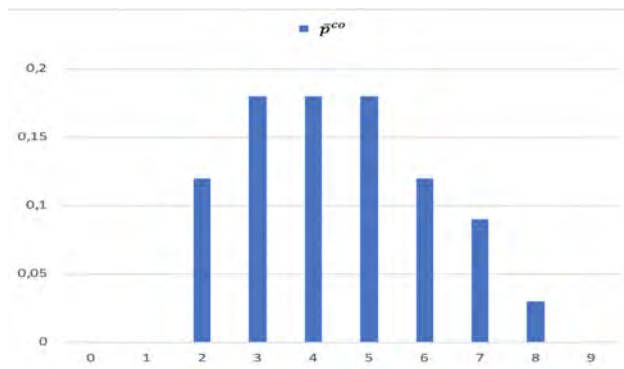


Figure 5: From T^c to T^o

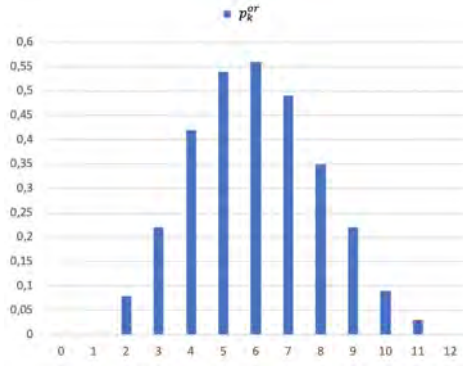


Figure 6: From T^o to T^r

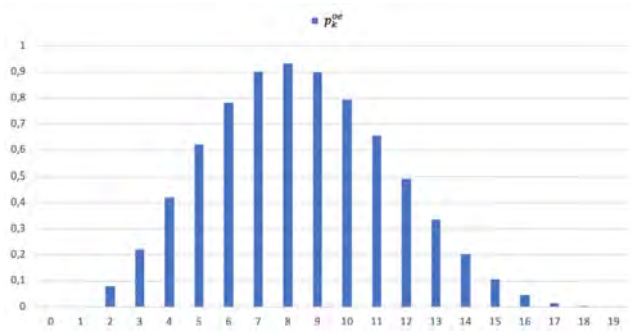


Figure 7: From T^o to T^e

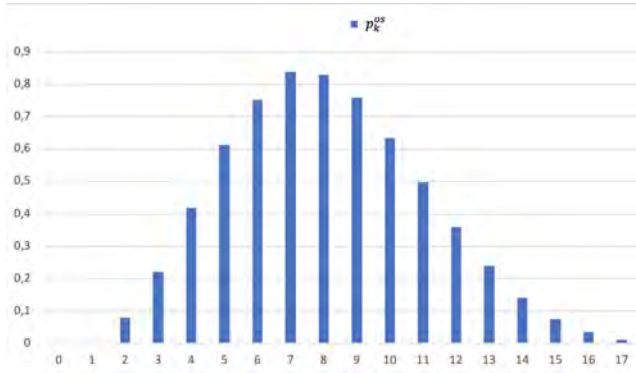


Figure 8: From T^o to T^s

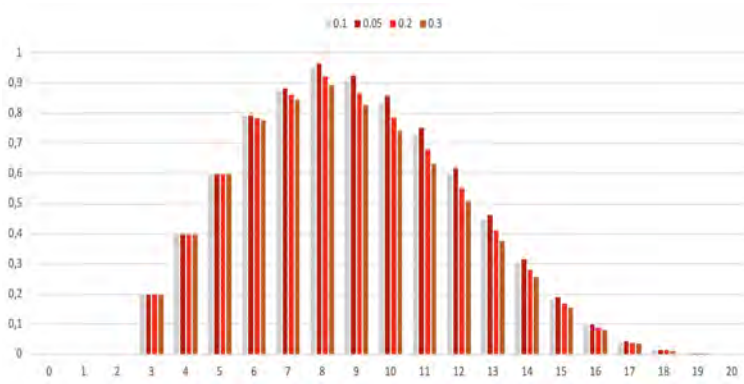


Figure 9: The Cohort Composition Kernel - Variations of $\lambda\nu$

The risk of being a fallen angel and the corporate dash for cash in the midst of COVID

Viral V. Acharya¹ and Sascha Steffen²

Date submitted: 21 April 2020; Date accepted: 21 April 2020

As a response to the COVID-19 pandemic, governments globally closed down major parts of their economies potentially plunging a vast majority of their firms into a liquidity crisis. Using a novel dataset of daily credit line drawdowns at the firm-loan-level, we study in a descriptive exercise the resulting “dash for cash” among firms and how the stock market priced firms differentially based on liquidity. In particular, we show that the U.S. stock market rewarded firms with access to liquidity through either cash or committed lines of credit from banks. AAA-A-rated firms, i.e., high-quality investment-grade firms, issued bonds in public capital markets, particularly after the Federal Reserve Bank initiated its corporate bond buying program. In contrast, bond issuances of BBB-rated firms, i.e., the lowest-rated investment-grade firms, remained mostly flat; instead, these firms rushed to convert their credit line commitments from banks into cash accounting for about half of all the credit line drawdowns. We document that consistent with the risk of becoming a fallen angel, this “dash for cash” has been driven by the lowest-quality BBB-rated firms. The risk of such precautionary drawdowns of credit lines remains an important consideration for stress-test based assessments of banking sector capital adequacy.

1 C.V. Starr Professor of Economics, New York University Stern School of Business.

2 Professor of Finance, Frankfurt School of Finance & Management.

Introduction

The COVID-19 pandemic had an immediate impact on the global economy as governments have undertaken drastic lockdown steps to contain the spread of the virus. The resulting economic standstill has affected the corporate sector adversely, as firms' cash flows in the near term are anticipated to drop as much as 100%, while other fixed costs (including paying workers, rents and servicing debt) – operating and financial leverage – remain sticky. In particular, firms in industries such as retail, hotel and travel have experienced an immediate drop in cash flows and thus have an unusual high demand for liquidity during the economic shutdown. However, other firms also appear to be scrambling for liquidity because of the high uncertainty as to when and how much economic activity might recover.

Faced with this liquidity stress, firms that have secured access to different sources of liquidity before the crisis should on average have an advantage over firms lacking in such access. To investigate this issue empirically, we first study whether the U.S. stock markets differentially rewarded firms with access to liquidity. Then, we analyze which firms have been able to raise liquidity through outside funding sources (e.g., the bond market) and which firms decided to convert committed credit lines from banks into cash using a novel dataset of daily credit line drawdowns at the firm-loan-level. How did the initial interventions from the Federal Reserve Bank and the U.S. Treasury affect the possible “dash for cash”?³

Importantly, over the last decade, the outstanding debt of particularly low investment-grade firms, *i.e.* BBB-rated firms, has quadrupled, and a case has been made that a large percentage of these firms might actually be of worse quality – similar to non-investment grade or “junk” firms (Altman, 2020). Do these lowest-quality investment-grade firms, in an attempt to avoid the “cliff risk” of a possible downgrade to junk grade status and the associated acceleration of borrowing costs, increase their cash holdings by drawing down their credit lines? Finally, we draw capital and liquidity implications of this cliff risk for exposed banks, focusing on the energy sector that has been adversely impacted by oil price crash during the pandemic.

Are firms rewarded for having more access to liquidity?

We first investigate whether firms benefit from access to liquidity during the COVID-19 crisis using stock market data. If the access to (committed) sources of liquidity helps firms weather better the unexpected shock of the crisis, then stock prices should reflect this and the stock price performance should be better of those firms that have secured ex-ante access to liquidity. We collect data for all publicly listed firms in the U.S. as of Q4: 2019 from the Capital IQ database, drop those with total assets below USD 100 million, and keep all firms that we can match to CRSP/Compustat.

Firms have access to liquidity through two main sources (without issuing new bonds, loans or commercial paper in the spot market):

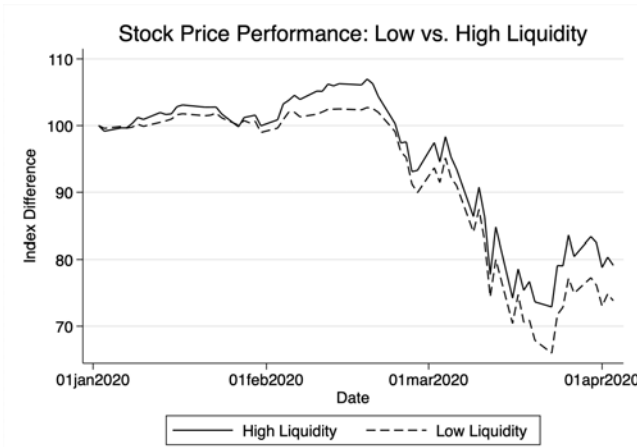
- *Unused Credit Lines*: The sum of undrawn revolvers, undrawn credit lines as backup for commercial paper, and undrawn term loans.
- *Cash and Short-Term Investments*: The sum of cash and short-term investments.

³ Platt et al. used this term recently in their article in the Financial Times ([“Dash for cash: companies draw \\$124bn from credit lines”](#)) on March 25, 2020.

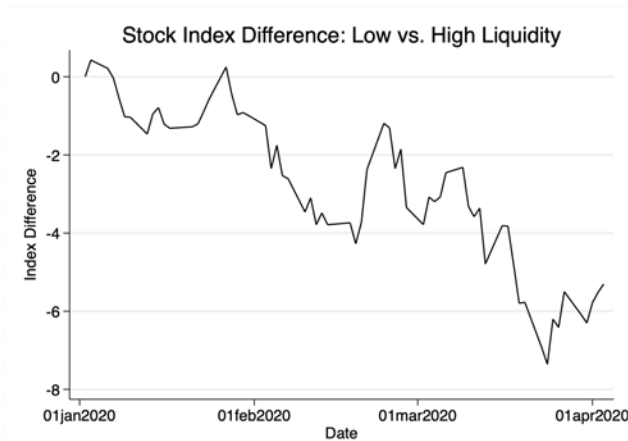
Hence, we construct a comprehensive measure of firm liquidity as:

$$Liquidity = \frac{Unused\ credit\ lines + cash\ and\ short\ term\ investments - short\ term\ debt}{Total\ assets}$$

where *Short-term debt* is the current portion of debt. Using a median split based on *Liquidity*, we classify firms as having high or low access to liquidity. We create a stock index for each subsample of firms indexed at Jan 2, 2020 using their (market-value weighted) average stock returns and plot the stock price development for both types of firms in panel A of Figure 1. We also calculate the difference of the two indices, *i.e.*, low liquidity minus high liquidity indices, and plot the difference in panel B of Figure 1.



Panel A. Stocks of firms with low vs. high liquidity



Panel B. Stock price difference

Figure 1. Stock price performance of firm with high / low access to liquidity for the period 1 Jan 2020 – 9 April 2020

Covid Economics 10, 27 April 2020: 49-66

The stock price performance suggests that firms have been rewarded in the stock market during the recent stress episode for having access to liquidity through cash holdings and unused credit lines. While stock prices naturally decline on average across all firms, the market value of firms with more liquidity drops significantly less so, particularly when the COVID crisis accelerated and lockdowns had to be put in place in mid-March 2020.

How do firms raise liquidity during the COVID-19 crisis?

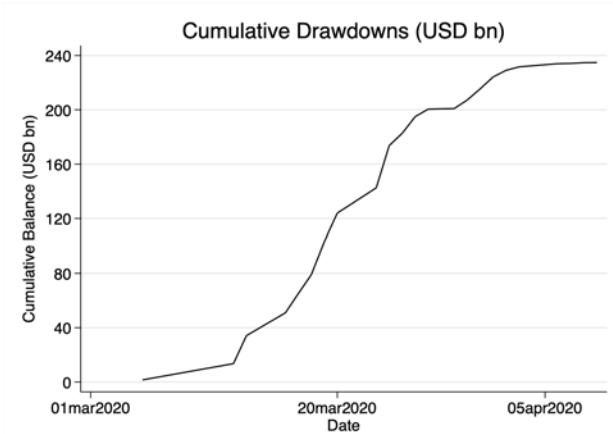
Evidence from credit lines usage

Having documented that lack of ex-ante access to liquidity has led to adverse stock market reaction for firms, we next use micro-level data to examine how this ex-ante risk might manifest during the COVID-19 crisis: Is there a dash for cash? If yes, how do firms raise cash? Do they draw down credit lines and/or issue bonds? And, are accelerated credit line drawdowns reflected in banks' stock prices?

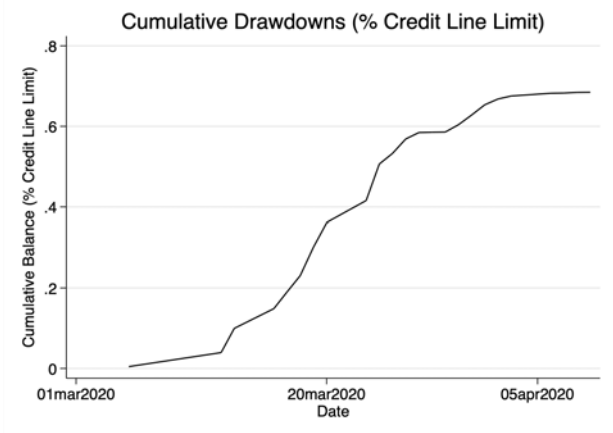
We combine several data sources that provide timely data to investigate these questions. S&P's Loan Commentary and Data (LCD) provides a novel dataset including daily updates on credit line drawdowns based on public company filings. LCD provide the drawn amount, the company rating, and the date as well as the agent bank on the original loan contract. In addition to undrawn credit line exposures at the end of 2019, Capital IQ also provides us the *Altman Z'Score* (referred henceforth simply as *Z-score*) as a measure of ex-ante credit risk of firms as well as other firm balance-sheet measures.⁴ We obtain bond issuance data from Dealogic.

Figure 2 shows the total cumulative drawdowns of credit lines since March 1, 2020. Panel A of Figure 2 shows the cumulative dollar amount of drawdowns and the panel B the cumulative drawdown percentage of the total credit line limit of those firms that have undertaken drawdowns during the period March 1, 2020 to April 9, 2020. As the figures reveal, credit line usage accelerated rather early during this stress period and became somewhat flat by the end of March 2020. Total drawdowns up to April 9, 2020 accumulate to more than USD 225 billion and close to 70% of the originally available credit line commitments.

⁴ The *Z'Score* is calculated as described in Altman (1986).



Panel A. Cumulative drawdowns (in USD bn)



Panel B. Drawdowns as % of credit limit

Figure 2. Cumulative drawdowns and drawdown percentage rate for the period 1 March 2020 – 9 April 2020

Figure 3 shows cumulative drawdowns of credit lines since March 1, 2020 for different rating classes, AAA-A (the high-quality investment grade), BBB (the lowest-quality investment grade), non-investment grade (NonIG) und unrated (NR) firms. The first companies to utilize their credit lines were NonIG and not-rated firms, which is reasonable given that these firms are likely to have had difficulties accessing other forms of credit once the crisis started. While the credit line usage of AAA-A rated and unrated firms is flat and does not exceed USD 20bn, NonIG and particularly BBB-rated firms have drawn down their credit lines at an accelerating rate.

Covid Economics 10, 27 April 2020: 49-66

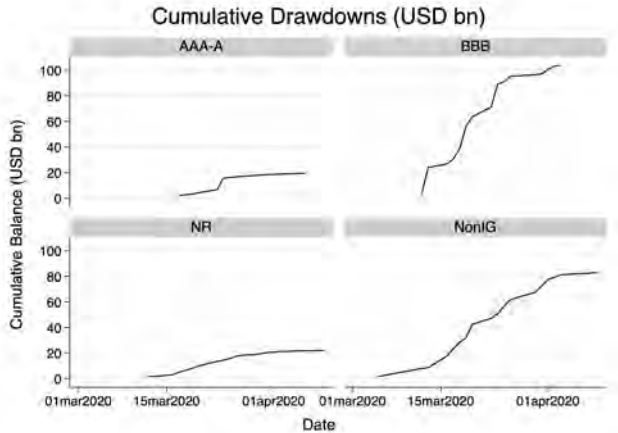
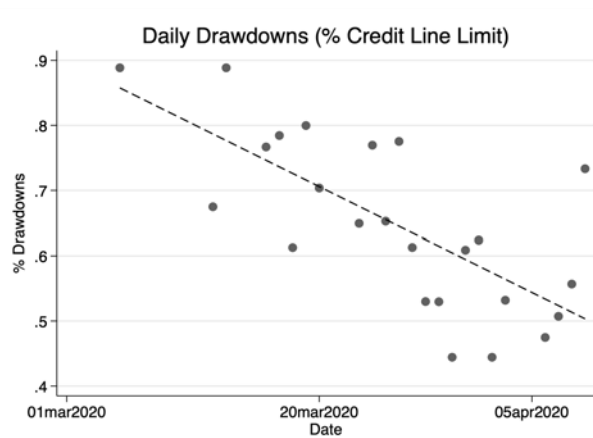


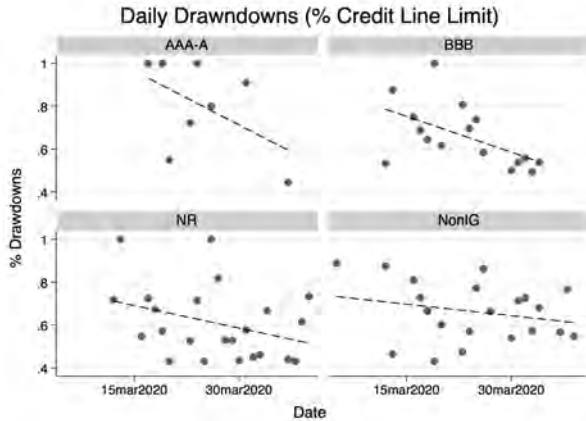
Figure 3. Cumulative drawdowns by rating class for the period 1 March 2020 – 9 April 2020

Figure 4 shows daily drawdown intensities (*i.e.*, daily borrowing amounts relative to a firm’s credit line limit on this day). Panel A of Figure 4 shows percentage drawdowns for the full sample of firms, panel B for each rating category. The full sample figure shows a significant decline in drawdown intensity, a result that extends broadly to all rating categories. That is, at the beginning of the crisis, arguably when uncertainty was at its peak, we observe a “run” on bank credit lines with firms almost fully using their credit lines. At the end of our sample period, daily credit line drawdowns are lower but still about 50% of the credit limit (conditional on firms borrowing).



Panel A. Daily drawdowns (all firms)

Covid Economics 10, 27 April 2020: 49-66



Panel B. Daily drawdowns (by rating category)

Figure 4. Daily percentage drawdowns by rating class for the period 1 March 2020 – 9 April 2020

How do these drawdowns compare to previous recession periods? In Acharya and Steffen (2020), we outline stress scenarios for banks with respect to expected credit line drawdowns. In one scenario, we use the end of 2008 (global financial crisis, *GFC* henceforth) drawdown rate, immediately after the failure of Lehman Brothers in September 2008. We use the GFC stress-scenario drawdown rates (which are based on end-of-2008 realized drawdowns) for different rating classes to calculate an expected volume of credit line drawdowns. We then compare this estimate to the actual US dollar amount of credit line drawdowns since the beginning of March 2020. Table 1 shows this comparison expressed in million USD.

	Unused Credit Lines	Expected Drawdown Rate (2008)	Expected Drawdowns	Actual Drawdowns	Difference	Actual Drawdown Rate
AAA-A	322,183	17.00%	54,771	19,372	-35,399	6.01%
BBB	449,817	23.80%	107,056	103,616	-3,441	23.04%
Non-IG	309,163	28.50%	88,111	82,345	-5,767	26.63%
Not Rated	162,725	39.20%	63,788	20,006	-43,783	12.29%
Total	1,243,888		313,727	225,338	-88,389	

Table 1: Expected versus actual drawdowns (in USD mn).

As we observed earlier in Figure 2, U.S. firms have drawn down USD 225bn from outstanding credit lines between March 1 and April 9. Out of this aggregate amount, the lion’s share of USD185bn (*i.e.*, more than 80%) was drawn by BBB and NonIG-rated firms. Interestingly, and comparing COVID-19 drawdowns to those observed during the GFC, we find that the credit line usage of BBB (about 23%) and Non-IG (about 27%) rated firms is similar to the GFC. However, and in contrast, AAA-A rated and unrated firms draw down much less, only about one-third of what we would have expected based on previous crisis episodes.⁵ In other words, banks’ loan portfolios have expanded by USD 185bn in borderline investment-grade and non-investment-grade debt since the beginning of March 2020.

⁵ AAA-A rated firms might use other forms of credit (e.g., bond issuances) to raise cash. Unrated firms, however, have limited external finance options. Either they have sufficient cash on balance sheet to decide not to use their liquidity insurance, or they raise cash through loan issuances in the loan market, or they rely on trade

To get a better understanding of the risks associated with the credit line usage, we use the Z-Score as a firm-specific measure of credit risk that allows us to compare the risk of default of firms within and across rating classes when they draw down credit lines. In other words, we want to study the relation between firm-specific credit-line usage and firm-specific default risk across rating categories on a specific day and over time within a rating class.

Figure 5 plots for each rating group on a given day the average across firms of credit-line drawdown intensities (left-hand scale) together with their Z-Score (right-hand scale).⁶ Somewhat surprisingly, unrated firms appear to be less risky than both BBB- and NonIG-rated firms. In all rating categories, firms that drew down credit lines early had lower Z-Scores, *i.e.*, higher default risk. The average quality of borrowers improves over time, possibly because the riskiest firms have already used their outstanding credit lines. Importantly, those firms that continue to use their credit lines towards the end of the sample period, appear to be, on average, riskier, when high-quality firms might have been able to issue bonds in public capital markets, an issue we investigate next.

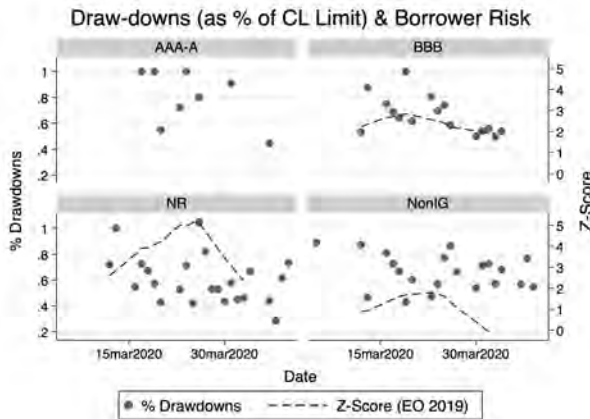


Figure 5. Drawdowns and borrower risk by rating class for the period 1 March 2020 – 9 April 2020

Who issues bonds?

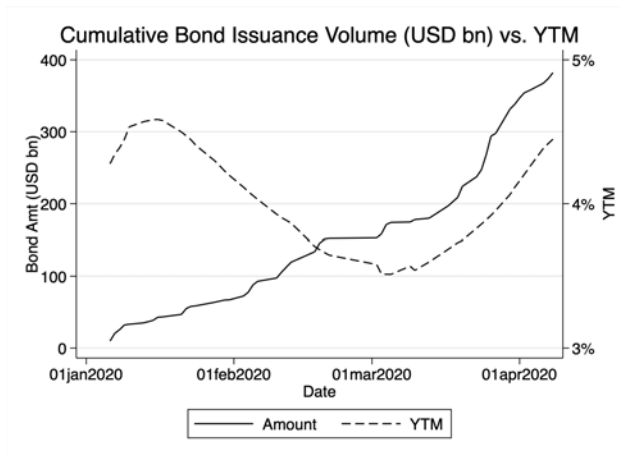
An alternative way for firms with a credit rating to raise cash is to access the bond market. We obtain corporate bond issuance data for U.S. firms from Dealogic and plot in Figure 6 the cumulative bond issuance volume (solid line, left-hand axis) and each day's average yield to maturity of newly issued bonds (dotted line, right-hand axis) since January 1st, 2020 for the full sample in panel A and for different rating classes in panel B (note that all bond issuers are rated, *i.e.*, there is no “unrated” category).

credit. This remains an open area for further inquiry. As such, working-capital related loan issuances have been muted since March 2020.

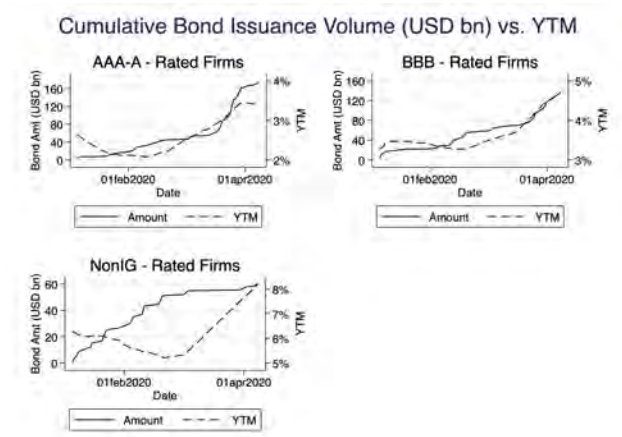
⁶ We use a smoothing function to plot the Z-Score estimates. As only few AAA-A rated firms draw down their credit lines, we cannot compute these estimates for the AAA-A rating category.

In total, U.S. non-financial firms issued about USD 150bn until mid-February. From then, issuance volume was muted until mid-March as spreads in the investment-grade and high-yield market were elevated. Since mid-March, however, issuance volume increased within from USD 180bn to close to USD 400bn.⁷

The data suggest that NonIG-rated or “junk” firms have lost access to public debt market since the beginning of March 2020; between March 4 and March 30, there has been no single NonIG bond issue. Cumulative bond issuance volume of BBB-rated firms was flat from middle of February until the end of March 2020, *i.e.*, they hardly issued any new bonds during this time period. The surge in bond issuances that started after March 15, 2020 was driven almost exclusively by AAA-A rated firms. Evidently, firms that issued bonds during the COVID-crisis could only do so at substantially higher yields compared to the period before middle of February (as the dotted line suggests).



Panel A. Full Sample



Panel B. Bond issuances by rating class

Figure 6. Cumulative bond issuances by U.S. non-financial firms for the period 1 March 2020 – 9 April 2020

⁷ We exclude the bond issuance of about USD 20bn on April 2, 2020 by T-Mobile to finance the Sprint merger.

To reconcile the evidence from the loan and the bond market, observe that AAA-A rated firms do not need to utilize their liquidity insurance as they can access public bond markets. Only few (likely high-quality) BBB-rated firms issued public bonds until end of March 2020 consistent with the surge in credit line usage over this period. It appears that NonIG-rated firms have not been able to access public capital markets and therefore had to draw down their credit lines. Similarly, unrated firms cannot access bond markets and need to rely on bank finance. This is consistent with the evidence we showed in Figures 3 and 4 that both NonIG-rated and unrated groups of firms used their credit lines early on in the crisis.

The impact of the U.S. fiscal and monetary policy measures on corporate debt market

To address the unfolding crisis in the economy and associated stress in the financial markets, the Federal Reserve Bank (Fed) and the U.S. Treasury reacted introducing a series of measures.

The Fed introduced a set of measures to address the economic fallout from the Corona virus. After having reduced the fed fund rate close to zero and reinstating its Treasury and agency MBS quantitative easing program, the Fed introduced a series of programs, among those: I announced the Commercial Paper Funding Facility (CPFF), the Primary Dealer Credit Facility (PDCF) and the Money Market Mutual Fund Facility (MMFF) on March 15. On March 17, it announced a USD 5tn repurchase program. The Fed introduced two facilities to support credit to large firms, the Primary Market Corporate Credit Facility (PMCCF) and the Secondary Market Corporate Credit Facility (SMCCF), through which the Fed can purchase investment-grade rated corporate bonds. This program was announced on March 23. On March 25, the Senate voted for a USD 2tn fiscal package (that was approved by the House on March 27).

While the Fed targeted short-term funding markets with its earlier initiatives, the corporate bond buying program that was announced on March 23, 2020 likely affects long-term corporate funding options. This should be particularly valuable for BBB and NonIG-rated firms that have – up to this point – been constrained to borrow in public capital markets as documented above. To assess this empirically, we study the effect of the announcement of the corporate bond buying program on stock and loan market returns. A lacking access to liquidity was an important driver of firms' stock price decline at the beginning of the stress period, alleviating funding problems might help reversing this trend. Moreover, the secondary loan market is an important indicator for funding stress in corporate debt markets (Saunders et al., 2020).⁸

⁸ To investigate loan market returns, we use an index of about 1,500 loans issued by U.S. non-financial firms that are traded in the secondary loan market with a market value of about USD 1.5 trillion as of 2 Jan 2020.

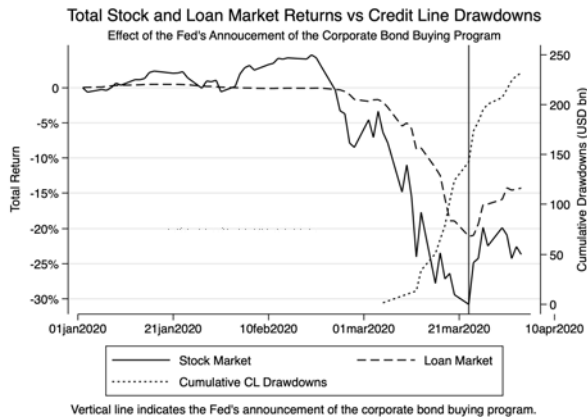


Figure 7. Total stock and loan market return vs. credit line drawdowns

We plot stock and loan market returns in Figure 7. Also loan market returns fell about 20% since the beginning of January 2020 indicating the lack of supply of credit to firms. Both stocks and loans increased significantly after the announcement of the corporate bond buying program on 23 March 2020. Stock (loan) market returns increased by about 10pp (5pp) after the announcement suggesting that the program might have to some degree reduced liquidity problems for U.S. non-financial firms.

When we add the cumulative credit line drawdowns since the beginning of March 2020 to the figure, we observe that – if anything – credit line drawdowns even accelerated after the announcement of the bond buying program. This is puzzling as – in contrast to an increase in stock and loan returns – this implies that funding problems of some firms persisted even after the Fed's announcements to buy investment-grade-rated corporate bonds.

Investigating corporate bond issuances around this announcement might help us understand this. Figure 8 focuses on the 13 March 2020 to 30 March 2020 to investigate the effects of the announcement of the corporate bond buying program on bond issuances of U.S. non-financial firms, overall as well as by rating category. It seems that the impact on corporate debt markets is asymmetric. While NonIG firms are still not able to borrow in public bond markets, only AAA-A rated firms benefit from the Fed interventions in the corporate sector with a surge in issuance volumes from USD 40bn to USD 80bn within a few days. The dollar volume of cumulative bond issues of BBB-rated firms is muted relative to AAA-A rated firms and amounts to about USD 10bn in the same period. About 75% of all bonds during this period have been issued by AAA-A-rated forms. In other words, most of BBB-rated firms, therefore, continued to rely on banks, which is consistent with an additional demand for loans and drawdown of committed credit lines in the corporate loan market.

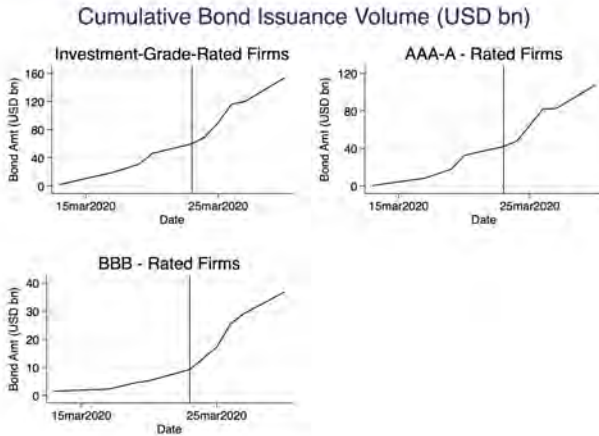


Figure 8. Cumulative bond issuances by U.S. non-financial firms for the period 13 March 2020 – 30 March 2020

“Cliff risk” of BBB-rated firms and the dash for cash

Since the 2008 to 2009 global financial crisis, the volume of BBB-rated debt has more than quadrupled.⁹ Within this rating class, credit geared towards riskier customers with high leverage, raising concerns as to whether its rating meaningfully reflect the risk of the company and about possible future downgrades to non-investment grade status. Altman (2020) estimates that about 34 % of BBB-rated firms can be classified as NonIG firms based on their Z-Score.

Rating agencies usually hesitate to downgrade a firm into non-investment-grade territory as such a downgrade might have severe consequences. E.g. many institutional investors are limited to holding investment-grade-rated debt and would be forced to sell. Moreover, the initial corporate bond buying program announced on 23 March 2020 included only the purchases of investment-grade corporate debt. Also, borrowing costs in the loan market might increase in addition to higher collateral requirements or an increase in covenant strictness. Taken together, BBB-rated firms likely face a steep a reduction in the access to credit and a steep increase in their funding costs after a downgrade.

A deep and prolonged recession because of the economic lockdown might result in the downgrade of some of these BBB-rated firms and stock market prices might already reflect the risk of being a “fallen angel”. In Figure 9, we plot the stock price of U.S. non-financial firms by rating class. AAA-A rated companies perform much better compared to lower-rated firms. These firms have healthier balance sheets and better access to credit markets in case of liquidity needs (as shown also above). Interestingly, BBB and NonIG-rated firms perform very similar as markets appear to be worried about the sustainability of the leverage of BBB-rated firms.

⁹ During the 2015 to 2019 period alone, U.S. firms issued about USD 4.5 trillion in corporate bonds. BBB-rated firms alone issued USD 1.4 trillion, *i.e.*, about 31% of the overall corporate bond volume.

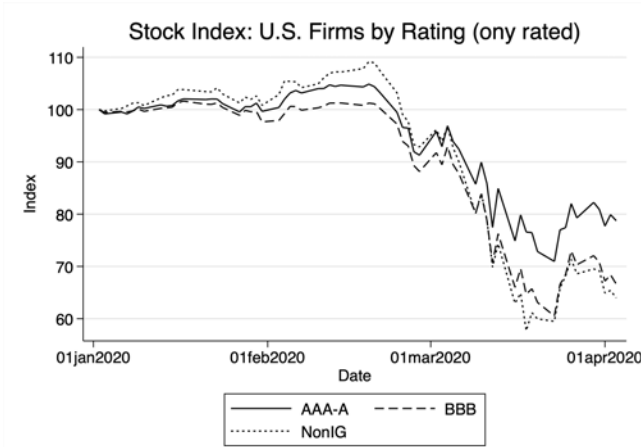


Figure 9. Stock price performance by rating class

We test this more formally and investigate the stock price performance of firms at the investment-grade boundary, *i.e.*, we compare BBB to BB-rated firms. We use the *Z-Score* as a continuous measure to match firms from both rating classes that have very similar *Z-Scores* (and therefore similar default risk) but one firm is investment-grade and the other firm is non-investment grade rated. We then simply compare their cumulative stock returns during the March 1, 2020 – March 23, 2020 period.

	Sample	Treated BBB	Controls BB	Difference	S.E.	T-stat
Stock return	Unmatched	-0.49	-0.612	0.13	0.032	3.79
	Matched Sample (<i>Z-Score</i>)	-0.49	-0.54	0.05	0.047	1.11

Table 2: Matched sample of BBB and BB-rated firms

Note: The results are based on a propensity score matched sample. We calculate the propensity score using a logit model where the dependent variable is an indicator that is one if the firm has a BBB-rating and zero if it has a BB-rating. The regressor is the *Z-Score*.

Simply comparing all firms from both rating classes (without matching) shows that BB-rated firms perform worse. The average stock price drops about 61% during this period compared with a 49% drop of BBB-rated firms. However, comparing the return of those firms with similar *Z-Score* shows that the stock performance of both group firms is not significantly different from each other. The average stock market decline of the matched control (*i.e.*, BB-rated) firms is about 54% and thus similar to the performance of BBB-rated firms.

That is, the stock market performance suggests that BBB-rated firms are probably of worse quality than their credit rating suggests. These firms, therefore, might face a downgrade if the crisis deepens. It is thus an interesting question to ask whether they increase borrowing by drawing down their credit lines to avoid a downgrade and the associated steep increase in borrowing costs if a downgrade materializes.

We analyze the cross-section of credit lines drawdowns during the March 1 to March 23, 2020 period and ask whether firms that are more likely to be downgraded to a NonIG category use their credit lines more compared to other firms. For each firm, we construct a

measure of total drawdowns as the natural logarithm of total drawdowns during this period ($\text{Log}(\text{Total Drawdown})$). This is our dependent variable.

Our explanatory variables include indicator variables for each rating class and their interaction with two different (continuous) measures of credit quality, (1) the *Z-Score* and (2) the *Debt/EBITDA* ratio. BBB-rated firms with a higher (lower) *Z-Score* (*Debt/EBITDA* ratio) have lower default risk. We include them individually in models shown in columns (1) and (2) of Table 3. In column (1), we add the *Z-Score* as control variables in addition to industry fixed effects. We do not add other balance sheet characteristics as the *Z-Score* is constructed from these measures. In column (2), we use firm characteristics that might affect drawdown behavior such as $\text{Log}(\text{Assets})$, *Debt/EBITDA*, *return on assets (ROA)* and *Liquidity* (as defined above) in addition to industry fixed effects.

As expected, using the full sample of firms, those BBB-rated firms that have a higher likelihood to be downgraded – as measured by a lower *Z-Score* or a higher *Debt/EBITDA* ratio – use their credit lines more compared to safer firms. Our results in column (2) also show that lower quality NonIG-rated firms draw down more consistent with our earlier result that absolute drawdowns of NonIG firms were similar to those of BBB-rated firms. The coefficients of BBB and NonIG-rated firms interacted with their *Debt/EBITDA* ratio are not significantly different.

We then perform a matched sample exercise and focus exclusively on BBB and BB-rated firms. We match these firms in two different ways using (1) Altman's *Z-Score* and (2) using a set of firm characteristics ($\text{Log}(\text{Assets})$, *Debt/EBITDA*, *return on assets (ROA)* and *Liquidity* in addition to industry fixed effects). That is, we focus on a set of firms that are most similar in terms of their characteristics (such as default risk) and only differ as one firm is investment-grade rated and the other firm is non-investment-grade rated.

The results are reported in columns (3) to (6) and we always compare differences in credit line drawdowns in the matched sample to the unmatched sample. Consistent with a “dash for cash” of firms that are at risk of being a fallen angel, we find that BBB-rated firms draw down significantly more than comparable, BB-rated firms.

Using the matched sample based on different balance sheet characteristics is likely the most conservative approach and produces economically somewhat smaller results, which are still statistically highly significant. The coefficient suggests that matched BBB-rated firms draw down, on average, about USD 2.66 billion more from their credit line compared to similar BB-rated firms during our sample period.

	Full Sample		Log (Total Drawdowns)			
	(1)	(2)	Cliff (BBB vs BB rated firms)			
			Unmatched (3)	PS-Matched (Z-Score) (4)	Unmatched (5)	PS-Matched (Controls) (6)
AAA-A x Z-Score	-0.2655 (-.25)					
BBB x Z-Score	-0.5701 (-3.06)					
NonIG x Z-Score	0.0385 (.79)					
AAA-A x Debt/EBITDA		-0.207 (.31)				
BBB x Debt/EBITDA		0.023 (3.8)				
NonIG x Debt/EBITDA		0.051 (1.72)				
AAA-A	3.007 (.5)	0.068 (.07)				
BBB	3.044 (5.55)	0.258 (1.61)	1.174 (4.51)	1.392 (3.31)	1.193 (4.85)	0.9768 (2.12)
NonIG	-1.416 (-4.78)	-0.156 (.85)				
Controls		Log(Assets), Debt/EBITDA, ROA, Liquidity				
Industry FE	Yes	Yes	Yes	Yes	Yes	Yes
N	129	139	59	59	63	63
R ²	48.62%	83.51%	26.33%		27.83%	
Treated				27		29
Control				32		34

Table 3: Cliff risk and credit line drawdowns

Note: The results in columns (4) and (6) are based on a propensity score matched sample. We calculate the propensity score using logit models where the dependent variable is an indicator that is one if the firm has a BBB-rating and zero if it has a BB-rating. The regressor is the Z-Score for the Z-Score matched sample (column (4)) and the set of controls used in column (2), *i.e.*, *Log(Assets)*, *Debt/EBITDA*, *ROA*, *Liquidity*, for the control matched sample analysis shown in column (6). We also include industry fixed effects in both logit models. T-statistics are in parentheses.

Not all fallen angels are the same

Some firms have already been downgraded to non-investment-grade by credit rating agencies at the end of March 2020 (so-called “fallen angels”). Based on our earlier analysis of the stock price response of BBB vs. BB-rated firms, we would expect to observe a significantly worse performance of fallen angels relative to other BBB-rated firms during our sample period. Figure 10 compares the stock market performance of these fallen angels with other BBB-rated firms since January 1, 2020.¹⁰ Consistent with our previous discussion, fallen angels perform significantly worse, particularly since the begin of the COVID-19 crisis, where stock prices dropped by about 40% relative to their 1 January 2020 values and did not recover.

¹⁰ The fallen angels that are stock exchange listed and thus included in our dataset are Apache Corporation (APA), Continental Resources (CLR), Delta Airlines (DAL), Ford (F), Macy’s (M), Occidental Petroleum (OXY) and Patterson Energy (PTEN).

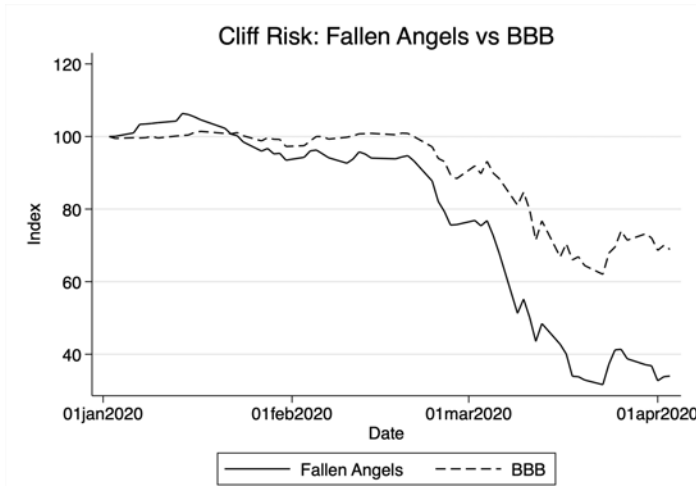


Figure 10. Stock prices: Fallen Angels vs. BBB-rated firms

In a final step, we focus on the 6 publicly listed fallen angels in our sample and investigate their stock market performance before they were downgraded. We plot their stock prices since 1 January 2020 in Figure 11. We observe that firms from the oil & gas industry experience a sharp drop in their share price on March 9, 2020, when the oil price dropped by more than 20% on a single day. In an environment, in which global demand for oil was already weak – also as a consequence of the COVID-19 pandemic – both Saudi Arabia and Russia, the two world’s largest oil producers, decided to increase their oil output considerably when both countries could not enter into an agreement with OPEC on possible production cuts. The share price of the other firms declined more gradually by about 50% before they were eventually downgraded.¹¹

The downgrade to the status of a non-investment-grade rated company does not only have an impact on the firms themselves but also on the banks that provide loans to these firms (in the form of both credit lines and term loans). The fallen angels from the oil & gas sector alone have an outstanding loan volume of more than USD 34 billion, out of which about USD 15 billion is held by US banks alone (see Table 4).

¹¹ Interestingly, the fallen angels from the energy sector (in contrast to the firms from the other sectors) did not draw down their credit line before they were downgraded. A possible reason might be a contractual mechanism specific to loans issued by firm in the energy sector. So-called “borrowing base” conditions require banks to regularly assess the present value of future cash flows of these firms. If the present value falls too much, lenders can reduce the committed credit line. If borrowers have already used their credit line beyond this point, lenders can either demand repayment or request additional collateral.

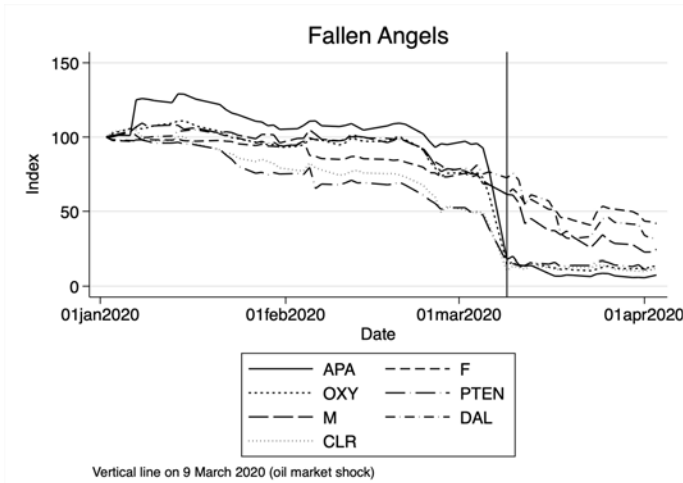


Figure 11. Stock prices of fallen angels

For some banks, this exposure alone is substantial relative to their Tier 1 capital. In other words, the increasing speed of credit line drawdowns, particularly of riskier firms, that we have observed since beginning of March 2020, also impacts the balance sheet of lenders with likely spillovers into the real economy.

Bank	Exposure Fallen	
	Angel	% of Tier 1
PNC Bank	2,663	7.34%
US Bancorp	2,838	6.80%
Comerica Inc	288	4.16%
Zions Bancorp	176	2.81%
Citi	2,920	1.87%
Truist Financial	721	1.77%
BofA	2,809	1.49%
Wells Fargo & Co	1,547	0.97%
JP Morgan	1,184	0.55%
Total	15,147	3.08%

Table 4: US banks' exposure to fallen (energy) angels

Conclusion

The lockdown as a response to the COVID-19 pandemic caused a high demand for liquidity for firms affected by the crisis. Using a novel dataset of daily credit line drawdowns at the firm-loan-level, we provide evidence consistent a “cash for cash” of BBB-rated firms, particularly those that might be more similar in terms of credit quality to non-investment-grade rated firms. The announcement of an investment-grade corporate bond buying program by the Federal Reserve did not alleviate this cliff risk of being downgraded and these firms continue to convert committed credit lines into cash.

This “dash for cash” also impacts the balance sheets of banks when commitments turn into loans as banks have to fund these exposures with equity. Worse, banks usually hold additional term loan exposure to the same firms, *i.e.*, they accumulate a concentrated exposure to firms

at the risk of being downgraded. Even though banks are better capitalized compared to 2007 and before the global financial crisis, the accelerated drawdowns of credit lines and provision for possible future credit losses for on-balance sheet exposures might bring them closer to the regulatory minimum capital requirement, which not only endangers their financial stability but can constrain future intermediation with likely spillovers into the real economy.¹²

Regulators should therefore insist that banks do everything possible to conserve capital. Requiring them to withhold dividend payments or stop repurchasing shares can only be the minimum response at the beginning of a crisis, which the International Monetary Fund describes as possibly the “worst economic downturn since the Great Depression” and an unprecedented challenge for the global economy. In an Op-Ed in the *Financial Times*, the president of the Federal Reserve Bank of Minneapolis, Neel Kashkari, recently requested that banks raise USD 200bn now, which compares to the amount raised privately by the U.S. banks following the stress tests of 2009. As it seems within reasonable chance that this crisis will eventually dwarf what we observed in the 2008 to 2009 global financial crisis, it might be desirable to have an immediate regulatory prescription to banks to raise an even larger amount to build resilience in their balance-sheets and lend well to the real economy in the phase of economic recovery.

References

Acharya, V. and N. Mora, 2015, A Crisis of Banks as Liquidity Providers, *Journal of Finance*, 70(1), 1-44.

Acharya, V. and S. Steffen, 2020, ‘Stress tests’ for banks as liquidity insurers in a time of COVID, VoxEU.org

Altman, E., 1986, Financial Ratios, Discriminant Analysis and the Prediction of Corporate Bankruptcy, *Journal of Finance*.

Altman, E., 2020, The Credit Cycle Before And After The Market’s Awareness Of The Coronavirus Crisis In The U.S., NYU Working Paper.

Beltratti, A. and R. Stulz, 2012, The credit crisis around the globe: Why did some banks perform better?, *Journal of Financial Economics*, 2012, v105(1), 1-17.

Saunders, A., A. Spina, S. Steffen and D. Streit, 2020, What’s in the Spread? The Predictive Power of Loan vs. Bond Spreads, Working Paper.

¹² Some large U.S. banks have already reported a significant increase in quarterly provisions for credit losses compared to previous quarters. E.g. JP Morgan increased its provisions from USD 1.4bn in Q4:2019 to USD 8.3bn for the first quarter of 2020.

Modeling the consumption response to the CARES Act¹

Christopher D. Carroll,² Edmund Crawley,³ Jiri Slacalek⁴
and Matthew N. White⁵

Date submitted: 17 April 2020; Date accepted: 19 April 2020

To predict the effects of the 2020 U.S. 'CARES' act on consumption, we extend a model that matches responses of households to past consumption stimulus packages. The extension allows us to account for two novel features of the coronavirus crisis. First, during the lockdown, many types of spending are undesirable or impossible. Second, some of the jobs that disappear during the lockdown will not reappear when it is lifted. We estimate that, if the lockdown is short-lived, the combination of expanded unemployment insurance benefits and stimulus payments should be sufficient to allow a swift recovery in consumer spending to its pre-crisis levels. If the lockdown lasts longer, an extension of enhanced unemployment benefits will likely be necessary if consumption spending is to recover.

1 Thanks to the Consumer Financial Protection Bureau for funding the original creation of the Econ-ARK toolkit, whose latest version we used to produce all the results in this paper; and to the Sloan Foundation for funding its extensive further development that brought it to the point where it could be used for this project. The toolkit can be cited by its digital object identifier, 10.5281/zenodo.1001068, as is done in the paper's own references as Carroll, White, and Econ-ARK (2017). We are grateful to Kiichi Tokuoka, who provided valuable feedback and input as this project progressed, and to Mridul Seth, who created the dashboard and configurator. The views presented in this paper are those of the authors, and should not be attributed to the Federal Reserve Board or the European Central Bank.

2 Professor of Economics, Johns Hopkins University.

3 Economist, Federal Reserve Board.

4 Economist, European Central Bank.

5 Assistant Professor of Economics, University of Delaware.

“Economic booms are all alike; each recession contracts output in its own way.”
— with apologies to Leo Tolstoy

I Introduction

In the decade since the Great Recession, macroeconomics has made great progress by insisting that models be consistent with microeconomic evidence (see Krueger, Mitman, and Perri (2016) for a survey). From the new generation of models, we take one specifically focused on reconciling apparent conflicts between micro and macro evidence about consumption dynamics (Havranek, Rusnak, and Sokolova (2017)) and adapt it to incorporate two aspects of the coronavirus crisis. First, because the tidal wave of layoffs for employees of shuttered businesses will have a large impact on their income and spending, assumptions must be made about the employment dynamics of laid off workers. Second, even consumers who remain employed will have restricted spending options (nobody can eat dinner at a shuttered restaurant).

On the first count, we model the likelihood that many of the people unemployed during the lockdown will be able to quickly return to their old jobs (or similar ones) by assuming that the typical job loser has a two-thirds chance of being reemployed in the same or a similar job after each quarter of unemployment. However, we expect that some kinds of jobs will not come back quickly after the lockdown,¹ and that people who worked in these kinds of jobs will have more difficulty finding a new job. We call these people the ‘deeply unemployed’ and assume that there is a one-third chance each quarter that they become merely ‘normal unemployed.’ The ‘normal unemployed’ have a jobfinding rate that matches average historical unemployment spell of 1.5 quarters (as a ‘normal unemployed’ person). Thus a deeply unemployed person expects to remain in the ‘deep unemployment’ state for three quarters on average, and then unemployed for another one and a half quarters. When the pandemic hits, we assume that 10 percent of model households become normal unemployed and an additional 5 percent become deeply unemployed; in line with empirical evidence, the unemployment probabilities are skewed toward households who are young, unskilled and have low income. (All of these assumptions can be adjusted using our [dashboard](#); changing several parameters simultaneously requires installation of the [software toolkit](#).)

On the second count, we model the restricted spending options by assuming that during the lockdown spending is less enjoyable (there is a negative shock to the ‘marginal utility of consumption.’) Based on a tally of sectors that we judge to be substantially shuttered during the ‘lockdown,’ we calibrate an 11 percent reduction to spending. Thus households will prefer to defer some of their consumption into the future, when it will yield them greater utility. (See Carvalho, Garcia, Hansen, Ortiz, Rodrigo, Rodriguez, and Ruiz (2020) for Spanish data already showing a strong effect of this kind in recent weeks, and Andersen, Hansen, Johannesen, and Sheridan (2020) for similar evidence from Denmark).² In our primary scenario, we assume that this condition is removed with probability one-half after each quarter, so on average remains for two quarters. When the ‘lockdown’ ends, the buildup of savings by households who did not lose their jobs but whose spending was suppressed should result in a partial recovery in consumer spending, but in our primary scenario (without the CARES act), total consumer spending remains below its pre-crisis peak through the foreseeable future.

¹The cruise industry, for example, is likely to take a long time to recover.

²A shock to marginal utility may not perfectly capture the essence of what depresses consumption spending, but it accomplishes our purposes and is a kind of shock commonly studied in the literature. Any analysis of the welfare consequences of the lockdown would probably need a richer treatment to be credible.

Our model captures the two primary features of the CARES Act that aim to bolster consumer spending:

1. The boost to unemployment insurance benefits, amounting to \$7,800 if unemployment lasts for 13 weeks.
2. The direct stimulus payments to households, amounting to \$1,200 per adult.

We estimate that the combination of expanded unemployment insurance benefits and stimulus payments should be sufficient to allow a swift recovery in consumer spending to its pre-crisis levels under our primary scenario in which the lockdown ends after two quarters on average. Overall, unemployment benefits account for about 30 percent of the total aggregate consumption response and stimulus payments explain the remainder.

Our analysis partitions households into three groups based on their employment state when the pandemic strikes and the lockdown begins.

First, households in our model who do not lose their jobs will initially build up their savings, both because of the lockdown-induced suppression of spending and because most of these households will receive a significant stimulus check, much of which the model says will be saved. Even without the lockdown, we estimate that only about 20 percent of the stimulus money would be spent immediately upon receipt, consistent with evidence from prior stimulus packages about spending on nondurable goods and services. Once the lockdown ends, the spending of the always-employed households rebounds strongly thanks to their healthy household finances.

The second category of households are the ‘normal unemployed,’ job losers who perceive that it is likely they will be able to resume their old job (or get a similar new job) when the lockdown is over. Our model predicts that the CARES Act will be particularly effective in stimulating their consumption, given the perception that their income shock will be largely transitory. Our model predicts that by the end of 2021, the spending of this group will recover to the level it would have achieved in the absence of the pandemic (‘baseline’); without the CARES Act, this recovery would take more than a year longer.

Finally, for households in the deeply unemployed category, our model says that the marginal propensity to consume (MPC) from the checks will be considerably smaller, because they know they must stretch that money for longer. Even with the stimulus from the CARES Act, we predict that consumption spending for these households will not fully recover until the middle of 2023. Even so, the act makes a big difference to their spending, particularly in the first six quarters after the crisis. For both groups of unemployed households, the effect of the stimulus checks is dwarfed by the increased unemployment benefits, which arrive earlier and are much larger (per recipient).

Perhaps surprisingly, we find the effectiveness of the combined stimulus checks and unemployment benefits package for aggregate consumption is not substantially different from a package that distributed the same quantity of money equally between households. The reason for this is twofold: first, the extra unemployment benefits in the CARES Act are generous enough that many of the ‘normally’ unemployed remain financially sound and can afford to save a good portion of those benefits; second, the deeply unemployed expect their income to remain depressed for some time and therefore save more of the stimulus for the future. In the model, the fact that they do *not* spend immediately is actually a reflection of how desperately they anticipate these funds will be needed to make it through a long period of uncertainty. While unemployment benefits do not strongly stimulate current consumption of the deeply unemployed, they do provide important disaster relief for those who may not be able to return to work for several quarters (see Krugman (2020) for an informal discussion).

In addition to our primary scenario's relatively short lockdown period, we also consider a worse scenario in which the lockdown is expected to last for four quarters and the unemployment rate increases to 20 percent. In this case, we find that the return of spending toward its no-pandemic path takes roughly three years. Moreover, the spending of deeply unemployed households will fall steeply unless the temporary unemployment benefits in the CARES Act are extended for the duration of the lockdown.

Our modeling assumptions — about who will become unemployed, how long it will take them to return to employment, and the direct effect of the lockdown on consumption utility — could prove to be off, in either direction. Reasonable analysts may differ on all of these points, and prefer a different calibration. To encourage such exploration, we have made available our modeling and prediction software, with the goal of making it easy for fellow researchers to test alternative assumptions. Instructions for installing and running our code can be found [here](#); alternatively, you can explore adjustments to our parametrization with an interactive dashboard [here](#).

There is a potentially important reason our model may underpredict the bounceback in consumer spending when the lockdown ends: 'pent up demand.' This term captures the fact that purchases of 'durable' goods can be easily postponed, but that when the reason for postponement abates some portion of the missing demand is made up for. (We put 'durable' in quotes because 'memorable' goods, Hai, Krueger, and Postlewaite (2013), have effectively the same characteristics.) For simplicity, our model does not include durable goods as modeling spending on durables is a formidable challenge. But it is plausible that, when the lockdown ends, people may want to spend *more* than usual on memorable or durable goods to make up for earlier missing spending.

Existing Work on the Effects of the Pandemic

Many papers have recently appeared on the economic effects of the pandemic and policies to manage it. Several papers combine the classic susceptible–infected–recovered (SIR) epidemiology model with dynamic economic models to study the interactions between health and economic policies (Eichenbaum, Rebelo, and Trabandt (2020) and Alvarez, Argente, and Lippi (2020), among others). Guerrieri, Lorenzoni, Straub, and Werning (2020) shows how an initial supply shock (such as a pandemic) can be amplified by the reaction of aggregate demand. The ongoing work of Kaplan, Moll, and Violante (2020) allows for realistic household heterogeneity in how household income and consumption are affected by the pandemic. Glover, Heathcote, Krueger, and Ríos-Rull (2020) studies distributional effects of optimal health and economic policies. Closest to our paper, work analyzing the effects of the fiscal response to the pandemic includes Faria-e-Castro (2020b), in a two-agent DSGE model, and Bayer, Born, Luetticke, and Müller (2020) in a HANK model.

All of this work accounts for general equilibrium effects on consumption and employment, which we omit, but none of it is based on a modeling framework explicitly constructed to match micro and macroeconomic effects of past stimulus policies, as ours is.

A separate strand of work focuses on empirical studies of how the economy reacts to pandemics; see, e.g., Baker, Farrokhnia, Meyer, Pagel, and Yannelis (2020), Jorda, Singh, and Taylor (2020) and Correia, Luck, and Verner (2020).

II Modeling Setup

A The Baseline Model

Our model extends a class of models explicitly designed to capture the rich empirical evidence on heterogeneity in the marginal propensity to consume (MPC) across different types of household (employed, unemployed; young, old; rich, poor). This is motivated by the fact that the act distributes money unevenly across households, particularly targeting unemployed households. A model that does not appropriately capture both the degree to which the stimulus money is targeted, and the differentials in responses across differently targeted groups, is unlikely to produce believable answers about the spending effects of the stimulus.

Specifically, we use a *lifecycle model* calibrated to match the income paths of high school dropouts, high school graduates, and college graduates.³ Households are subject to permanent and transitory income shocks, as well as unemployment spells.⁴ Within each of these groups, we construct an *ex ante* distribution of discount factors to match their distribution of liquid assets. Matching the distributions of liquid assets allows us to achieve a realistic distribution of marginal propensities to consume according to education group, age, and unemployment status, and thus to assess the impact of the act for these different groups.⁵

B Adaptations to Capture the Pandemic

To model the pandemic, two new features are introduced to the model.

First, our new category of ‘deeply unemployed’ households was created to capture the likelihood that the pandemic will have long-lasting effects on some kinds of businesses and jobs (e.g., the cruise industry), even if the CARES act manages to successfully cushion much of the financial hit to total household income.

Each quarter, our ‘deeply unemployed’ households have a two-thirds chance of remaining deeply unemployed, and a one-third chance of becoming ‘normal unemployed.’ The expected time to employment for a ‘deeply unemployed’ household is four and a half quarters, much longer than the historical average length of a typical unemployment spell. Reflecting recent literature on the ‘scarring effects’ of unemployment spells, permanent income of both ‘normal’ and ‘deeply’ households declines by 0.5 percent each quarter due to ‘skill rot’ (rather than following its usual age profile).

Second, a temporary negative shock to the *marginal utility of consumption* captures the idea that, during the period of the pandemic, many forms of consumption are undesirable or even impossible.⁶

The pandemic is modeled as an unexpected (MIT) shock, sending many households into both normal and deep unemployment, as well as activating the negative shock to marginal utility. Households understand and respond in a forward-looking way to their new circumstances (according to their beliefs about its duration), but their decisions prior to the pandemic did not account for any probability that it would occur.

³The baseline model is very close to the lifecycle model in Carroll, Slacalek, Tokuda, and White (2017).

⁴Households exit unemployment with a fixed probability each quarter — the expected length of an unemployment spell is one and a half quarters.

⁵For a detailed description of the model and its calibration see Appendix A.

⁶For the purposes of our paper, with log utility, modeling lockdowns as a shock to marginal utility is essentially equivalent to not allowing consumers to buy a subset of goods (which are combined into composite consumption by a Cobb–Douglas aggregator). However, the two approaches would yield different implications for normative evaluations of economic policies.

Calibration

The calibration choices for the pandemic scenario are very much open for debate. Here we have tried to capture something like median expectations from early analyses, but there is considerable variation in points of view around those medians. Section III.B below presents a more adverse scenario with a long lockdown and a larger increase in unemployment.

Unemployment forecasts for Q2 2020 range widely, from less than 10 percent to over 30 percent, but all point to an unprecedented sudden increase in unemployment.⁷ We choose a total unemployment rate in Q2 2020 of just over 15 percent, consisting of five percent ‘deeply unemployed’ and ten percent ‘normal unemployed’ households.

We calibrate the likelihood of becoming unemployed to match empirical facts about the relationship of unemployment to education level, permanent income and age, which is likely to matter because the hardest hit sectors skew young and unskilled.⁸ Figure 1 shows our assumptions on unemployment along these dimensions. In each education category, the solid line represents the probability of unemployment type (‘normal’ or ‘deep’) for a household with the median permanent income at each age, while the dotted lines represent the probability of unemployment type for a household at the 5th and 95th percentile of permanent income at each age; Appendix A with Table A2 detail the parametrization and calibration we used.

To calibrate the drop in marginal utility, we estimate that 10.9 percent of the goods that make up the consumer price index become highly undesirable, or simply unavailable, during the pandemic: food away from home, public transportation including airlines, and motor fuel. We therefore multiply utility from consumption during the period of the epidemic by a factor of 0.891. Furthermore, we choose a one-half probability of exiting the period of lower marginal utility each quarter, accounting for the possibility of a ‘second wave’ if restrictions are lifted too early — see Cyranoski (2020).⁹

The CARES Act

We model the two elements of the CARES Act that directly affect the income of households:

- The stimulus check of \$1,200 for every adult taxpayer, means tested for previous years’ income.¹⁰
- The extra unemployment benefits of \$600 for up to 13 weeks, a total of \$7,800. For normal unemployed, we assume they receive only \$5,200 to reflect the idea that they may not be unemployed the entire 13 weeks.

We model the stimulus checks as being announced at the same time as the crisis hits. However, only a quarter of households change their behavior immediately at the time of announcement, as calibrated to past experience. The remainder do not respond until their stimulus check arrives,

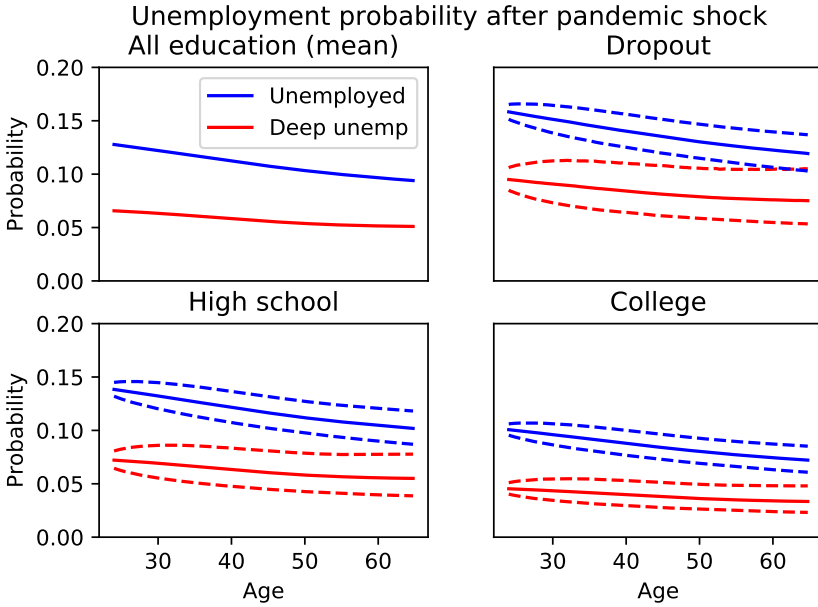
⁷As of April 16, about 22 million new unemployment claims have been filed in four weeks, representing a loss of over 14 percent of total jobs. JP Morgan Global Research forecast 8.5 percent unemployment (JPMorgan (2020), from March 27); Treasury Secretary Steven Mnuchin predicted unemployment could rise to 20 percent without a significant fiscal response (Bloomberg (2020a)); St. Louis Fed president James Bullard said the unemployment rate may hit 30 percent (Bloomberg (2020b) — see Faria-e-Castro (2020a) for the analysis behind this claim. Based on a survey that closely follows the CPS, Bick and Blandin (2020) calculate a 20.2 percent unemployment rate at the beginning of April.

⁸See Gascon (2020), Leibovici and Santacreu (2020) and Adams-Prassl, Boneva, Golin, and Rauh (2020) for breakdowns of which workers are at most risk of unemployment from the crisis. See additional evidence in Kaplan, Moll, and Violante (2020) and modeling of implications for optimal policies in Glover, Heathcote, Krueger, and Ríos-Rull (2020).

⁹The CBO expects social distancing to last for three months, and predicts it to have diminished, on average and in line with our calibration, by three-quarters in the second half of the year; see Swagel (2020).

¹⁰The act also includes \$500 for every child. In the model, an agent is somewhere between a household and an individual. While we do not model the \$500 payments to children, we also do not account for the fact that some adults will not receive a check. In aggregate we are close to the Joint Committee on Taxation’s estimate of the total cost of the stimulus checks.

Figure 1 Unemployment Probability in Q2 2020 by Demographics



which we assume happens in the following quarter. The households that pay close attention to the announcement of the policy are assumed to be so forward looking that they act as though the payment will arrive with certainty next period; the model even allows them to borrow against it if desired.¹¹

The extra unemployment benefits are assumed to both be announced and arrive at the beginning of the second quarter of 2020, and we assume that there is no delay in the response of unemployed households to these benefits.

Figure 2 shows the path of labor income — exogenous in our model — in the baseline and in the pandemic, both with and without the CARES Act. Income in quarters Q2 and Q3 2020 is substantially boosted (by around 10 percent) by the extra unemployment benefits and the stimulus checks. After two years, aggregate labor income is almost fully recovered. (See below for a brief discussion of analyses that attempt to endogenize labor supply and other equilibrium variables).

III Results

This section presents our simulation results for the scenario described above. In addition, we then model a more pessimistic scenario with longer lockdown and higher initial unemployment rate.

¹¹See Carroll, Crawley, Slacalek, Tokuoka, and White (2020) for a detailed discussion of the motivations behind this way of modeling stimulus payments, and a demonstration that this model matches the empirical evidence of how and when households have responded to stimulus checks in the past — see Parker, Souleles, Johnson, and McClelland (2013), Broda and Parker (2014) and Parker (2017), among others.

Figure 2 Labor and Transfer Income

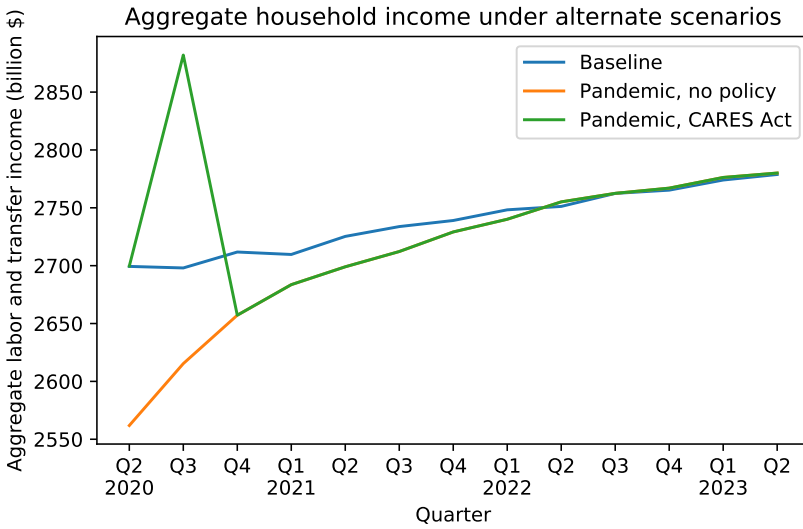
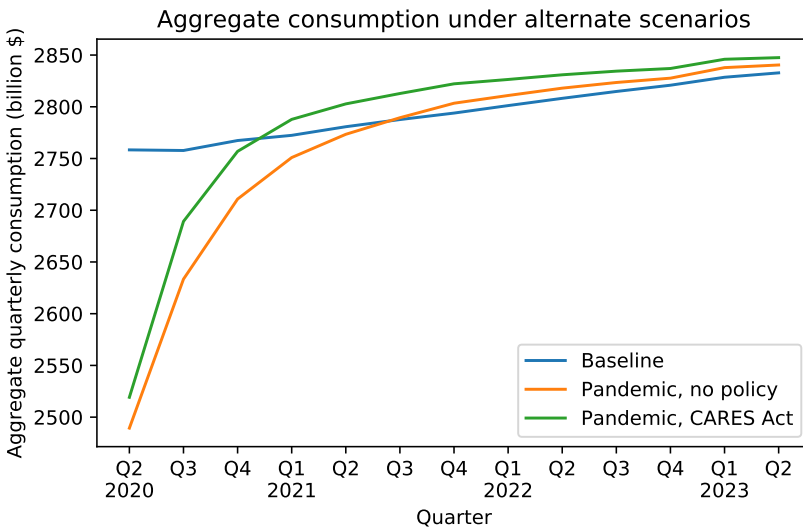


Figure 3 Consumption Response to the Pandemic and the Fiscal Stimulus



Covid Economics 10, 27 April 2020: 67-91

A Short-lived Pandemic

Figure 3 shows three scenarios for quarterly aggregate consumption: (i) the baseline with no pandemic; (ii) the pandemic with no fiscal response; (iii) the pandemic with both the stimulus checks and extended unemployment benefits in the CARES Act. The pandemic reduces consumption by ten percentage points in Q2 2020 relative to the baseline.

Without the CARES Act, consumption remains depressed through to the second half of 2021, at which point spending actually rises above the baseline, as a result of the buildup of liquid assets during the pandemic by households that do not lose their income. We capture the limited spending options during the lockdown period by a reduction in the utility of consumption, which makes household save more than they otherwise would usual during the pandemic, with the result that they build up liquid assets. When the lockdown ends, the pent up savings of the always-employed become available to finance a resurgence in their spending, but the depressed spending of the two groups of unemployed people keeps total spending below the baseline until most of them are reemployed, at which point their spending (mostly) recovers while the always-employed are still spending down their extra savings built up during the lockdown.

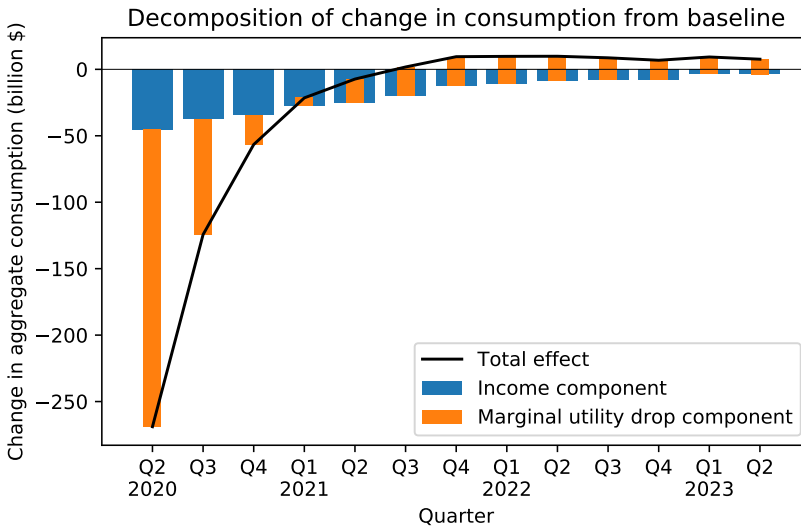
Figure 4 decomposes the effect of the pandemic on aggregate consumption (with no fiscal policy response), separating the drop in marginal utility from the reduction in income due to mass layoffs. The figure illustrates that the constrained consumption choices are quantitatively key in capturing the expected depth in the slump of spending, which is already under way; see Baker, Farrokhnia, Meyer, Pagel, and Yannelis (2020) and Armantier, Kosar, Pomerantz, Skandalis, Smith, Topa, and van der Klaauw (2020) for early evidence. The marginal utility shock hits all households, and directly affects their spending decisions in the early quarters after the pandemic; its effect cannot be mitigated by fiscal stimulus. The loss of income from unemployment is large, but affects only a fraction of households, who are disproportionately low income and thus account for a smaller share of aggregate consumption. Moreover, most households hold at least some liquid assets, allowing them to smooth their consumption drop — the 5 percent decrease in labor income in Figure 2 induces only a 1.5 percent decrease in consumption in Figure 4.

Figure 5 shows how the consumption response varies depending on the employment status of households in Q2 2020. For each employment category (employed, unemployed, and deeply unemployed), the figure shows consumption relative to the same households' consumption in the baseline scenario with no pandemic (dashed lines).¹² The upper panel shows consumption without any policy response, while the lower panel includes the CARES Act. The figure illustrates an important feature of the unemployment benefits that is lost at the aggregate level: the response provides the most relief to households whose consumption is most affected by the pandemic. For the unemployed — and especially for the deeply unemployed — the consumption drop when the pandemic hits is much shallower and returns faster toward the baseline when the fiscal stimulus is in place.

Indeed, this targeted response is again seen in Figure 6, showing the extra consumption relative to the pandemic scenario without the CARES Act. The dashed lines show the effect of the stimulus check in isolation (for employed workers this is the same as the total fiscal response). For unemployed households, this is dwarfed by the increased unemployment benefits. These benefits both arrive earlier and are much larger. Specifically, in Q3 2020, when households receive the stimulus checks, the effect of unemployment benefits on consumption makes up

¹²Households that become unemployed during the pandemic might or might not have been unemployed otherwise. We assume that all households that would have been unemployed otherwise are either unemployed or deeply unemployed in the pandemic scenario. However, there are many more households that are unemployed in the pandemic scenario than in the baseline.

Figure 4 Decomposition of Effect of the Pandemic on Aggregate Consumption (No Policy Response)



about 70 percent and 85 percent of the total effect for the normally and deeply unemployed, respectively.

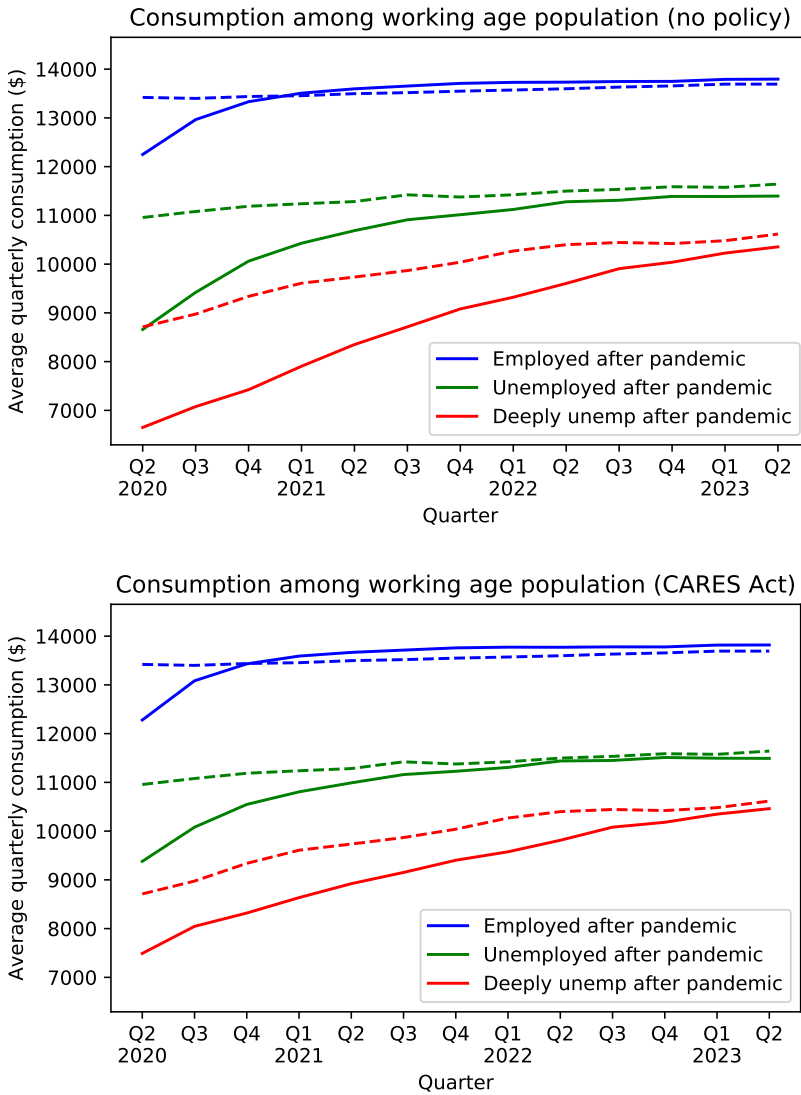
Figure 7 aggregates the decomposition of the CARES Act in Figure 6 across all households. In our model economy, the extra unemployment benefits amount to \$544 per household, while the stimulus checks amount to \$1,054 per household (as means testing reduces or eliminates the stimulus checks for high income households). Aggregated, stimulus checks amount to \$267 billion, while the extended unemployment benefits amount to just over half that, \$137 billion.¹³ The figure shows that during the peak consumption response in Q3 2020, the stimulus checks account for about 70 percent of the total effect on consumption for the average household and the unemployment benefits for about 30 percent. Thus, although the unemployment benefits make a much larger difference to the spending of the individual recipients than the stimulus checks, a small enough proportion of households becomes unemployed that the total extra spending coming from these people is less than the total extra spending from the more widely distributed stimulus checks.

The previous graphs show the importance of the targeted unemployment benefits at the individual level, but the aggregate effect is less striking. Figure 8 compares the effect of the CARES Act (both unemployment insurance and stimulus checks) to a policy of the same absolute size that distributes checks to everybody. While unemployment benefits arrive sooner, resulting in higher aggregate consumption in Q2 2020, the un-targeted policy leads to higher aggregate consumption in the following quarters.

The interesting conclusion is that, while the net spending response is similar for alternative ways of distributing the funds, the choice to extend unemployment benefits means that much more of the extra spending is coming from the people who will be worst hurt by the crisis. This has obvious implications for the design of any further stimulus packages that might be necessary if the crisis lasts longer than our baseline scenario assumes.

¹³See Appendix B for details on how we aggregate households.

Figure 5 Consumption Response by Employment Status



Covid Economics 10, 27 April 2020: 67-91

Figure 6 Effect of CARES Act by Employment Status

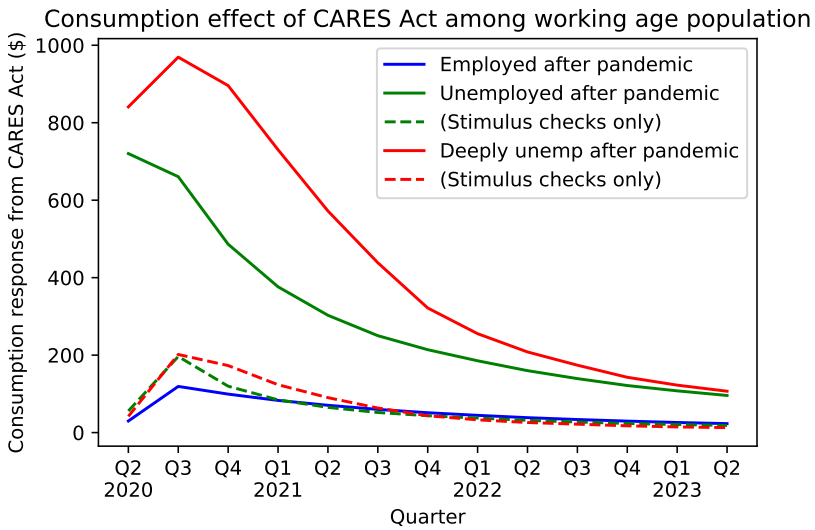
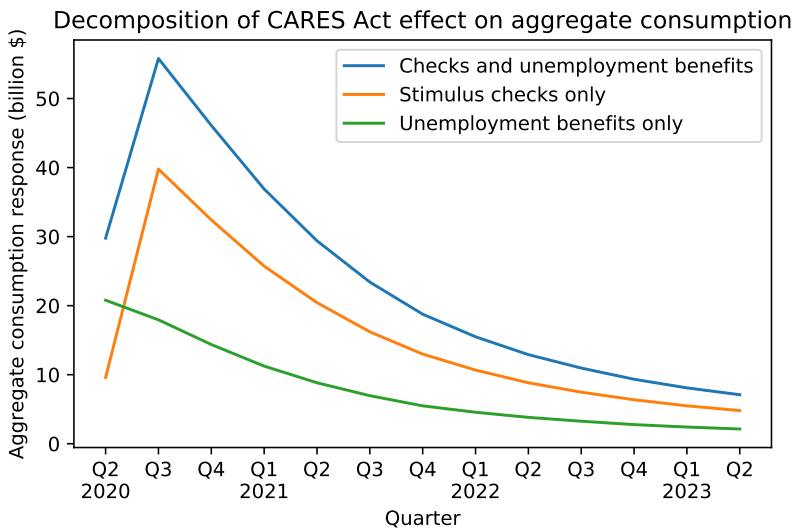
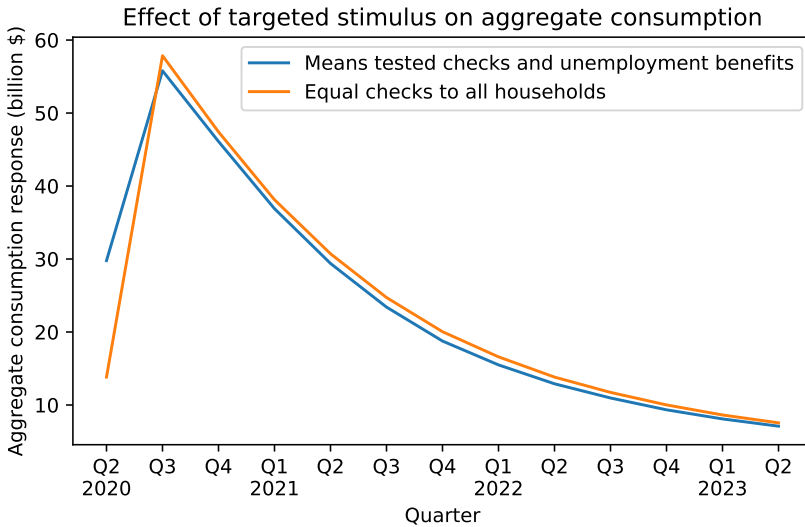


Figure 7 Aggregate Consumption Effect of Stimulus Checks vs Unemployment Benefits



Covid Economics 10, 27 April 2020: 67-91

Figure 8 Effect of Targeting the CARES Act Consumption Stimulus



Covid Economics 10, 27 April 2020: 67-91

B Alternative Scenario: Long, Deep Pandemic

Given the uncertainty about how long and deep the current recession will be, we investigate a more pessimistic scenario in which the lockdown is expected to last for four quarters. In addition, the unemployment rate will increase to 20 percent, consisting of 15 percent of deeply unemployed and 5 percent of normal unemployed. In this scenario we compare how effectively the CARES package stimulates consumption, also considering a more generous plan in which the unemployment benefits continue until the lockdown is over. We model the receipt of unemployment benefits each quarter as an unexpected shock, representing a series of policy renewals.

Figure 9 compares the effects of the two fiscal stimulus scenarios on income. The persistently high unemployment results in a substantial and long drop in aggregate income (orange), compared to the no pandemic scenario. The CARES stimulus (green) provides only a short term support to income for the first two quarters. In contrast, the scenario with unemployment benefits extended as long as the lockdown lasts (red) keeps aggregate income elevated through the recession.

Figure 10 shows the implications of the two stimulus packages for aggregate consumption. The long lockdown causes a much longer decline in spending than the shorter lockdown in our primary scenario. In the shorter pandemic scenario (Figure 3) consumption returns to the baseline path after roughly one year, while in the long lockdown shown here the recovery takes around three years; that is, the CARES stimulus shortens the consumption drop to about 2 years. The scenario with extended unemployment benefits ensures that aggregate spending returns to the baseline path after roughly one year, and does so by targeting the funds to the people who are worst hurt by the crisis and to whom the cash will make the most difference.

Figure 9 Labor and Transfer Income During the Long, Four-Quarter Pandemic

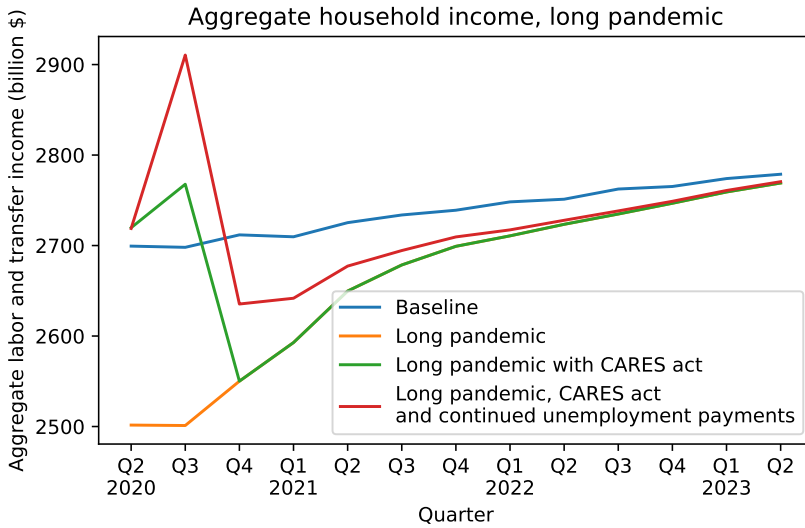
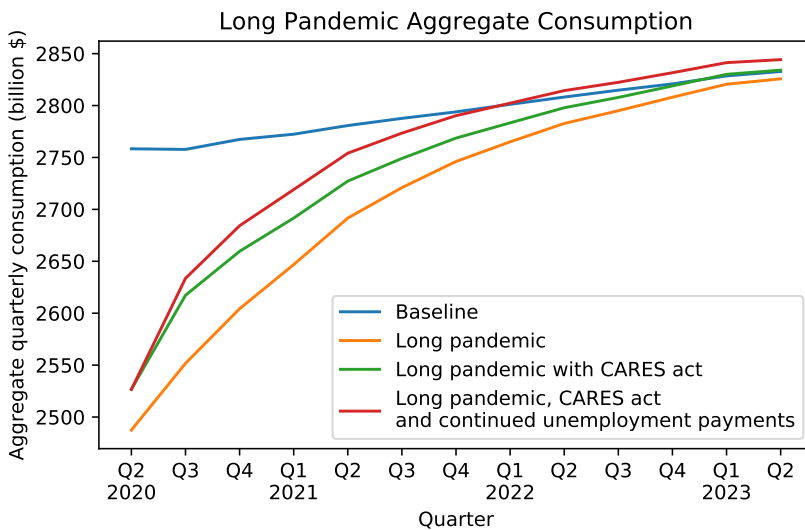


Figure 10 Consumption Response to the Long, Four-Quarter Pandemic



Covid Economics 10, 27 April 2020: 67-91

IV Conclusions

Our model suggests that there may be a strong consumption recovery when the social-distancing requirements of the pandemic begin to subside. We invite readers to test the robustness of this conclusion by using the associated software toolkit to choose their own preferred assumptions on the path of the pandemic, and of unemployment, to understand better how consumption will respond.

One important limitation of our analysis is that it does not incorporate Keynesian demand effects or other general equilibrium responses to the consumption fluctuations we predict. In practice, Keynesian effects are likely to cause movements in aggregate income in the same direction as consumption; in that sense, our estimates can be thought of as a “first round” analysis of the dynamics of the crisis, which will be amplified by any Keynesian response. (See Bayer, Born, Luetticke, and Müller (2020) for estimates of the multiplier for transfer payments). These considerations further strengthen the case that the CARES Act will make a substantial difference to the economic outcome. A particularly important consideration is that forward-looking firms that expect consumer demand to return forcefully in the third and fourth quarters of 2020 are more likely to maintain relations with their employees so that they can restart production quickly.

The ability to incorporate Keynesian demand effects is one of the most impressive achievements of the generation of heterogeneous agent macroeconomic models that have been constructed in the last few years. But the technical challenges of constructing those models are such that they cannot yet incorporate realistic treatments of features that our model says are quantitatively important, particularly differing risks of (and types of) unemployment, for different kinds of people (young, old; rich, poor; high- and low-education). This rich heterogeneity is important both to the overall response to the CARES act, and to making judgments about the extent to which it has been targeted to provide benefits to those who need them most. A fuller analysis that incorporates both the kinds of heterogeneity that are of interest to policymakers and a satisfying treatment of general equilibrium will have to wait for another day, but that day is likely not far off.

References

- ADAMS-PRASSL, ABI, TEODORA BONEVA, MARTA GOLIN, AND CHRISTOPHER RAUH (2020): “Inequality in the Impact of the Coronavirus Shock: New Survey Evidence for the US,” mimeo, Oxford University.
- ALVAREZ, FERNANDO, DAVID ARGENTE, AND FRANCESCO LIPPI (2020): “A Simple Planning Problem for COVID-19 Lockdown,” BFI working paper 34, University of Chicago.
- ANDERSEN, ASGER LAU, EMIL TOFT HANSEN, NIELS JOHANNESSEN, AND ADAM SHERIDAN (2020): “Consumer Responses to the COVID-19 Crisis: Evidence from Bank Account Transaction Data,” *Covid Economics*, 7, 88–111.
- ARMANTIER, OLIVIER, GIZEM KOSAR, RACHEL POMERANTZ, DAPHNE SKANDALIS, KYLE SMITH, GIORGIO TOPA, AND WILBERT VAN DER KLAUW (2020): “Coronavirus Outbreak Sends Consumer Expectations Plummeting,” URL link retrieved on 04/07/2020 [here](#).
- BAKER, SCOTT R., R. A. FARROKHANIA, STEFFEN MEYER, MICHAELA PAGEL, AND CONSTANTINE YANNELIS (2020): “How Does Household Spending Respond to an Epidemic? Consumption During the 2020 COVID-19 Pandemic,” working paper 26949, National Bureau of Economic Research.

- BAYER, CHRISTIAN, BENJAMIN BORN, RALPH LUETTICKE, AND GERNOT J. MÜLLER (2020): “The Coronavirus Stimulus Package: How Large Is the Transfer Multiplier?,” discussion paper 14600, CEPR.
- BICK, ALEXANDER, AND ADAM BLANDIN (2020): “Real Time Labor Market Estimates During the 2020 Coronavirus Outbreak,” Working paper, Arizona State University.
- BLOOMBERG (2020a): “Mnuchin Warns Virus Could Yield 20% Jobless Rate Without Action,” Press article, Bloomberg.
- (2020b): “U.S. Jobless Rate May Soar to 30%, Fed’s Bullard Says,” Press article, Bloomberg.
- BRODA, CHRISTIAN, AND JONATHAN A. PARKER (2014): “The Economic Stimulus Payments of 2008 and the Aggregate Demand for Consumption,” *Journal of Monetary Economics*, 68(S), 20–36.
- BROWN, JEFFREY, JEFFREY B. LIEBMAN, AND JOSHUA POLLETT (2002): “Estimating Life Tables That Reflect Socioeconomic Differences in Mortality,” in *The Distributional Aspects of Social Security and Social Security Reform*, ed. by Martin Feldstein, and Jeffrey B. Liebman, pp. 447–457. University of Chicago Press.
- CAGETTI, MARCO (2003): “Wealth Accumulation Over the Life Cycle and Precautionary Savings,” *Journal of Business and Economic Statistics*, 21(3), 339–353.
- CARROLL, CHRISTOPHER D. (2006): “The Method of Endogenous Gridpoints for Solving Dynamic Stochastic Optimization Problems,” *Economics Letters*, 91(3), 312–320.
- CARROLL, CHRISTOPHER D., EDMUND CRAWLEY, JIRI SLACALEK, KIICHI TOKUOKA, AND MATTHEW N. WHITE (2020): “Sticky Expectations and Consumption Dynamics,” *American Economic Journal: Macroeconomics*, Forthcoming.
- CARROLL, CHRISTOPHER D., JIRI SLACALEK, KIICHI TOKUOKA, AND MATTHEW N. WHITE (2017): “The Distribution of Wealth and the Marginal Propensity to Consume,” *Quantitative Economics*, 8, 977–1020, At <http://econ.jhu.edu/people/ccarroll/papers/cstwMPC>.
- CARROLL, CHRISTOPHER D., MATTHEW N WHITE, AND TEAM ECON-ARK (2017): “econ-ark/HARK: 0.8.0,” Available at via doi:10.5281/zenodo.1001068 or at <https://doi.org/10.5281/zenodo.1001068>.
- CARVALHO, V.M, J.R. GARCIA, S. HANSEN, A. ORTIZ, T. RODRIGO, J.V. MORA RODRIGUEZ, AND J. RUIZ (2020): “Tracking the COVID-19 Crisis with High-Resolution Transaction Data,” Discussion paper, Cambridge University.
- CORREIA, SERGIO, STEPHAN LUCK, AND EMIL VERNER (2020): “Pandemics Depress the Economy, Public Health Interventions Do Not: Evidence from the 1918 Flu,” mimeo, MIT Sloan.
- CYRANOSKI, DAVID (2020): “‘We need to be alert’: Scientists fear second coronavirus wave as China’s lockdowns ease,” *Nature*.
- EICHENBAUM, MARTIN S., SERGIO REBELO, AND MATHIAS TRABANDT (2020): “The Macroeconomics of Epidemics,” working paper 26882, National Bureau of Economic Research.
- FARIA-E-CASTRO, MIGUEL (2020a): “Back-of-the-Envelope Estimates of Next Quarter’s Unemployment Rate,” Blog post, Federal Reserve Bank, St. Louis.
- (2020b): “Fiscal Policy during a Pandemic,” *Covid Economics*, 2, 67–101.

- GASCON, CHARLES (2020): “COVID-19: Which Workers Face the Highest Unemployment Risk?,” Blog post, Federal Reserve Bank, St. Louis.
- GLOVER, ANDREW, JONATHAN HEATHCOTE, DIRK KRUEGER, AND JOSÉ-VÍCTOR RÍOS-RULL (2020): “Health versus Wealth: On the Distributional Effects of Controlling a Pandemic,” *Covid Economics*, 6, 22–64.
- GUERRIERI, VERONICA, GUIDO LORENZONI, LUDWIG STRAUB, AND IVAN WERNING (2020): “Macroeconomic Implications of COVID-19: Can Negative Supply Shocks Cause Demand Shortages?,” working paper 26918, National Bureau of Economic Research.
- HAI, RONG, DIRK KRUEGER, AND ANDREW POSTLEWAITE (2013): “On the Welfare Cost of Consumption Fluctuations in the Presence of Memorable Goods,” working paper 19386, National Bureau of Economic Research.
- HAVRANEK, TOMAS, MAREK RUSNAK, AND ANNA SOKOLOVA (2017): “Habit formation in consumption: A meta-analysis,” *European Economic Review*, 95, 142–167.
- JORDA, OSCAR, SANJAY R. SINGH, AND ALAN M. TAYLOR (2020): “Longer-run Economic Consequences of Pandemics,” *Covid Economics*, 1, 1–15.
- JPMORGAN (2020): “Fallout from COVID-19: Global Recession, Zero Interest Rates and Emergency Policy Actions,” Blog post, JPMorgan.
- KAPLAN, GREG, BENJAMIN MOLL, AND GIOVANNI L. VIOLANTE (2020): “Pandemics According to HANK,” mimeo, Princeton University.
- KRUEGER, DIRK, KURT MITMAN, AND FABRIZIO PERRI (2016): “Macroeconomics and Household Heterogeneity,” *Handbook of Macroeconomics*, 2, 843–921.
- KRUGMAN, PAUL (2020): “Notes on Coronacoma Economics,” mimeo, City University of New York.
- LEIBOVICI, FERNANDO, AND ANA MARIA SANTACREU (2020): “Social Distancing and Contact-Intensive Occupations,” Blog post, Federal Reserve Bank, St. Louis.
- PARKER, JONATHAN A. (2017): “Why Don’t Households Smooth Consumption? Evidence from a \$25 Million Experiment,” *American Economic Journal: Macroeconomics*, 4(9), 153–183.
- PARKER, JONATHAN A, NICHOLAS S SOULELES, DAVID S JOHNSON, AND ROBERT MCCLELLAND (2013): “Consumer spending and the economic stimulus payments of 2008,” *The American Economic Review*, 103(6), 2530–2553.
- SABELHAUS, JOHN, AND JAE SONG (2010): “The Great Moderation in Micro Labor Earnings,” *Journal of Monetary Economics*, 57(4), 391–403.
- SWAGEL, PHILL (2020): “Updating CBO’s Economic Forecast to Account for the Pandemic,” Blog post, Congressional Budget Office.

Appendices

A Model Details

The baseline model is adapted and expanded from Carroll, Slacalek, Tokuoka, and White (2017). The economy consists of a continuum of expected utility maximizing households with a common CRRA utility function over consumption, $u(\mathbf{c}, \eta) = \eta \mathbf{c}^{1-\rho} / (1-\rho)$, where η is a marginal utility shifter. Households are *ex ante* heterogeneous: household i has a quarterly time discount factor $\beta_i \leq 1$ and an education level $e_i \in \{D, HS, C\}$ (for dropout, high school, and college, respectively). Each quarter, the household receives (after tax) income, chooses how much of their market resources \mathbf{m}_{it} to consume \mathbf{c}_{it} and how much to retain as assets \mathbf{a}_{it} ; they then transition to the next quarter by receiving shocks to mortality, income, their employment state, and their marginal utility of consumption.

For each education group e , we assign a uniform distribution of time preference factors between $\beta_e - \nabla$ and $\beta_e + \nabla$, chosen to match the distribution of liquid wealth and retirement assets. Specifically, the calibrated values in Table A1 fit the ratio of liquid wealth to permanent income in aggregate for each education level, as computed from the 2004 Survey of Consumer Finance. The width of the distribution of discount factors was calibrated to minimize the difference between simulated and empirical Lorenz shares of liquid wealth for the bottom 20%, 40%, 60%, and 80% of households, as in Carroll, Slacalek, Tokuoka, and White (2017).

When transitioning from one period to the next, a household with education e that has already lived for j periods faces a D_{ej} probability of death. The quarterly mortality probabilities are calculated from the Social Security Administration's actuarial table (for annual mortality probability) and adjusted for education using Brown, Liebman, and Pollett (2002); a household dies with certainty if it (improbably) reaches the age of 120 years. The assets of a household that dies are completely taxed by the government to fund activities outside the model. Households who survive to period $t + 1$ experience a return factor of R on their assets, assumed constant.

Household i 's state in period t , at the time it makes its consumption–saving decision, is characterized by its age j ,¹⁴ a level of market resources $\mathbf{m}_{it} \in \mathbb{R}_+$, a permanent income level $\mathbf{p}_{it} \in \mathbb{R}_{++}$, a discrete employment state $\ell_{it} \in \{0, 1, 2\}$ (indicating whether the individual is employed, normal unemployed, or deeply unemployed), and a discrete state $\eta_{it} \in \{1, \underline{\eta}\}$ that represents whether its marginal utility of consumption has been temporarily reduced ($\underline{\eta} < 1$). Denote the joint discrete state as $n_{it} = (\ell_{it}, \eta_{it})$.

Each household inelastically participates in the labor market when it is younger than 65 years ($j < 164$) and retires with certainty at age 65. The transition from working life to retirement is captured in the model by a one time large decrease in permanent income at age $j = 164$.¹⁵ Retired households face essentially no income risk: they receive Social Security benefits equal to their permanent income with 99.99% probability and miss their check otherwise; their permanent income very slowly degrades as they age. The discrete employment state ℓ_{it} is irrelevant for retired households.

Labor income for working age households is subject to three risks: unemployment, permanent income shocks, and transitory income shocks. Employed ($\ell_{it} = 0$) households' permanent income grows by age-education-conditional factor Γ_{ej} on average, subject to a mean one lognormal permanent income shock ψ_{it} with age-conditional underlying standard deviation of σ_{ψ_j} . The household's labor income \mathbf{y}_{it} is also subject to a mean one lognormal transitory shock ξ_{it}

¹⁴Households enter the model aged 24 years, so model age $j = 0$ corresponds to being 24 years, 0 quarters old.

¹⁵The size of the decrease depends on education level, very roughly approximating the progressive structure of Social Security: $\Gamma_{D164} \approx 0.56$, $\Gamma_{HS164} \approx 0.44$, $\Gamma_{C164} \approx 0.31$.

with age-conditional underlying standard deviation of σ_{ξ_j} . The age profiles of permanent and transitory income shock standard deviations are approximated from the results of Sabelhaus and Song (2010), and the expected permanent income growth factors are adapted from Cagetti (2003). Normal unemployed and deeply unemployed households receive unemployment benefits equal to a fraction $\underline{\xi} = 0.3$ of their permanent income, $\mathbf{y}_{it} = \underline{\xi}\mathbf{p}_{it}$; they are not subject to permanent nor transitory income risk, but their permanent income degrades at rate $\underline{\Gamma}$, representing “skill rot”.¹⁶

The income process for a household can be represented mathematically as:

$$\mathbf{p}_{it} = \begin{cases} \psi_{it}\Gamma_{ej}\mathbf{p}_{it-1} & \text{if } \ell_{it} = 0, j < 164 & \text{Employed, working age} \\ \underline{\Gamma}\mathbf{p}_{it-1} & \text{if } \ell_{it} > 0, j < 164 & \text{Unemployed, working age} \\ \Gamma_{ret}\mathbf{p}_{it-1} & \text{if } j \geq 164 & \text{Retired} \end{cases}$$

$$\mathbf{y}_{it} = \begin{cases} \xi_{it}\mathbf{p}_{it} & \text{if } \ell_{it} = 0, j < 164 & \text{Employed, working age} \\ \underline{\xi}\mathbf{p}_{it} & \text{if } \ell_{it} > 0, j < 164 & \text{Unemployed, working age} \\ \mathbf{p}_{it} & \text{if } j \geq 164 & \text{Retired} \end{cases}$$

A working-age household’s employment state ℓ_{it} evolves as a Markov process described by the matrix Ξ , where element k, k' of Ξ is the probability of transitioning from $\ell_{it} = k$ to $\ell_{it+1} = k'$. During retirement, all households have $\ell_{it} = 0$ (or any other trivializing assumption about the “employment” state of the retired). We assume that households treat $\Xi_{0,2}$ and $\Xi_{1,2}$ as zero: they do not consider the possibility of ever attaining the deep unemployment state $\ell_{it} = 2$ from “normal” employment or unemployment, and thus it does not affect their consumption decision in those employment states.

We specify the unemployment rate during normal times as $\bar{U} = 5\%$, and the expected duration of an unemployment spell as 1.5 quarters. The probability of transitioning from unemployment back to employment is thus $\Xi_{1,0} = \frac{2}{3}$, and the probability of becoming unemployed is determined as the flow rate that offsets this to generate 5% unemployment (about 3.5%). The deeply unemployed expect to be unemployed for *much* longer: we specify $\Xi_{2,0} = 0$ and $\Xi_{2,1} = \frac{1}{3}$, so that a deeply unemployed person remains so for three quarters on average before becoming “normal” unemployed (they cannot transition directly back to employment). Thus the unemployment spell for a deeply unemployed worker is 2 quarters at a minimum and 4.5 quarters on average.¹⁷

Like the prospect of deep unemployment, the possibility that consumption might become less appealing (via marginal utility scaling factor $\eta_{it} < 1$) does not affect the decision-making process of a household in the normal $\eta_{it} = 1$ state. If a household does find itself with $\eta_{it} = \underline{\eta}$, this condition is removed (returning to the normal state) with probability 0.5 each quarter; the evolution of the marginal utility scaling factor is represented by the Markov matrix H . In this way, the consequences of a pandemic are fully unanticipated by households, a so-called “MIT shock”; households act optimally once in these states, but did not account for them in their consumption–saving problem during “normal” times.¹⁸

¹⁶Unemployment is somewhat persistent in our model, so the utility risk from receiving 15% of permanent income for one quarter (as in Carroll, Slacalek, Tokunaka, and White (2017)) is roughly the same as the risk of receiving 30% of permanent income for 1.5 quarters in expectation.

¹⁷Our computational model allows for workers’ beliefs about the average duration of deep unemployment to differ from the true probability. However, we do not present results based on this feature and thus will not further clutter the notation by formalizing it here.

¹⁸Our computational model also allows households’ beliefs about the duration of the reduced marginal utility state (via social distancing) to deviate from the true probability. The code also permits the possibility that the reduction in marginal utility is lifted as an aggregate or shared outcome, rather than idiosyncratically. We do not present results utilizing these features here, but invite the reader to investigate their predicted consequences using our public repository.

The household's permanent income level can be normalized out of the problem, dividing all boldface variables (absolute levels) by the individual's permanent income \mathbf{p}_{it} , yielding non-bold normalized variables, e.g., $m_{it} = \mathbf{m}_{it}/\mathbf{p}_{it}$. Thus the only state variables that affect the choice of optimal consumption are normalized market resources m_{it} and the discrete Markov states n_{it} . After this normalization, the household consumption functions $c_{e,j}$ satisfy:

$$\begin{aligned} v_{e,j}(m_{it}, n_{it}) &= \max_{c_{e,j}} u(c_{e,j}(m_{it}, n_{it}), \eta_{it}) + \beta_i(1 - D_{e,j}) \mathbb{E}_t \left[\widehat{\Gamma}_{it+1}^{1-\rho} v_{e,j+1}(m_{it+1}, n_{it+1}) \right] \\ &\text{s.t.} \\ a_{it} &= m_{it} - c_{e,j}(m_{it}, n_{it}), \\ m_{it+1} &= (R/\widehat{\Gamma}_{it+1})a_{it} + y_{it}, \\ n_{it+1} &\sim (\Xi, H), \\ a_{it} &\geq 0, \end{aligned}$$

where $\widehat{\Gamma}_{it+1} = \mathbf{p}_{it+1}/\mathbf{p}_{it}$, the realized growth rate of permanent income from period t to $t + 1$. Consumption function $c_{e,j}$ yields optimal *normalized* consumption, the ratio of consumption to the household's permanent income level; the actual consumption level is simply $\mathbf{c}_{it} = \mathbf{p}_{it}c_{e,j}(m_{it}, n_{it})$.

Starting from the terminal model age of $j = 384$, representing being 120 years old (when the optimal choice is to consume all market resources, as death is certain), we solve the model by backward induction using the endogenous grid method, originally presented in Carroll (2006). Substituting the definition of next period's market resources into the maximand, the household's problem can be rewritten as:

$$\begin{aligned} v_{e,j}(m_{it}, n_{it}) &= \max_{c_{it} \in \mathbb{R}_+} u(c_{it}, \eta_{it}) + \beta_i(1 - D_{e,j}) \mathbb{E}_t \left[\widehat{\Gamma}_{it+1}^{1-\rho} v_{e,j+1}((R/\widehat{\Gamma}_{it+1})a_{it} + y_{it}, n_{it+1}) \right] \\ &\text{s.t. } a_{it} = m_{it} - c_{it}, \quad a_{it} \geq 0, \quad n_{it+1} \sim (\Xi, H). \end{aligned}$$

This problem has one first order condition, which is both necessary and sufficient for optimality. It can be solved to yield optimal consumption as a function of (normalized) end-of-period assets and the Markov state:

$$\underbrace{\eta_{it} c_{it}^{-\rho}}_{= \frac{\partial u}{\partial c}} - \underbrace{\beta_i R(1 - D_{e,j}) \mathbb{E}_t \left[\widehat{\Gamma}_{it+1}^{-\rho} v_{e,j+1}^m((R/\widehat{\Gamma}_{it+1})a_{it} + y_{it}, n_{it+1}) \right]}_{\equiv v_{e,j}^a(a_{it}, n_{it})} = 0 \implies c_{it} = \left(\frac{v_{e,j}^a(a_{it}, n_{it})}{\eta_{it}} \right)^{-\frac{1}{\rho}}.$$

To solve the age- j problem numerically, we specify an exogenous grid of end-of-period asset values $a \geq 0$, compute end-of-period marginal value of assets at each gridpoint (and each discrete Markov state), then calculate the unique (normalized) consumption that is consistent with ending the period with this quantity of assets while acting optimally. The beginning-of-period (normalized) market resources from which this consumption was taken is then simply $m_{it} = a_{it} + c_{it}$, the *endogenous gridpoint*. We then linearly interpolate on this set of market resources-consumption pairs, adding an additional bottom gridpoint at $(m_{it}, c_{it}) = (0, 0)$ to represent the liquidity-constrained portion of the consumption function $c_{e,j}(m_{it}, n_{it})$.

The standard envelope condition applies in this model, so that the marginal value of market resources equals the marginal utility of consumption when consuming optimally:

$$v_{e,j}^m(m_{it}, n_{it}) = \eta_{it} c_{e,j}(m_{it}, n_{it})^{-\rho}.$$

The marginal value function for age j can then be used to solve the age $j - 1$ problem, iterating backward until the initial age $j = 0$ problem has been solved.

When the pandemic strikes, we draw a new employment state (employed, unemployed, deeply unemployed) for each working age household using a logistic distribution. For each household i at $t = 0$ (the beginning of the pandemic and lockdown), we compute logistic weights for the employment states as:

$$\mathbb{P}_{i,\ell} = \alpha_{\ell,e} + \alpha_{\ell,p} \mathbf{P}_{i0} + \alpha_{\ell,j} j_{i0} \quad \text{for } \ell \in \{1, 2\}, \quad \mathbb{P}_{i,0} = 0,$$

where $e \in \{D, H, C\}$ for dropouts, high school graduates, and college graduates and j is the household's age. The probability that household i draws employment state $\ell \in \{0, 1, 2\}$ is then calculated as:

$$\Pr(\ell_{it} = \ell) = \exp(\mathbb{P}_{i,\ell}) / \sum_{k=0}^2 \exp(\mathbb{P}_{i,k}).$$

Our chosen logistic parameters are presented in Table A2.

B Aggregation

Households are modeled as individuals and incomes sized accordingly. We completely abstract from family dynamics. To get our aggregate predictions for income and consumption, we take the mean from our simulation and multiply by 253 million, the number of adults (over 18) in the United States in 2019. To size the unemployment benefits correctly, we multiply the benefits per worker by 0.8 to account for the fact that 20 percent of the working-age population is out of the labor force, so the average working-age household consists of 0.8 workers and 0.2 non-workers. With this adjustment, there are 151 million workers eligible for unemployment benefits in the model. Aggregate consumption in our baseline for 2020 is just over \$11 trillion, a little less than total personal consumption expenditure, accounting for the fact that some consumption does not fit in the usual budget constraint.¹⁹ Aggregating in this way underweights the young, as our model excludes those under the age of 24.

Our model estimates the aggregate size of the stimulus checks to be \$267 billion, matching the the Joint Committee on Taxation's estimate of disbursements in 2020.²⁰ This is somewhat of a coincidence: we overestimate the number of adults who will actually receive the stimulus, while excluding the \$500 payment to children.

The aggregate cost of the extra unemployment benefits depends on the expected level of unemployment. Our estimate is \$137 billion, much less than the \$260 billion mentioned in several press reports, but in line with the extent of unemployment in our pandemic scenario. We do not account for the extension of unemployment benefits to the self-employed and gig workers.

Households enter the model at age $j = 0$ with zero liquid assets. A 'newborn' household has its initial permanent income drawn lognormally with underlying standard deviation of 0.4 and an education-conditional mean. The initial employment state of households matches the steady state unemployment rate of 5%.²¹

We assume annual population growth of 1%, so older simulated households are appropriately down-weighted when we aggregate idiosyncratic values. Likewise, each successive cohort is

¹⁹PCE consumption in Q4 2019, from the NIPA tables, was \$14.8 trillion. Market based PCE, a measure that excludes expenditures without an observable price was \$12.9 trillion. Health care, much of which is paid by employers and not in the household's budget constraint, was \$2.5 trillion.

²⁰The JCT's 26 March 2020 publication JCX-11-20 predicts disbursements of \$267 billion in 2020, followed by \$24 billion in 2021.

²¹This is the case even during the pandemic and lockdown, so the death and replacement of simulated agents is a second order contribution to the profile of the unemployment rate.

slightly more productive than the last, with aggregate productivity growing at a rate of 1% per year. The profile of average income by age in the population at any moment in time thus has more of an inverted-U shape than implied by the permanent income profiles from Cagetti (2003).

Table A1 Parameter Values in the Baseline Model

Description	Parameter	Value
Coefficient of relative risk aversion	ρ	1
Mean discount factor, high school dropout	β_D	0.9637
Mean discount factor, high school graduate	β_{HS}	0.9705
Mean discount factor, college graduate	β_C	0.9756
Discount factor band (half width)	∇	0.0253
Employment transition probabilities:		
– from normal unemployment to employment	$\Xi_{1,0}$	2/3
– from deep unemployment to normal unemployment	$\Xi_{2,1}$	1/3
– from deep unemployment to employment	$\Xi_{2,0}$	0
Proportion of high school dropouts	θ_D	0.11
Proportion of high school graduates	θ_{HS}	0.55
Proportion of college graduates	θ_C	0.34
Average initial permanent income, dropout	\bar{p}_{D0}	5000
Average initial permanent income, high school	\bar{p}_{HS0}	7500
Average initial permanent income, college	\bar{p}_{C0}	12000
Steady state unemployment rate	\bar{U}	0.05
Unemployment insurance replacement rate	ξ	0.30
Skill rot of all unemployed	$\bar{\Gamma}$	0.995
Quarterly interest factor	R	1.01
Population growth factor	N	1.0025
Technological growth factor	λ	1.0025

Table A2 Pandemic Assumptions

Description	Parameter	Value
Short-lived Pandemic		
Logistic parametrization of unemployment probabilities		
Constant for dropout, regular unemployment	$\alpha_{1,D}$	-1.15
Constant for dropout, deep unemployment	$\alpha_{2,D}$	-1.5
Constant for high school, regular unemployment	$\alpha_{1,H}$	-1.3
Constant for high school, deep unemployment	$\alpha_{2,H}$	-1.75
Constant for college, regular unemployment	$\alpha_{1,C}$	-1.65
Constant for college, deep unemployment	$\alpha_{2,C}$	-2.2
Coefficient on permanent income, regular unemployment	$\alpha_{1,p}$	-0.1
Coefficient on permanent income, deep unemployment	$\alpha_{2,p}$	-0.2
Coefficient on age, regular unemployment	$\alpha_{1,j}$	-0.01
Coefficient on age, deep unemployment	$\alpha_{2,j}$	-0.01
Marginal Utility Shock		
Pandemic utility factor	η	0.891
Prob. exiting pandemic each quarter	$\bar{H}_{1,0}$	0.5
Long, Deep Pandemic		
Logistic parametrization of unemployment probabilities		
Constant for dropout, regular unemployment	$\alpha_{1,D}$	-1.45
Constant for dropout, deep unemployment	$\alpha_{2,D}$	-0.3
Constant for high school, regular unemployment	$\alpha_{1,H}$	-1.6
Constant for high school, deep unemployment	$\alpha_{2,H}$	-0.55
Constant for college, regular unemployment	$\alpha_{1,C}$	-1.95
Constant for college, deep unemployment	$\alpha_{2,C}$	-1.00
Coefficient on permanent income, regular unemployment	$\alpha_{1,p}$	-0.2
Coefficient on permanent income, deep unemployment	$\alpha_{2,p}$	-0.2
Coefficient on age, regular unemployment	$\alpha_{1,j}$	-0.01
Coefficient on age, deep unemployment	$\alpha_{2,j}$	-0.01
Marginal Utility Shock		
Pandemic utility factor	η	0.891
Prob. exiting pandemic each quarter	$\bar{H}_{1,0}$	0.25

Table A3 Fiscal Stimulus Assumptions, CARES Act

Description	Value
Stimulus check	\$1,200
Means test start (annual)	\$75,000
Means test end (annual)	\$99,000
Stimulus check delay	1 quarter
Fraction that react on announcement	0.25
Extra unemployment benefit for:	
Normal unemployed	\$5,200
Deeply unemployed	\$7,800

Note: The unemployment benefits are multiplied by 0.8 to account for the fact that 20 percent of the working age population is out of the labor force. See aggregation details in Appendix B.

The natural and unnatural histories of Covid-19 contagion

Michael Beenstock¹ and Xieer Dai²

Date submitted: 19 April 2020; Date accepted: 21 April 2020

We study the epidemiology of Covid-19 using an overlapping-generations method in which successive cohorts of infectives are temporarily contagious. We use this method to estimate RO (natural rate of contagion) and Re (effective rate of contagion) for Covid-19 in various countries and over time using data on confirmed morbidity and estimates of unconfirmed morbidity. We use these estimates to study the effect of mitigation policy on Re . We show that even in the absence of mitigation policy Re tends to decrease by week 3 of the epidemic due to endogenous social distancing. Several methods for estimating the treatment effect of mitigation policy on R suggest that mitigation policy accelerates the decrease in Re . A "Chinese crystal ball" method is proposed for projecting and simulating contagion with an empirical illustration for Israel.

¹ Professor of Economics (emeritus), Hebrew University of Jerusalem.

² PhD candidate Department of Geography, Hebrew University of Jerusalem.

The natural history of contagion is expressed by the basic reproductive number R_0 , which is the average number of susceptibles that infectives are expected to infect until they cease to be contagious. However, the natural history of contagion is rarely observed because it is concealed by mitigating action undertaken by individuals and governments, such as quarantine, social distancing, travel restrictions and lockdown. The unnatural history of contagion, measured by the effective rate of contagion (R_e), is observed instead, which is inevitably smaller than its natural counterpart. This applies to Covid-19 in particular because in contrast to previous epidemics, mitigation policy has been unusually activist.

In this paper we make three contributions. First, we propose an "overlapping generations method" for calculating R . We argue that this method provides more reliable estimates of R than the canonical SIR (susceptible – infective – removed) method widely used by epidemiologists since 1927 (Bailey 1975). It also calculates R in real time. Second, the true number of infectives is typically much larger than the measured number due to delays in diagnosis and because carriers may be completely asymptomatic (Bendavid et al 2020). We propose a method to impute the true number of infectives from official data on infectives. Third, we study the causal effect of mitigation policy on R . We introduce the concept of "corona equilibrium" in which mitigation and R are mutually dependent. To resolve the identification problem for estimating treatment effects in corona equilibrium, we explore a number of methodologies, including triple differences-in-differences, vector autoregressions, and a leading indicator method, which we call the "Chinese crystal ball".

Measuring R in Real Time

Overlapping Generations Method

Let τ denote the infective period measured in days, and suppose that infectives are diagnosed immediately. "Corona time" begins on day 0 when the first infectives are diagnosed. We denote the true number of ever-infectives by C and corona days by t , hence C_0 is the initial number of infectives. We assume that the daily rate of contagion is R_0/τ so that after τ days infectives infect R_0 susceptibles, i.e. the temporal distribution of contagiousness is uniform. The number of new infectives on day 1 is $C_0 R_0/\tau$, so that the number of infectives at the end of day 1 is $C_1 = C_0$

+C₀R0/τ. Until t = τ the number of infectives is C_t = (1 + R0/τ)C_{t-1}. Repeated backward substitution implies that C_t = C₀(1 + R0/τ)^t and C_τ = C₀(1 + R0/τ)^τ.

On day τ + 1 the original infectives cease to be contagious. Henceforth, we distinguish between the ever-infected (C) and contagious carriers or infectives (C*). According to the "perpetual inventory method" the current number of contagious carriers equals the number diagnosed over the previous τ days. Hence, C_t^{*} = ∑_{j=0}^{τ-1} ΔC_{t-j} = C_t - C_{t-τ-1} = Δ_{1+τ}C_t. The number of ever-infected by the end of day τ + 1 is C_{τ+1} = (1 + R0/τ)(C_τ - C₀) where the last term is the number of infectives on day τ. By day 2τ all infectives up to day τ cease to be contagious. More generally, C_{τ+j} = (1 + R0/τ)(C_{τ+j-1} - ΔC_{j-1}), which implies that by day 2τ the number of ever-infected is:

$$C_{2\tau} = C_{\tau} \left(1 + \frac{R0}{\tau}\right)^{\tau} - \frac{R0}{\tau} \left(1 + \frac{R0}{\tau}\right)^{\tau-1} C_0 \quad (1)$$

Suppose initially there is only one infective (C₀ = 1), infectives are contagious for 14 days (τ = 14), and by the end of day 14 there are 70 infectives (C_τ = 70), the implicit value for R0 during the first "generation" is 4.9636, which is the average rate of infection during the first 14 days of the epidemic. If this rate of infection applied over the next 14 days, equation (1) implies that the number of ever-infected by the end of day 28 of the epidemic will be 4881.7. If the number of ever-infected is less than this, R0 during the second generation must have decreased. For example, if the number is 4000, equation (1) implies that R0 during days 14 – 28 is 4.6968 instead of 4.9636.

We have ignored the fact that the number of susceptibles decreases over time because in the early stages of epidemics the ever-infected constitute a tiny fraction of the population. More generally, however, if the least fit succumb first to the epidemic and the fittest succumb last, or even do not succumb at all, R would tend to decrease over time.

R0/τ refers to the daily rate of contagion (ROD), which varies directly with R0 and inversely with the duration of contagion (τ). The number of ever-infected obviously varies directly with the daily rate of contagion since:

$$\frac{\partial C_t}{\partial ROD} = \ln(1 + ROD) [C_t - (1 + ROD)C_{t-\tau-1}] > 0 \quad (2)$$

Where $t = \tau + j$. Equation (2) is positive because the term in square brackets is positive. Given ROD, the number of ever-infected varies directly, but perhaps less obviously, with the duration of contagion since:

$$\frac{\partial C_t}{\partial \tau} = ROD \ln(1 + ROD) C_{t-\tau-1} > 0 \tag{3}$$

Finally, when ROD is not given, the separate effects of R0 and are determined by:

$$dC_t = \ln(1 + ROD) (C_t - C_{t-\tau-1}) \frac{1}{\tau} (dR0 - RODd\tau) \tag{4}$$

The number of ever-infected varies directly with R0 and inversely with the duration of contagion (τ). The reason for this apparent paradox is that when τ increases, the daily rate of contagion (ROD) decreases. Therefore, what matters is not R0, but the daily rate of contagion and the duration of contagion.

In summary, the generating process for the number of ever-infected is:

$$C_t = \left(1 + \frac{R_{t-1}}{\tau}\right) C_{t-1} - \frac{R_{t-\tau-2}}{\tau} C_{t-\tau-2} \tag{5}$$

where R_{t-1} refers to the OLG estimate of the average number of susceptibles infected by the generation of carriers on day t-1 and $R_{t-\tau-2}$ is its counterpart for the previous generation.

The "doubling time" (the time in which C doubles) is equal to $\ln 2 / \ln(1 + ROD)$. For example, if $R0 = 3$ and $\tau = 14$ days, the doubling time is 3.23 days. The doubling time varies inversely with R and directly with τ . Doubling time has become a popular concept for measuring contagion during the corona epidemic.

OLG Estimates of R using Morbidity Data

Many health authorities have set isolation periods at two weeks, suggesting that τ is 14 days. However, clinical evidence suggests that viral shedding may have a mean of 20 days (Zhou et al 2020) and that contagiousness may not be uniformly distributed. Since OLG estimates the daily rate of contagion ($R0/\tau$), the estimate of R0 varies proportionately with τ . In the previous numerical example, in which the doubling time is 3.23 days, R0 would have been 4.286 instead of 3 if τ is 20 instead of 14 days. Hence, given the OLG estimate of ROD, R0 is proportionate to τ .

Figures 1 – 3 report rolling OLG estimates of R based on official morbidity data as of April 24 for a variety of countries and Chinese provinces assuming τ is 14 days. In Figures 1 and 2 time is measured in corona days where day 0 occurs when morbidity is 100 in large countries and proportionately smaller in less populated countries. This is why the last data point appears to refer to different days. In Figure 1 the epidemic occurred earliest in Italy and latest in Russia. In Figure 2 the epidemic occurred earliest in Singapore and latest in Sweden. In Figure 3A the horizontal axis is measured in calendar time. The epidemic occurred earliest in Hubei province and latest in Xingjiang province.

Although R in Figures 1 – 3 vary by country, they share a common dynamic profile. R initially increases steeply before decreasing gradually. Recall that if R exceeds 1 the number of infectives increases, and it decreases when R is less than 1. In the latter case, the battle is won. When R is zero the war is won. Several countries are on course for winning the battle, while the war appears to have been won in most provinces of China and in S. Korea. Japan and Singapore are exceptions in that R did not increase steeply, it has fluctuated around 1 in Japan, and it has increased gradually to 1.5 in Singapore.

Figure 1 Rates of Contagion

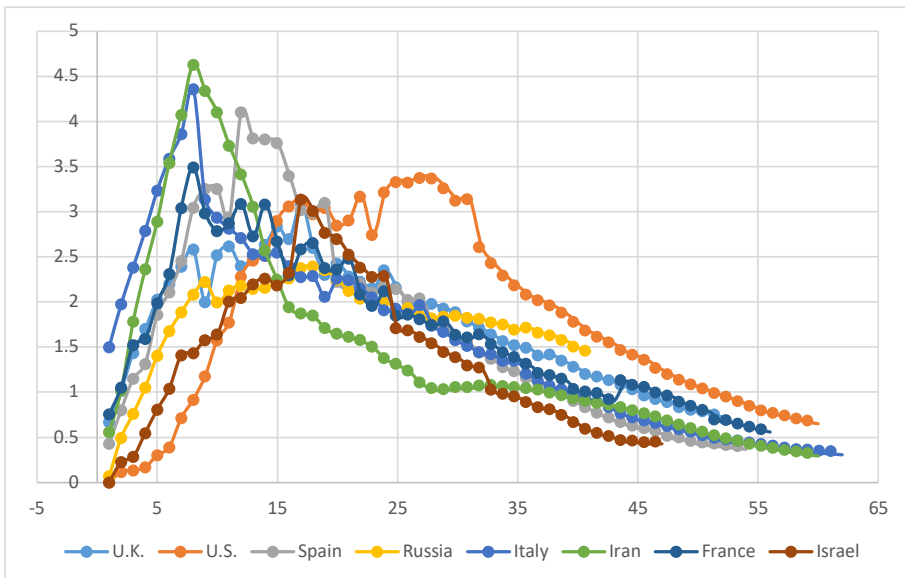
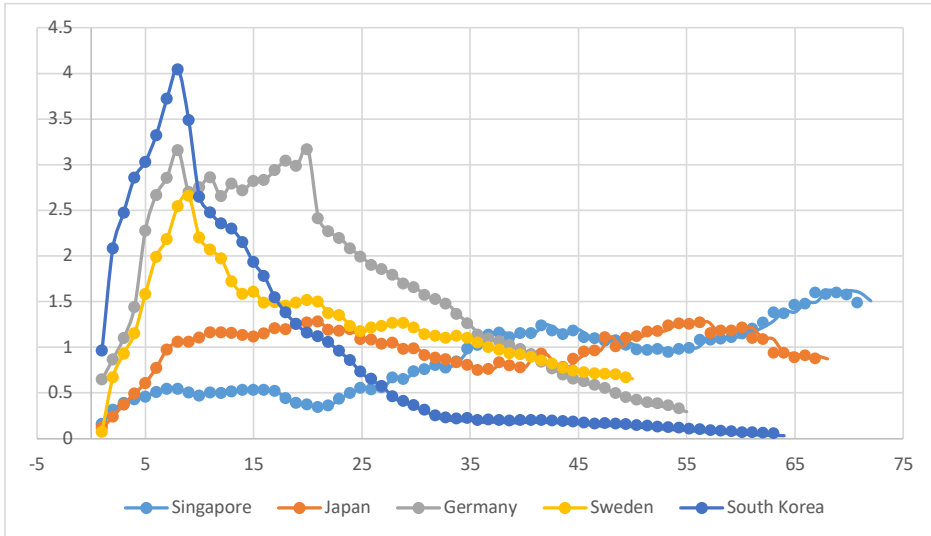


Figure 2 Rates of Contagion in Countries with Minimal Mitigation



Sweden has been a focus of international attention because she has undertaken minimal mitigation (Figure 6). Nevertheless, the dynamic profile for R has followed the international trend, and is currently less than 1. Unfortunately, Sweden is the only example. Hence, it is difficult to judge whether Sweden is an outlier, or whether it may serve as a counterfactual for what might have happened had countries not practiced mitigation, as discussed further below. Also, South Korea has followed a policy of mass testing and isolation, which has enabled it to reduce R to zero without intensive mitigation.

China has had the longest experience with Covid-19. Indeed, we argue below that in many respects, we may look to China to project the future course of the epidemic in other countries. In March, lockdown policy that had been in force since January 24 began to be reversed, and by late April had been reversed completely. Therefore, it is particularly interesting to ask whether the epidemic resurged subsequently. Figure 3B seems to suggest that in some provinces resurgence occurred, especially in Hong Kong and Inner Mongolia. However, almost all of this resurgence was imported because Chinese citizens abroad, who were unable to return to China beforehand, were allowed to return in March. Indeed, there have been few cases of indigenous contagion. In the vast majority of provinces R continues to be almost zero more than a month after the reversal of lockdown.

Figure 3A Rates of Contagion in China

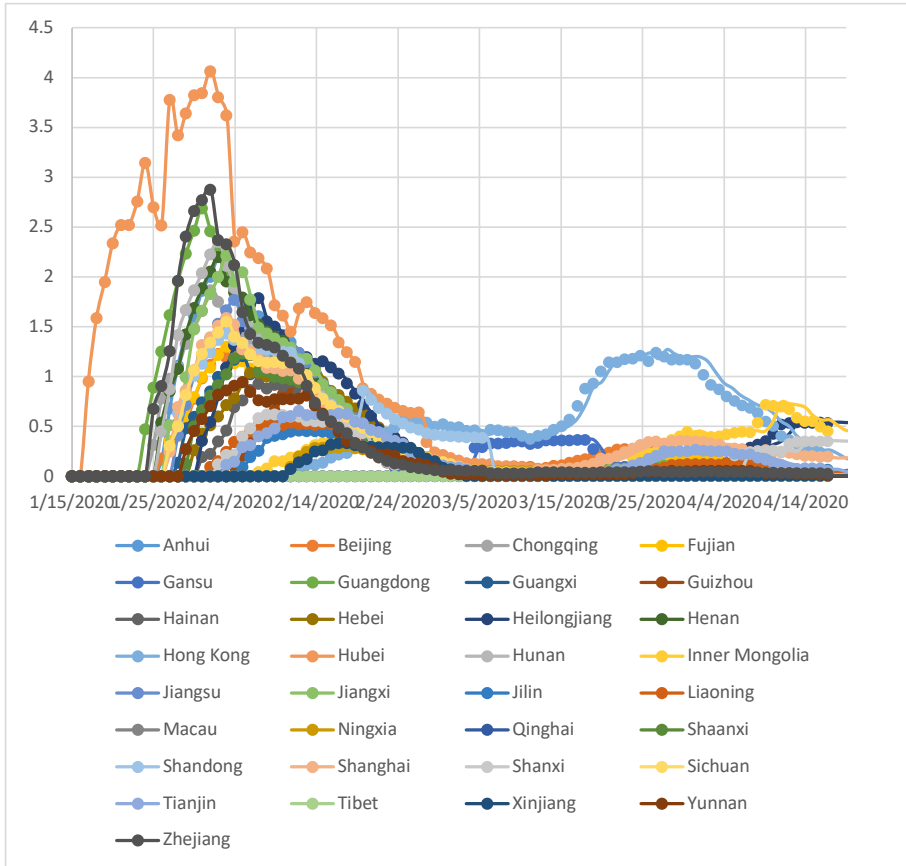
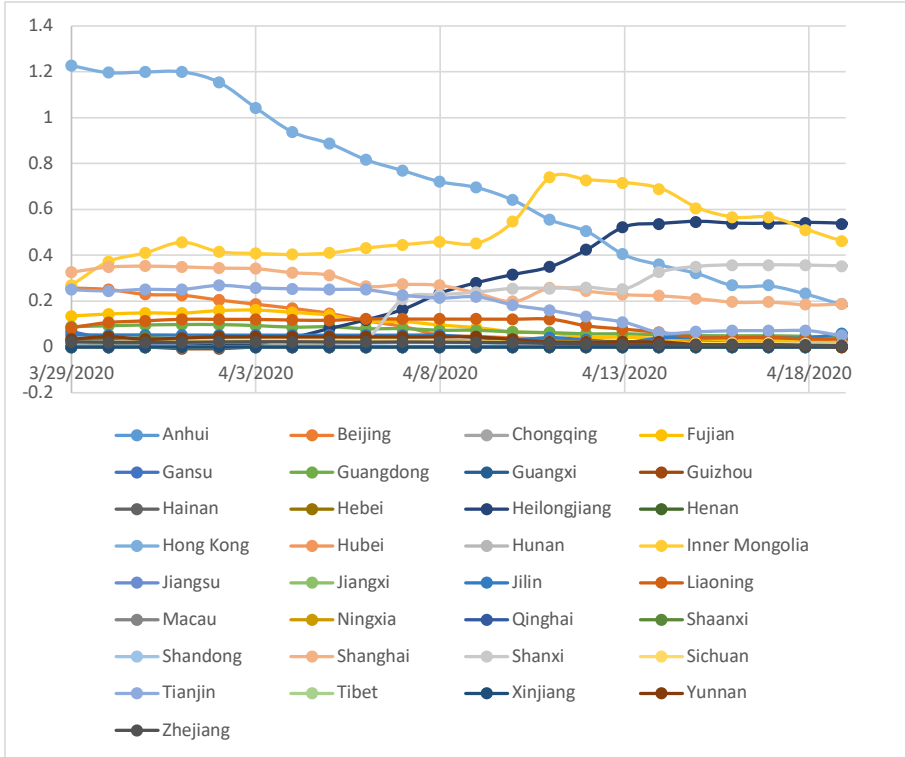


Figure 3B Contagion in China since the Reversal of Lockdown

Covid Economics 10, 27 April 2020: 92-120



Diagnostic Delay and Hidden Infectives

Suppose infectives are not diagnosed immediately so that the true number of ever-infected (C) is greater than the number of diagnosed infected denoted by D . We assume that a proportion ϕ of infectives are never diagnosed; they remain hidden as "corona zombies", and that on each day a proportion θ of other infectives become symptomatic and are diagnosed:

$$\Delta D_t = \theta[(1 - \phi)C_{t-1} - D_{t-1}] \quad (6)$$

The terms in square brackets is the backlog of asymptomatic and symptomatic infectives yet to be diagnosed. Note that θ will depend on the testing capacity of the health authorities.

The general solution for the number of diagnosed cases is:

$$D_t = A(1 - \theta)^t + \theta(1 - \phi) \sum_{j=0}^{t-1} (1 - \theta)^j C_{t-1-j} \quad (7)$$

Covid Economics 10, 27 April 2020: 92-120

Where A is an arbitrary constant determined by initial conditions D_0 , and C_t is determined as in equation (1). Equation (7) states the number of diagnosed infected lags behind the number of carriers, of whom some will never be diagnosed. If, for expositional simplicity there are C infectives, equation (7) simplifies to:

$$D_t = A(1 - \theta)^t + (1 - \phi)C \tag{8}$$

Where $A = D_0 - (1 - \phi)C$. Since $1 - \theta$ is a positive fraction and $\phi - 1$ is a negative fraction, equation (8) states that the number of diagnosed cases converges from below, as expected, to the number of non-hidden infectives. It implies that if x percent of them are diagnosed within d days θ would be:

$$\theta = 1 - \left[\frac{(1 - \phi)(x - 1)C}{A} \right]^{1/d} \tag{9}$$

If, according to the Director of CDC, 25 percent of infectives are corona zombies ($\phi = 0.25$), there are a hundred infectives ($C = 100$) of which 5 have been diagnosed ($D_0 = 5$), equation (9) implies that 90 percent ($x = 0.9$) will be diagnosed within 10 days, if $\theta = 0.2$.

By reverse engineering, equation (6) implies that the true number of infectives is:

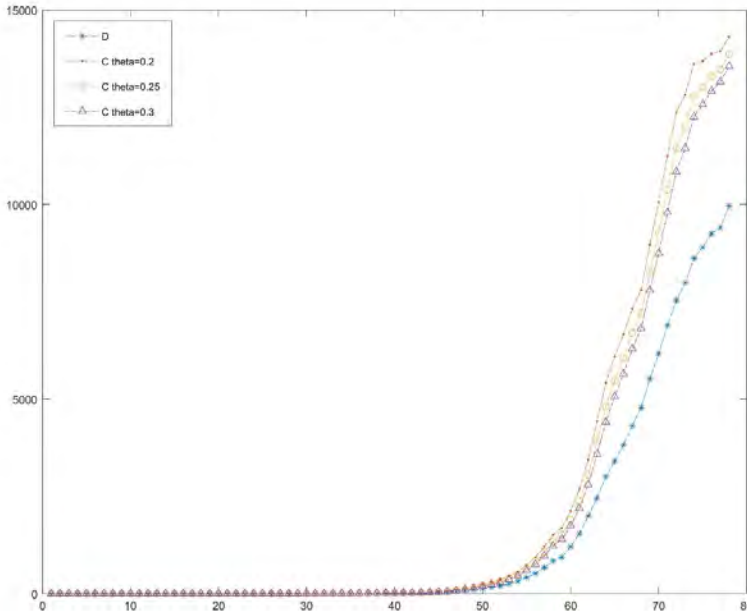
$$C_{t-1} = \frac{1}{1 - \phi} \left(\frac{\Delta D_t}{\theta} + D_{t-1} \right) \tag{10}$$

For example, if $\phi = 0.25$, $\theta = 0.2$, the number of diagnosed cases yesterday was 10,000 (D_{t-1}) and there are 800 newly diagnosed cases today (ΔD_t), the true number of infectives yesterday is 18,666 (C_{t-1}). In principle ϕ may be estimating by randomized testing for covid-19 in the population. Icelandic test data, which are not randomized, suggest that 0.43 percent of the population are asymptomatic carriers of Covid-19. Without supplementary data on the proportion of carriers who eventually became symptomatic, randomized testing provides at best an upper bound for ϕ .

In Figure 4A equation (10) is used to calculate C using Israeli morbidity data for D, setting $\phi = 0.25$ for different values of θ . For these purposes a 4th order moving average of ΔD is specified to ensure that C cannot decrease. The difference between D and C naturally varies inversely with θ . By the end of the period (April 10) the number of diagnosed cases under-estimated the number of undiagnosed cases by

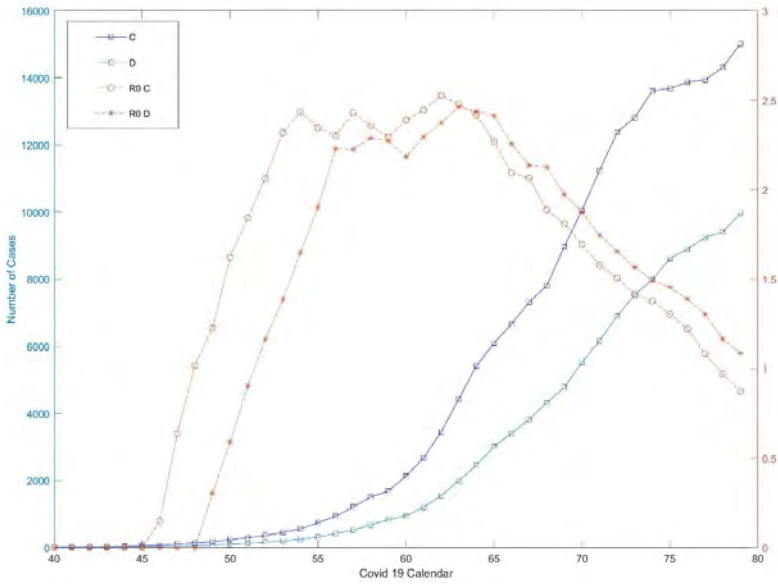
about 29 percent. By construction 25 percent were corona zombies (since $\phi = 0.25$) and 4 percent would have been diagnosed eventually.

Figure 4A Diagnosed and Undiagnosed Covid-19 Carriers in Israel



In Figure 4B we report OLG estimates of R using the imputed data for C from Figure 4A, which are compared with their counterparts using official morbidity data (D). As expected, R is initially larger for C than it is for D. The former precedes the latter by about 5 days. However, the trends are similar, and both measures peak at the same level of R. Subsequently, R based on C is less than R based on D. This means that just as conventional estimates of R understate the rate of contagion when R is increasing, they overstate it when R decreases. It also means that although R based on D lags behind R based on C, the former provides a reliable indicator of trends and turning points in contagion.

Figure 4B OLG Estimates of R including Asymptomatics (Israel)



Quarantine

Let q denote the proportion of infectives in quarantine. Because quarantine shortens the period during which infectives are contagious, the OLG model becomes:

$$C_t = [1 + (1 - q_{t-1})R0D](C_{t-1} - C_{t-\tau-1}) \quad (11)$$

It is obvious that quarantine mitigates the propagation of coronavirus because it reduces the daily rate of contagion. Since only diagnosed infectives can be quarantined, the proportion of infectives in quarantine at the beginning of day t (the end of day $t-1$) is assumed to be $q_{t-1} = D_{t-1}/C_{t-1}$. This assumes that once diagnosed, infectives are quarantined.

We modify equation (6) by defining D in terms of the diagnosed who are contagious instead of the ever-diagnosed by subtracting patients who recovered or died:

$$\Delta D_t = \theta[(1 - \phi)C_{t-1} - D_{t-1}] - rD_{t-1} \quad (12)$$

where the recovery/mortality rate is denoted by r . In the early stages of the epidemic D is zero, because it takes time for infectives to be diagnosed, in which case q is initially zero. Subsequently, q becomes positive, which reduces the propagation of the

epidemic through equation (11). Substituting for q_{t-1} equation (11) may be rewritten as:

$$\Delta C_t = R0D(C_{t-1} - D_{t-1}) - C_{t-\tau-1} - \frac{C_{t-1} - D_{t-1}}{C_{t-1}} C_{t-\tau-1} \quad (13)$$

Equations (12) and (13) are simultaneous difference equations, which solve for true infectives (C) and diagnosed infectives (D). Because equation (12) is linear, but equation (13) is nonlinear, we are unable to obtain analytical solutions. Nevertheless, they obviously imply that q grows over time from zero to less than one if $R0D$ is positive. This means that OLG estimates of $R0$ tend to decrease after q becomes positive, as evidenced in Figures 1 – 3.

As suggested by Chudik, Pesaran and Rebucci (2020) q may also increase endogenously. As the public forms expectations about R , it spontaneously engages in social distancing with the result that R begins to decrease. Hence, the profiles in Figures 1 – 3 may occur spontaneously as in Sweden.

Regression Methods and Measurement Error

Suppose regression methods were used to estimate $R0D$. Denoting $1 + R0D$ by β , equation (1) suggests that β may be estimated by regression:

$$C_t = \beta(C_{t-1} - C_{t-1-\tau}) + u_t \quad (14)$$

Where $u \sim \text{iiN}(0, \sigma^2)$ denotes a residual error. Since C is unknown, β is estimated using morbidity data for D , which contains measurement error (m):

$$D_t = (1 - \phi)C_t + m_t \quad (15a)$$

$$m_t = \rho m_{t-1} + e_t \quad (15b)$$

Where e is distributed iiN with zero mean. Equations (6) implies that measurement error will be autocorrelated as in equation (15b). Since the unconditional expectation of m is zero, equations (15) imply that morbidity (D) lags behind its true value (C), of which only $1 - \phi$ percent of them are eventually diagnosed. Substituting equation (15a) into equation (14) implies that the regression model for D is:

$$D_t = \beta(D_{t-1} - D_{t-1-\tau}) + w_t \quad (16a)$$

$$w_t = (1 - \phi)u_t + m_t - \beta(m_{t-1} - m_{t-1-\tau}) \quad (16b)$$

From equation (15b) the sign of the covariance between D_{t-1} and m_{t-1} is $\rho - \beta$ and the sign of the covariance between $D_{t-1-\tau}$ and $m_{t-1-\tau}$ is negative. Hence, least squares estimates of β will be attenuated (biased downwards) especially if ρ is less than β . Since estimates of β are attenuated, so are estimates of the daily rate of contagion (R0D).

Regression methods may yield unbiased estimates of β provided that the measurement error model is taken into consideration. Substituting equation (6) with iid residual error d into equation (11), implies the following autoregressive model for D :

$$\Delta D_t = -\theta D_{t-1} + \beta \Delta_\tau \Delta D_{t-1} + \beta \theta \Delta_\tau D_{t-2} + \omega_t \quad (17a)$$

$$\omega_t = \theta(1 - \phi)u_{t-1} + d_t - \beta \Delta_\tau d_{t-1} \quad (17b)$$

Where Δ_τ denotes the "seasonal" difference operator ($\Delta_\tau X_t = X_t - X_{t-\tau}$). Since u and v are iid, so is ω . Therefore, constrained least squares estimates of β and θ are consistent. Note that equation (17a) delivers consistent estimates of β and θ . Hence, it identifies that daily rate of contagion (R0D) and the rate at which Covid-19 carriers are diagnosed (θ). Furthermore, it almost identifies the proportion of Covid-19 zombies (ϕ) since the variance of ω is:

$$\sigma_\omega^2 = \theta^2(1 - \phi)^2 \sigma_u^2 + (1 + 2\beta) \sigma_d^2 \quad (17c)$$

Using estimates of θ and β from equation (17a) and σ_ω^2 , combinations of ϕ and the variances of u and d are identified.

Comparison of OLG with SIR

The OLG method is conceptually different to the canonical SIR methodology, which is widely used to estimate R0. Whereas OLG directly calculates R0 from the data, SIR infers R0 by estimating a statistical model in which the entry rate into infection and the exit rate from infection are assumed to be exponential. The SIR estimate of R0 is the ratio of the entry rate to the exit rate. There are two methodological problems with this. If the entry and exit rates are not exponential, the estimate of R0 will be biased. Exponential exit implies that some patients recover almost instantaneously, while others recover extremely slowly. Evidence on recovery from Covid-19 suggests that recovery rates are not exponential (Zhou et al 2020). Second, exit rates are estimated by regressing recoveries on lagged infectives. Since, as discussed above, the latter

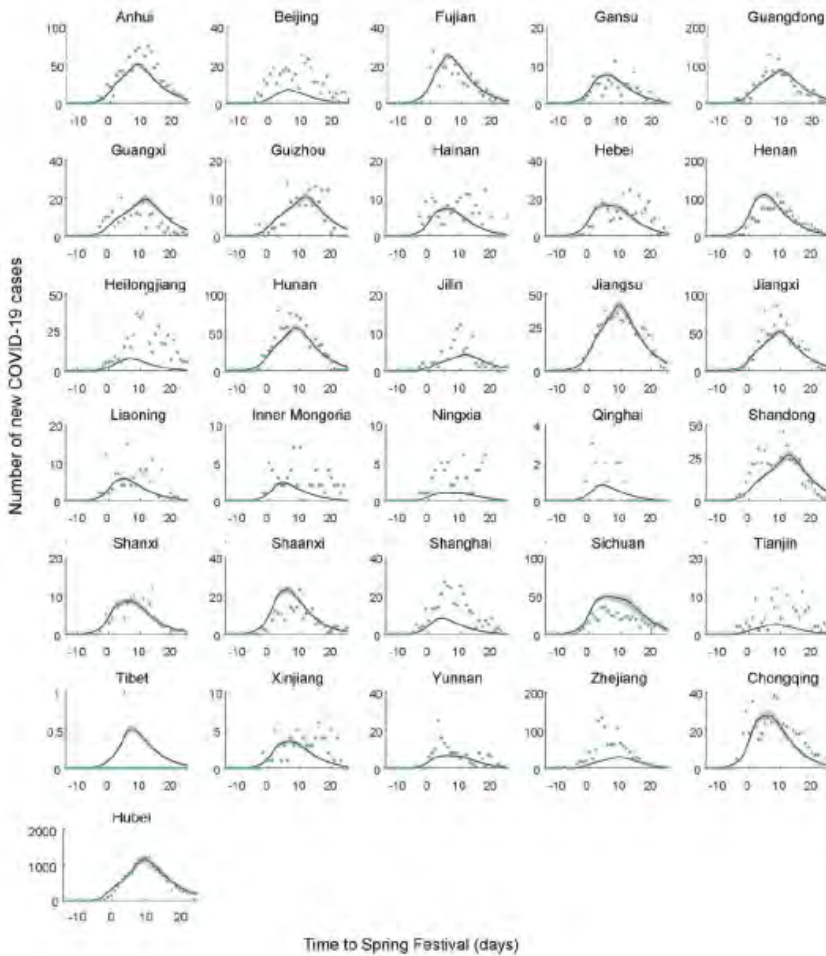
generally contain measurement error, the estimated exit rate is affected by attenuation bias. The SIR estimate of R_0 involves both types of bias. A third problem, which arises during the mature stage of epidemics is that susceptibility to Covid-19 is expected to decrease if the least resistant succumb first while the most resistant may not succumb at all. SIR usually ignores the effect of heterogeneity in resistance.

By contrast OLG does not involve statistical methods for inference. Hence, it is less sensitive to measurement error than SIR. On the other hand, OLG makes assumptions about τ . However, as already noted, the nature of the bias is known and equals the ratio of τ to its true value.

A further methodological criticism of SIR concerns the widespread use of the Metropolis – Hastings algorithm used to estimate Bayesian Markov-Chain Monte Carlo (MC^2) models (Berg 2004, Hamra, MacLehose and Richardson 2013). The starting point is that the model is correct, but its parameters are unknown and need to be estimated using data. The method is Bayesian in the sense that priors are chosen for these parameters, such as R_0 . It is first-order Markov because, for example, recoveries from Covid-19 today are assumed to be strictly proportional to the number of yesterday's infected. Hence the day before yesterday etc does not matter. It is Monte Carlo based because random shocks to exits and entries have to be sampled (using the Gibbs sampler). Parameter estimates for exit and entry rates, and their standard deviations, are represented by their posterior distributions. The latter are generally influenced by their priors and their anterior distributions.

If the priors are chosen badly, so might their MC^2 estimates. Since, recovery from Covid-19 is not exponential, a higher order Markov chain is required. Most importantly, since the model is assumed to be correct, it is never tested empirically. For example, Tian et al (2020) estimate R_0 and other parameters in a SIR-type model by MC^2 . However, their model poorly fits the data for Covid-19 incidence in almost all provinces in China (Figure 5). The posterior estimates of the entry and exit rates may be statistically significant to Bayesians but not to classical, frequentist statisticians. Wu, Leung and Leung (2020) apply MC^2 to data for Wuhan, and Liu et al (2020) show that estimates of R_0 vary widely (from 2 to 6.5) even using the same methodology.

Figure 5 Example of Badness-of-fit of SIR Models Estimated by MC^2



Source: Table SM3 from Tian et al (2020).

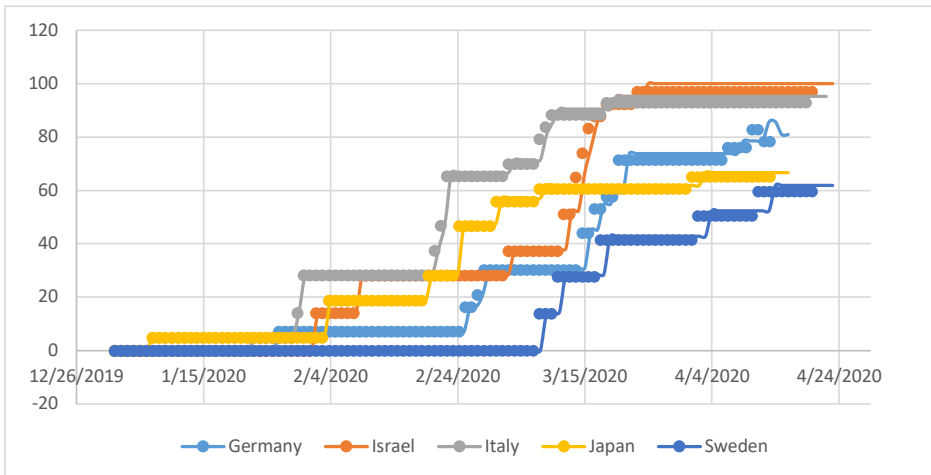
The Effect of Mitigation Policy on Contagion

Ideally, the study of infectious diseases should take place after they have occurred. Although four months have passed since coronavirus broke out in China, most countries have short histories of coronavirus (Figures 1 and 3). These histories get longer by the day, but they are arguably too short to study the treatment effects of mitigation policy on contagion especially because it took time before governments took mitigating action, and because it takes time for mitigation to affect morbidity

through its effect on R . Many countries ramped-up their mitigation policies during the second half of March (Figures 5 and 6), so it is too early to judge their treatment effects. However, other countries, especially China as well as Spain and Italy undertook such policies earlier.

Consequently, the empirical results we report on the efficacy of mitigation policy are inevitably reported with reservation. On the other hand, mitigation policy in China seems to have stopped coronavirus after two months (Figure 3). Within five weeks R began to decrease towards 1 in all Chinese provinces, and within ten weeks it continued to decrease towards zero. We therefore look for early signs that the same is happening in other countries. However, whereas in China mitigation policy was very stringent from the start, policy elsewhere was initially more variegated, but eventually became increasingly stringent.

Figure 6 OxCGRT Stringency Scores for Mitigation Policy



Corona Equilibrium and the Identification of Treatment Effects for Mitigation

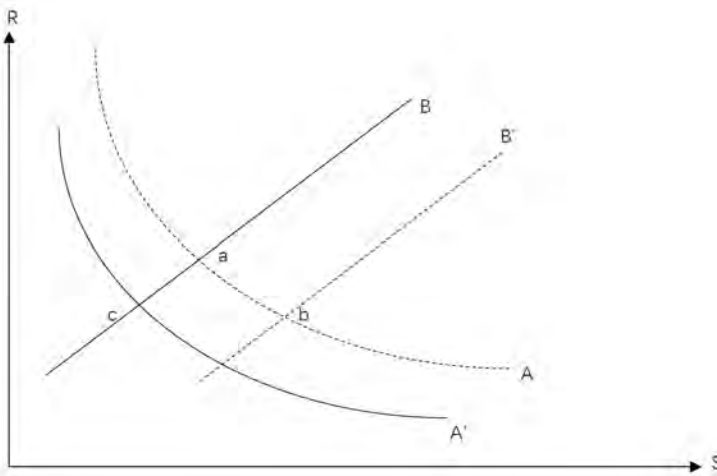
We use the stringency index (S) developed by Oxford Covid-19 Government Response Tracker (OxCGRT) to measure mitigation policy in different countries (Petherick, Hale and Phillips 2020). S ranges from 0 to 100 where the latter is maximal stringency. Our purpose is to identify the causal effect of mitigation policy on R when there may be reverse causality from contagion to mitigation policy. Indeed, in countries such as Japan and Singapore where Covid-19 prevalence was

Covid Economics 10, 27 April 2020: 92-120

low, mitigation policy has been minimal. By contrast, in China, Italy and Spain where prevalence was large, mitigation policy has been maximal.

Figure 6 illustrates the development of mitigation policy over time in a selection of countries. All countries have tended to ramp-up their mitigation policy over time, but some have done this sooner rather than later. Even Sweden and Japan, which have resisted mitigation have joined the trend. Nevertheless, mitigation in Sweden and Japan continues to be relatively light.

Figure 7 Corona Equilibrium



The identification problem is illustrated in Figure 7 where R is measured on the vertical axis and S on the horizontal. Schedule A plots the hypothesized negative causal effect of mitigation policy on R. The size of the treatment effect varies directly with its slope. Schedule B plots the policy response of mitigation to the rate of contagion. It expresses the idea that if morbidity and mortality are small, governments will mitigate less if at all. Governments more politically prone to mitigation will have flatter B schedules. The data for R and S are jointly determined at point a, where schedules A and B intersect. We refer to this as the "corona equilibrium"

Since the treatment effect of mitigation is reflected in the slope of schedule A, we ideally wish to apply an autonomous increase in S such that schedule B shifts to the right to B' in which the new corona equilibrium would be at point b. For example,

Covid Economics 10, 27 April 2020: 92-120

countries with fewer ICUs (Italy?) may resort to more stringent mitigation as in schedule B. The slope of schedule A between points a and b is the local average treatment effect (LATE).

Suppose the population in another country is less susceptible to corona e.g. because of indigenous social distancing as in schedule A', i.e. R is smaller given S. The corona equilibrium will be determined at point c instead of point a, at which both R and S are smaller (Sweden?). The unwitting might think that R is smaller because S is smaller, but this confuses cause and effect. The corona equilibrium in countries with low susceptibility (A') and plentiful ICUs (B) may involve zero mitigation.

To identify the treatment effect of mitigation policy on contagion, we experiment with three different methods. The first involves triple differences (Berck and Villas-Boas 2016). Next, we use time series data to estimate a VAR model for R and S in Israel from which we calculate the impulse response function from shocks to mitigation policy, represented by S, onto contagion measured by R. Third, we estimate a leading indicator model for R in Israel, which is dynamically related to R in Chinese provinces and S in Israel. We refer to the latter as the "Chinese crystal ball", because it exploits the longer history of contagion in China to make inferences regarding the much shorter history of contagion in Israel. Absent is the canonical instrumental variables method, in which mitigation stringency is randomized using instrumental variables for S. We have been unable to find statistically significant instruments for the timing and stringency of mitigation policy.

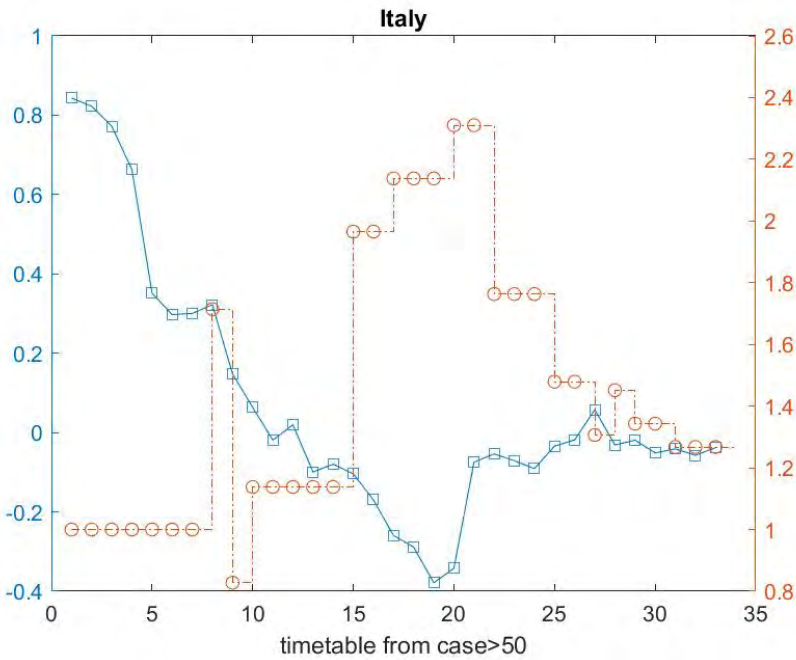
Harti, Wälde and Weber (2020) used structural break tests for nonstationary time series to estimate the treatment effect of mitigation policy in Germany. Since structural breaks may arise for reasons unrelated to mitigation policy, we do not apply their method here. Indeed, Figures 1 – 3 suggest that structural breaks are the norm even in countries that did not mitigate, or mitigated later. Chen and Qiu (2020) extend the SIR model so that the rate of contagion depends on mitigation policies such as school closure and lockdown under the assumption these policies are exogenous.

Triple Differences-in-Differences

We use a triple differences-in-differences (3DID) strategy in which the first two differences refer to the changes in R before and after the change in mitigation policy, and the third difference consists of a comparison with R in a country, which did not

mitigate. For example, Italy adopted a stringent mitigation policy after which R decreased. But so did R decrease in Sweden despite the fact that it refrained from mitigation. If, however, the decrease in R in Italy was greater than in Sweden, the difference may be attributed to the fact that Italy mitigated whereas Sweden did not.

Figure 8 Event Analysis: Italy v Sweden



In Figure 8 the left-hand vertical axis measures the logarithm of the ratio of R in Italy to R in Sweden. The right-hand vertical measures the ratio between stringency in Italy and Sweden. The horizontal axis measures corona time in days as of April 9. Initially R was much higher in Italy than in Sweden (blue). However, by day 19 it was considerably smaller in Italy, and towards the end R in Italy and Sweden were similar. On day 8 Italy began to mitigate, which was intensified on day 15 (brown schedule). On day 22 Sweden began to mitigate but by less than in Italy, hence the decrease in the brown schedule. Did the decrease in relative R result from the increase in relative S , and did the stabilization in relative R result from the subsequent decrease in relative S ? Sweden's partial *volte face* over its non-mitigation policy most probably came too late to affect relative R (blue).

Since relative S increased by about 0.9 and the log of relative R decreased by about 0.5, the semi-elasticity of relative R to relative S was about -0.56 for Italy. The semi-elasticity model implies:

$$\ln R_A = \ln R_B + \ln R_A^* - \ln R_B^* + \gamma \left[\left(\frac{S_A}{S_A^*} \right) - \left(\frac{S_B}{S_B^*} \right) \right] \quad (18)$$

where subscripts A and B refer to after and before treatment, * refers here to Sweden, and γ denotes the semi-elasticity. Semi-elasticities relative to Sweden for other countries are reported in Table 2. The absence of countries such as the UK is because mitigation policy came too late to calculate γ . However, in most countries such as Netherlands γ appeared to be zero. The results reported in Table 2 are obviously provisional. With the passage of time it may be possible to affirm them. However, because countries are increasingly adopting similar treatments in terms of more stringent mitigation policies, Sweden included, it naturally becomes more difficult to estimate treatment effects in this way.

Table 2 3DID Estimates of Treatment Effects for Mitigation Policy

Country	Semi-elasticity (γ)
Austria	-1.20
Denmark	-2.00
France	-0.45
Germany	-1.60
Israel	-0.78
Italy	-0.56
Norway	-1.8
Spain	-1.00
Switzerland	-0.43

Data as of April 9.

Equation (18) and the results in Table 2 imply that when Israel ramped-up its mitigation policy in mid-March, R subsequently decreased by 23 percent (approximately 0.64).

Vector Autoregressions

Corona equilibrium theory implies that contagion and policy mitigation are dynamically interdependent. If R increases S tends to increase subsequently, which in turn may reduce R in the future. Vector autoregression (VAR) models capture this dynamic interaction, and their impulse response functions shed light on how autonomous shocks to mitigation policy influence, or Granger-cause R. VAR models also shed light on how autonomous shocks to R Granger-cause mitigation policy. However, it is the former, which concerns us here.

The restricted VAR model for Israel is:

$$R_t = \underbrace{0.410}_{2.56} + \underbrace{0.998}_{20.44} R_{t-1} - \underbrace{0.0047}_{-2.34} S_{t-2} + \underbrace{0.0127}_{1.47} \Delta S_{t-3} + r_t \quad (19a)$$

Observations: March 11 – April 18 $R^2(\text{adj}) = 0.932$ $LM = 0.965$ $se = 0.196$

$$S_t = \underbrace{11.654}_{4.49} + \underbrace{0.883}_{32.03} S_{t-1} + \underbrace{0.384}_{3.14} \Delta S_{t-2} - \underbrace{4.659}_{-1.77} \Delta R_{t-1} + \underbrace{2.032}_{1.44} \Delta_3 R_t + s_t \quad (19b)$$

$R^2(\text{adj}) = 0.973$ $LM = 6.29$ $se = 2.482$

where t statistics are reported below their respective parameter estimates, r and s denote innovations, LM denotes the lagrange multiplier statistic for 4th order autocorrelated residuals (not significant), and se denotes the equation standard error. R and S Granger-cause each other. As expected, S Granger-causes R negatively, but so does ΔR Granger-cause S negatively. Also, equation (19a) contains a unit root and equation (19b) contains a near-unit root. After 10 days a temporary impulse equivalent to $\Delta S = 30$ induces a cumulative impulse response in R of -0.15, which continues to intensify through the unit root in R.

Note that Granger-causality is equivalent to causality when S_{t-2} in equation (19a) and R_{t-1} in equation (19b) are weakly exogenous (Greene 2012 p 357), necessary conditions for which are that the VAR innovations, r and s, are serially independent and independent of each other.

Chinese Crystal Ball

Whereas Sweden served as the comparator in the 3DID estimates reported in Table 2, here we use China as a comparator. Whereas Sweden undertook minimal mitigation until recently, the opposite was true in China. Moreover, Chinese exposure to corona is much longer than Sweden's. As noted in Figure 3, in March R converged to zero in all Chinese provinces. If a country adopted Chinese style mitigation, it might be plausible to assume that the temporal diffusion profile of R might be similar to China's. If so, what happened in China to R might serve as a crystal ball, or lead indicator, for countries elsewhere. Since in most other countries mitigation policy was less stringent than in China, the crystal ball needs to take account of mitigation policy.

To motivate the crystal ball model, we propose the following simple hypothesis in which relative contagion varies inversely with relative stringency as in equation (18). Let subscripts i , c , and 0 refer respectively to country i , China and a baseline country, which did not undertake mitigation. Hence, R in China relative to R in the baseline country is assumed to be:

$$\frac{R_c}{R_0} = \alpha_c - \beta_c \frac{S_c}{S_0} \quad (20a)$$

Normalizing $S_0 = 1$, equation (20a) states that if China had not practiced mitigation, R in China would have been larger than in the baseline country if $\alpha_c - \beta_c$ exceeds 1.

Importantly, the decrease in R in China has two components. The first results from maximal stringency. The second results from the decrease in R in the baseline.

Similarly, R in country i relative to R in China is assumed to be:

$$\frac{R_i}{R_c} = \alpha_i - \beta_i \frac{S_i}{S_c} \quad (20b)$$

If $\alpha_i - \beta_i$ exceeds 1, R in country i would exceed R in China if it undertook Chinese mitigation policy. If it did not, S_i/S_c is a fraction and R in country i may be larger or smaller than in China.

Equations (20a) and (20b) imply the following relation between R in country i and the baseline country:

$$R_i = R_0 \left(\alpha_i \alpha_c - \alpha_i \beta_c \frac{S_c}{S_0} - \alpha_c \beta_i \frac{S_i}{S_c} + \beta_i \beta_c \frac{S_i}{S_0} \right) \quad (20c)$$

According to equation (20c), R in country i varies proportionately with R in the baseline country. If the term in brackets exceeds 1, R in country i is larger than in the baseline country. If mitigation policy in China and country i are proportionate, and $\alpha_i - \beta_i$ exceeds 1, R in country i varies inversely with stringency in China and country i. Matters are more complicated when mitigation policy is not proportionate because the partial derivatives with respect to stringency in China and country i have ambiguous signs. If mitigation policy is entirely reversed in China and country i, the term in brackets equals $(\alpha_i - \beta_i)(\alpha_c - \beta_c)$. Therefore, if mitigation is entirely reversed, R in country i may be greater or smaller than in the baseline country.

A Crystal Ball for Israel

Representing country i by Israel, the crystal ball hypothesis predicts that R in Israel varies directly in corona time with R in China, and it varies inversely with the stringency of mitigation policy in Israel. In principle, what matters is relative stringency as in the triple difference method, but since stringency in China was maximal (until recently), its effect is absorbed into β_i . Note that the crystal ball hypothesis does not imply that had Israel mitigated maximally as in China, R in Israel would have been the same as R in China. It means, instead, that R in China serves as a lead indicator for R in Israel. Moreover, the relation between R in Israel and R in China is not instantaneous. Instead, it is dynamically related.

We report the following hybrid result for Hubei and Zhejiang provinces, where t refers to corona time in Israel, and calendar time in Hubei and Zhejiang. Note that in terms of calendar time Hubei is 54 days ahead of Israel and 10 days ahead of Zhejiang.

$$\ln R_t = \frac{0.338}{3.02} \ln R_{t-1} + \frac{0.626}{4.85} D \ln R_{t-1} + \frac{0.443}{3.69} \ln(1 + Z_{t-49}) - \frac{0.089}{-2.03} D \ln(1 + Z_{t-49}) + \frac{1.128}{2.23} \ln(1 + H_{t-53}) - \frac{0.528}{-4.37} D \ln(1 + H_{t-53}) - \frac{0.0018}{-3.30} S_{t-2} H_{t-53} - \frac{0.0079}{-7.10} S_{t-2} \tag{21}$$

Observations: March 11 – April 18 R(adj) = 0.9821 LM = 5.16 se = 0.073

Where H and Z denote R in Hubei and Zhejiang, and D is a dummy variable, which is 1 until R peaked in Israel and is zero afterwards. Equation (21) implies that the

weights on R in Hubei and Zhejiang were larger after R peaked in Israel, and there was a unit root until R until it peaked. It also implies that mitigation policy in Israel reduces R but this effect varies inversely with R in Hubei. Equation (21) implies, for example, that after R peaked the long run the elasticity of R in Israel with respect to its counterpart in Zhejiang is $0.669 \frac{Z}{1+Z}$, which tends to zero as Z tends to zero. The semi-elasticity with respect to stringency is $-(0.0119 + 0.02H)$, hence the mitigation effect decreases when R in Hubei decreases. There is no intercept term in equation (21) because it was not statistically significant. Also, the intercept affects what happens to R when the epidemic finally ends. When $Z = H = S = 0$, i.e. when the epidemic is over, the absence of an intercept would imply that $R = 0$ had equation (21) been specified in terms of $\ln(1 + R)$.

In summary, lead information on R in Hubei and Zhejiang predicts R in Israel, which varies inversely with mitigation policy in Israel relative to mitigation policy in China (which remained constant during the estimation period). The equation implies that with the passage of corona time, R in Israel follows the diffusion profile for R in Hubei, but the level of R in Israel varies inversely with stringency in Israel with a lag. Figure 9A plots in-sample tracking and residuals. Because the time series in equation (21) are nonstationary but the residuals are stationary, the parameter estimates are super-consistent (Greene 2012, p 1005). Consequently, the causal effect of mitigation policy in Israel on R is identified.

Figure 9A Tracking Performance of Crystal Ball Model

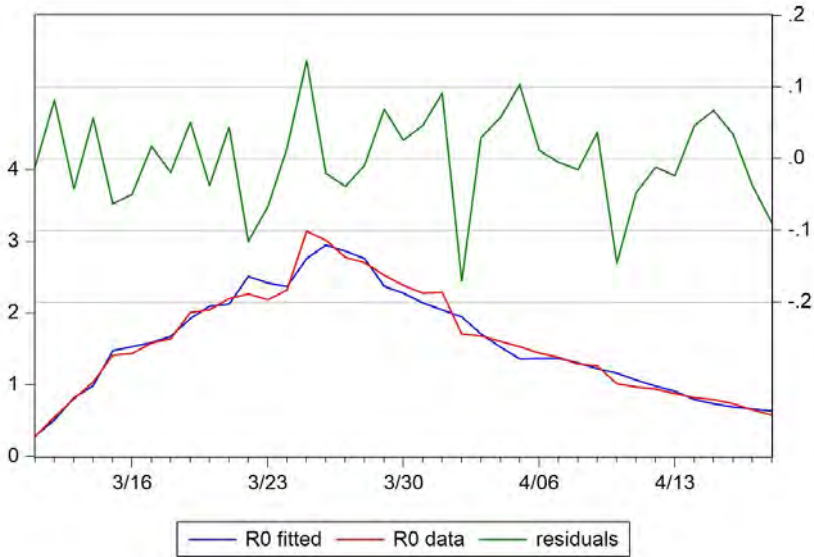
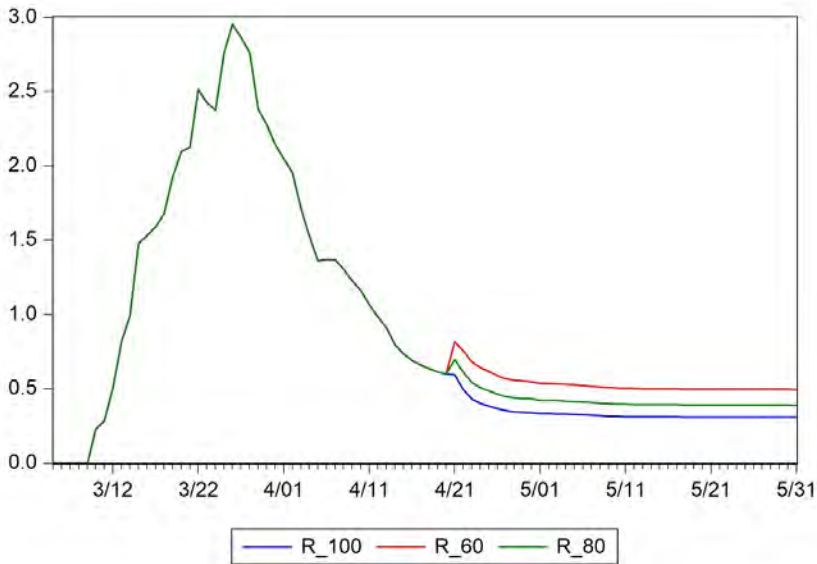


Figure 9B projects R in Israel using equation (21) under various assumptions for mitigation policy. The blue projection is based on the current policy of full mitigation ($S = 100$), according to which R is projected to decrease further to 0.4. Reversing mitigation policy increases R within the comfort zone of less than 1. The crystal ball model implies that R tends to a small number that exceeds zero.

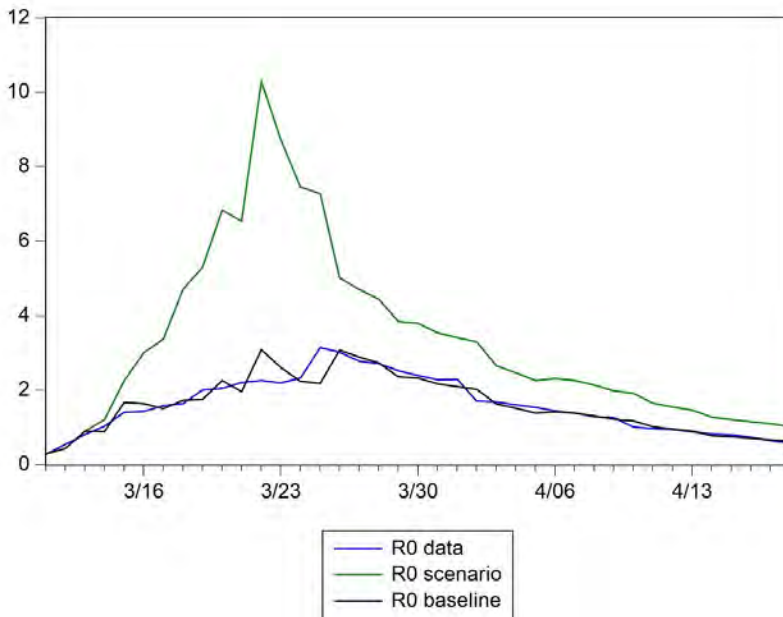
Figure 9B Crystal Ball Projections for R in Israel



The simulations in Figure 9B make the strong assumption that mitigation policy is symmetric; reversing mitigation policy has the same absolute effect on contagion as ramping it up. If mitigation policy increased public awareness of the importance of social distancing, its reversal is unlikely to decrease this awareness. Consequently, mitigation policy might be expected to be characterized by hysteresis. In its extreme form, reversal would have no effect on contagion. More generally, reversal is expected to have a smaller effect on contagion than ramping-up.

Ideally, it would be desirable to study empirically what happens to contagion when mitigation policy is reversed as in China. In the meanwhile, Figure 3B hints that mitigation policy may be asymmetric; it increases R by less when it is reversed than it decreases it when it was ramped-up. If this is true, the adverse effect on R of mitigation reversal in Figure 9B would be overstated.

Figure 9C No Lockdown since March 11



The issue of asymmetric response does not arise in counterfactual simulations, where we ask what would have happened to contagion if the government in Israel had not ramped-up its mitigation policy on March 11. Figure 9C is a counterfactual simulation in which the increase in mitigation stringency from 38 to 100 did not occur. In the absence of lockdown equation (21) implies that R would have increased sharply. This increase is induced by the unit root in equation (21) because the ramping-up occurred before R peaked. Subsequently, however, R decreases such that by the end of the simulation it is less than 2. The simulation shows that mitigation policy "flattened the curve" but it eventually made little difference to R . Lockdown simply brought forward a reduction in R that would have happened sooner or later. However, it avoided a possibly alarming increase in R . Unlike Israel most countries ramped-up mitigation policy after R had already peaked. In this case the crystal ball model would have generated a much milder increase R as in Figure 9B.

The empirical examples for Israel are intended to be illustrative. They may be applied elsewhere. For example, the Chinese crystal ball model may be applied in the United Kingdom or any other country to project contagion and to estimate the effect of mitigation policy and its reversal on the projected course for contagion.

Conclusion

In this paper we have been solely concerned with the measurement of contagion for Covid-19, the treatment effects of mitigation policy on contagion, and the projection and simulation of contagion. We have been concerned with morbidity to the exclusion of mortality. We do not consider here the crucial transitions from morbidity to intensive care and to mortality, which vary widely by country. These transitions have been disastrous for some but not all countries.

Whereas morbidity is essentially epidemiological, mortality is largely organizational and institutional. If there is inadequate provision of intensive care and ventilators, patients who would otherwise be curable die for lack of treatment. The corona epidemic is a drama, which turns into a crisis when there are insufficient or inefficient health services. This fundamental difference is overlooked by epidemiologists. For example, Ferguson et al (2020) treat ICU and ventilator capacity as hard and fixed constraints rather than an economic phenomenon, which are subject to market forces. Ventilator suppliers have responded to the increase in their price, as a result of which ventilator capacity is expanding. Epidemiological models, such as SIR, are too mechanical and ignore learning-by-doing. They assume that if there is a second wave of Covid-19 we shall have learnt nothing from the first wave to mitigate it. There is little in the way of endogeneity in epidemiological models.

Using Chinese data for January and February, Ferguson et al jumped to the conclusion that eventually 90 percent of the world's population will be infected and 40 millions will die in the absence suppression and mitigation. Toda (2020) reached similar conclusions regarding the contagiousness of Covid-19 based on SIR models estimated using cross country panel data for Covid-19 morbidity. It is ironical that by March 16 (when the Ferguson report was published) the rate of contagion had dropped to zero in almost all Chinese provinces, and was heading for zero even in countries that undertook almost no mitigation. It remains to be seen whether their predictions of further deadly rounds of Covid-19 are realistic.

References

Bailey N. (1975) *The Mathematical Theory of Infectious Diseases and its Application*. 2nd edition, Griffin, London.

- Bendavid E. et al (2020) Covid-19 antibody sero-prevalence in Santa Clara County, California. *mEDRxiv*, <https://doi.org/10.101/2020.04.14.20062463>.
- Berck P. and Villas-Boas S.B. (2016) A note on the triple difference in economic models. *Applied Economic Letters*, 23: 239-242.
- Berg B.A. (2004) *Markov Chain Monte Carlo Simulation and their Statistical Analysis*. World Scientific Press, Singapore.
- Chen X. and Qiu Z. (2020) Scenario analysis for non-pharmaceutical interventions on global Covid-19 transmissions. *Covid Economics*, 7: 46-67.
- Chudik A., Peseran M.H., and Rebucci A. (2020) Voluntary and mandatory social distancing: evidence on Covid-19 exposure rates for Chinese provinces and selected countries. Federal Reserve Bank of Dallas, <https://doi.org/10.24149gwp382>.
- Ferguson N. et al (2020) Impact of non-pharmaceutical interventions to reduce Covid-19 mortality and health care demand. doi:<https://doi.org/10.25561/77482>, London (March 16, 2020).
- Greene W, (2012) *Econometric Analysis*, 7th edition, Prentice Hall.
- Hamra G., MacLehose R. and Richardson D. (2013) Markov chain Monte Carlo: an introduction for epidemiologists. *International Journal of Epidemiology*, 42: 627-634.
- Harti T., Wälde K. and Weber E. (2020) Measuring the impact of the German public shutdown on the spread of Covid-19. *Covid Economics*, 1: 25-32.
- Liu Y., Gayle A.A., Wilder-Smith A. and Rocklöv J. (2020) The reproductive number of Covid-19 is higher compared to SARS coronavirus. *Journal of Travel Medicine*, doi:10.1093/jtm/taa.ao21.
- Tian et al (2020) The impact of transmission control measures during the first 50 days of the Covid-19 epidemic in China. *Science*, <https://doi.org/10.1126/science.abb6105>.
- Toda A.A. (2020) Susceptible -infective – recovered (SIR) dynamics of Covid-19 and economic impact. *Covid Economics*, 1: 43- .
- Wu J.T., Leung k. and Leung G.M. (2020) Nowcasting and forecasting the potential domestic and international spread of the 2019-nCov outbreak originating in Wuhan, China: a modelling study. *Lancet*, 395: 689-697.
- Zhou F. et al (2020) Clinical course and risk factors for mortality of adult inpatients with Covid-19 in Wuhan, China: a retrospective cohort study. *Lancet*, 395: 1054-1062.

The global macroeconomic impacts of COVID-19: Seven scenarios¹

Warwick McKibbin² and Roshen Fernando³

Date submitted: 22 April 2020; Date accepted: 23 April 2020

The outbreak of Coronavirus named COVID-19 world has disrupted the Chinese economy and is spreading globally. The evolution of the disease and its economic impact is highly uncertain, which makes it difficult for policymakers to formulate an appropriate macroeconomic policy response. In order to better understand possible economic outcomes, this paper explores seven different scenarios of how COVID-19 might evolve in the coming year using a modelling technique developed by Lee and McKibbin (2003) and extended by McKibbin and Sidorenko (2006). It examines the impacts of different scenarios on macroeconomic outcomes and financial markets in a global hybrid DSGE/CGE general equilibrium model. The scenarios in this paper demonstrate that even a contained outbreak could significantly impact the global economy in the short run. These scenarios demonstrate the scale of costs that might be avoided by greater investment in public health systems in all economies but particularly in less developed economies where health care systems are less developed and population density is high.

- 1 We gratefully acknowledge financial support from the Australian Research Council Centre of Excellence in Population Ageing Research (CE170100005). We thank Renee Fry-McKibbin, Will Martin Louise Shiner and David Wessel for comment and Peter Wilcoxon and Larry Weifeng Liu for their research collaboration on the GCubed model used in this paper. We also acknowledge the contributions to earlier research on modelling of pandemics undertaken with Jong-Wha Lee and Alexandra Sidorenko.
- 2 Professor of Public Policy & Director, Centre for Applied Macroeconomic Analysis, Crawford School of Public Policy, Australian National University.
- 3 PhD Student, Crawford School of Public Policy, Australian National University.

1. Introduction

The COVID-19 outbreak (previously 2019-nCoV) was caused by the SARS-CoV-2 virus. This outbreak was triggered in December 2019 in Wuhan city which is in the Hubei province of China. COVID-19 continues to spread across the world. Initially the epicenter of the outbreak was China with reported cases either in China or being travelers from China. At the time of writing this paper, at least four further epicenters have been identified: Iran, Italy, Japan and South Korea. Even though the cases reported from China are expected to have peaked and are now falling (WHO 2020), cases reported from countries previously thought to be resilient to the outbreak, due to stronger medical standards and practices, have recently increased. While some countries have been able to effectively treat reported cases, it is uncertain where and when new cases will emerge. Amidst the significant public health risk COVID-19 poses to the world, the World Health Organization (WHO) has declared a public health emergency of international concern to coordinate international responses to the disease. It is, however, currently debated whether COVID-19 could potentially escalate to a global pandemic.

In a strongly connected and integrated world, the impacts of the disease beyond mortality (those who die) and morbidity (those who are incapacitated or caring for the incapacitated and unable to work for a period) has become apparent since the outbreak. Amidst the slowing down of the Chinese economy with interruptions to production, the functioning of global supply chains has been disrupted. Companies across the world, irrespective of size, dependent upon inputs from China have started experiencing contractions in production. Transport being limited and even restricted among countries has further slowed down global economic activities. Most importantly, some panic among consumers and firms has distorted usual consumption patterns and created market anomalies. Global financial markets have also been responsive to the changes and global stock indices have plunged. Amidst the global turbulence, in an initial assessment, the International Monetary Fund expects China to slow down by 0.4 percentage points compared to its initial growth target to 5.6 percent, also slowing down global growth by 0.1 percentage points. This is likely to be revised in coming weeks.

This paper attempts to quantify the potential global economic costs of COVID-19 under different possible scenarios. The goal of the paper is to provide guidance to policy makers to the economic benefits of a globally-coordinated policy responses to tame the virus. The paper builds upon the experience gained from evaluating the economics of SARS (Lee & McKibbin 2003) and Pandemic Influenza (McKibbin & Sidorenko 2006). The paper first summarizes the

existing literature on the macroeconomic costs of diseases. Section 3 outlines the global macroeconomic model (G-Cubed) used for the study, highlighting its strengths to assess the macroeconomics of diseases. Section 4 describes how epidemiological information is adjusted to formulate a series of economic shocks that are input into the global economic model. Section 5 discusses the results of the seven scenarios simulated using the model. Section 6 concludes the paper summarizing the main findings and discusses some policy implications.

2. Related Literature

Many studies have found that population health, as measured by life expectancy, infant and child mortality and maternal mortality, is positively related to economic welfare and growth (Pritchett and Summers, 1996; Bloom and Sachs, 1998; Bhargava and et al., 2001; Cuddington et al., 1994; Cuddington and Hancock, 1994; Robalino et al., 2002a; Robalino et al., 2002b; WHO Commission on Macroeconomics and Health, 2001; Haacker, 2004).

There are many channels through which an infectious disease outbreak influences the economy. Direct and indirect economic costs of illness are often the subject of the health economics studies on the burden of disease. The conventional approach uses information on deaths (mortality) and illness that prevents work (morbidity) to estimate the loss of future income due to death and disability. Losses of time and income by carers and direct expenditure on medical care and supporting services are added to obtain the estimate of the economic costs associated with the disease. This conventional approach underestimates the true economic costs of infectious diseases of epidemic proportions which are highly transmissible and for which there is no vaccine (e.g. HIV/AIDS, SARS and pandemic influenza). The experience from these previous disease outbreaks provides valuable information on how to think about the implications of COVID-19

The HIV/AIDS virus affects households, businesses and governments - through changed labor supply decisions; efficiency of labor and household incomes; increased business costs and foregone investment in staff training by firms; and increased public expenditure on health care and support of disabled and children orphaned by AIDS, by the public sector (Haacker, 2004). The effects of AIDS are long-term but there are clear prevention measures that minimize the risks of acquiring HIV, and there are documented successes in implementing prevention and education programs, both in developed and in the developing world. Treatment is also available, with modern antiretroviral therapies extending the life expectancy and improving the quality of life of HIV patients by many years if not decades. Studies of the macroeconomic impact of

HIV/AIDS include (Cuddington, 1993a; Cuddington, 1993b; Cuddington et al., 1994; Cuddington and Hancock, 1994; Haacker, 2002a; Haacker, 2002b; Over, 2002; Freire, 2004; The World Bank, 2006). Several computable general equilibrium (CGE) macroeconomic models have been applied to study the impact of AIDS (Arndt and Lewis, 2001; Bell et al., 2004).

The influenza virus is by far more contagious than HIV, and the onset of an epidemic can be sudden and unexpected. It appears that the COVID-19 virus is also very contagious. The fear of 1918-19 Spanish influenza, the “deadliest plague in history,” with its extreme severity and gravity of clinical symptoms, is still present in the research and general community (Barry, 2004). The fear factor was influential in the world’s response to SARS – a coronavirus not previously detected in humans (Shannon and Willoughby, 2004; Peiris et al., 2004). It is also reflected in the response to COVID-19. Entire cities in China have closed and travel restrictions placed by countries on people entering from infected countries. The fear of an unknown deadly virus is similar in its psychological effects to the reaction to biological and other terrorism threats and causes a high level of stress, often with longer-term consequences (Hyams et al., 2002). A large number of people would feel at risk at the onset of a pandemic, even if their actual risk of dying from the disease is low.

Individual assessment of the risks of death depends on the probability of death, years of life lost, and the subjective discounting factor. Viscusi et al. (1997) rank pneumonia and influenza as the third leading cause of the probability of death (following cardiovascular disease and cancer). Sunstein (1997) discusses the evidence that an individual’s willingness to pay to avoid death increases for causes perceived as “bad deaths” – especially dreaded, uncontrollable, involuntary deaths and deaths associated with high externalities and producing distributional inequity. Based on this literature, it is not unreasonable to assume that individual perception of the risks associated with the new influenza pandemic virus similar to Spanish influenza in its virulence and the severity of clinical symptoms can be very high, especially during the early stage of the pandemic when no vaccine is available and antivirals are in short supply. This is exactly the reaction revealed in two surveys conducted in Taiwan during the SARS outbreak in 2003 (Liu et al., 2005), with the novelty, salience and public concern about SARS contributing to the higher than expected willingness to pay to prevent the risk of infection.

Studies of the macroeconomic effects of the SARS epidemic in 2003 found significant effects on economies through large reductions in consumption of various goods and services, an

increase in business operating costs, and re-evaluation of country risks reflected in increased risk premiums. Shocks to other economies were transmitted according to the degree of the countries' exposure, or susceptibility, to the disease. Despite a relatively small number of cases and deaths, the global costs were significant and not limited to the directly affected countries (Lee and McKibbin, 2003). Other studies of SARS include (Chou et al., 2004) for Taiwan, (Hai et al., 2004) for China and (Sui and Wong, 2004) for Hong Kong.

There are only a few studies of economic costs of large-scale outbreaks of infectious diseases to date: Schoenbaum (1987) is an example of an early analysis of the economic impact of influenza. Meltzer et al. (1999) examine the likely economic effects of the influenza pandemic in the US and evaluate several vaccine-based interventions. At a gross attack rate (i.e. the number of people contracting the virus out of the total population) of 15-35%, the number of influenza deaths is 89 – 207 thousand, and an estimated mean total economic impact for the US economy is \$73.1- \$166.5 billion.

Bloom et al. (2005) use the Oxford economic forecasting model to estimate the potential economic impact of a pandemic resulting from the mutation of avian influenza strain. They assume a mild pandemic with a 20% attack rate and a 0.5 percent case-fatality rate, and a consumption shock of 3%. Scenarios include two-quarters of demand contraction only in Asia (combined effect 2.6% Asian GDP or US\$113.2 billion); a longer-term shock with a longer outbreak and larger shock to consumption and export yields a loss of 6.5% of GDP (US\$282.7 billion). Global GDP is reduced by 0.6%, global trade of goods and services contracts by \$2.5 trillion (14%). Open economies are more vulnerable to international shocks.

Another study by the US Congressional Budget Office (2005) examined two scenarios of pandemic influenza for the United States. A mild scenario with an attack rate of 20% and a case fatality rate (i.e. the number who die relative to the number infected) of 0.1% and a more severe scenario with an attack rate of 30% and a case fatality rate of 2.5%. The CBO (2005) study finds a GDP contraction for the United States of 1.5% for the mild scenario and 5% of GDP for the severe scenario.

McKibbin and Sidorenko (2006) used an earlier vintage of the model used in the current paper to explore four different pandemic influenza scenarios. They considered a “mild” scenario in which the pandemic is similar to the 1968-69 Hong Kong Flu; a “moderate” scenario which is similar to the Asian flu of 1957; a “severe” scenario based on the Spanish flu of 1918-1919 ((lower estimate of the case fatality rate), and an “ultra” scenario similar to Spanish flu 1918-

19 but with upper-middle estimates of the case fatality rate. They found costs to the global economy of between \$US300 million and \$US4.4trillion dollars for the scenarios considered.

The current paper modifies and extends that earlier papers by Lee and McKibbin (2003) and McKibbin and Sidorenko (2006) to a larger group of countries, using updated data that captures the greater interdependence in the world economy and in particular, the rise of China's importance in the world economy today.

3. The Hybrid DSGE/CGE Global Model

For this paper, we apply a global intertemporal general equilibrium model with heterogeneous agents called the G-Cubed Multi-Country Model. This model is a hybrid of Dynamic Stochastic General Equilibrium (DSGE) Models and Computable General Equilibrium (CGE) Models developed by McKibbin and Wilcoxon (1999, 2013)

(9) The G-Cubed Model

The version of the G-Cubed (G20) model used in this paper can be found in McKibbin and Triggs (2018) who extended the original model documented in McKibbin and Wilcoxon (1999, 2013). The model has 6 sectors and 24 countries and regions. Table 1 presents all the regions and sectors in the model. Some of the data inputs include the I/O tables found in the GTAP database (Aguiar et al. 2019), which enables us to differentiate sectors by country of production within a DSGE framework. Each sector in each country has a KLEM technology in production which captures the primary factor inputs of capital (K) and labor (L) as well as the intermediate or production chains of inputs in energy (E) and materials inputs (M). These linkages are both within a country and across countries.

Table 1 – Overview of the G-Cubed (G20) model

<u>Countries (20)</u>	<u>Regions (4)</u>
Argentina	Rest of the OECD
Australia	Rest of Asia
Brazil	Other oil-producing countries
Canada	Rest of the world
China	
Rest of Eurozone	<u>Sectors (6)</u>
France	Energy
Germany	Mining
Indonesia	Agriculture (including fishing and hunting)
India	Durable manufacturing
Italy	Non-durable manufacturing
Japan	Services
Korea	
Mexico	<u>Economic Agents in each Country (3)</u>
Russia	A representative household
Saudi Arabia	A representative firm (in each of the 6 production sectors)
South Africa	Government
Turkey	
United Kingdom	
United States	

The approach embodied in the G-Cubed model is documented in McKibbin and Wilcoxon (1998, 2013). Several key features of the standard G-Cubed model are worth highlighting here.

First, the model completely accounts for stocks and flows of physical and financial assets. For example, budget deficits accumulate into government debt, and current account deficits accumulate into foreign debt. The model imposes an intertemporal budget constraint on all households, firms, governments, and countries. Thus, a long-run stock equilibrium obtains through the adjustment of asset prices, such as the interest rate for government fiscal positions or real exchange rates for the balance of payments. However, the adjustment towards the long-run equilibrium of each economy can be slow, occurring over much of a century.

Second, firms and households in G-Cubed must use money issued by central banks for all transactions. Thus, central banks in the model set short term nominal interest rates to target macroeconomic outcomes (such as inflation, unemployment, exchange rates, etc.) based on Henderson-McKibbin-Taylor monetary rules. These rules are designed to approximate actual monetary regimes in each country or region in the model. These monetary rules tie down the long-run inflation rates in each country as well as allowing short term adjustment of policy to smooth fluctuations in the real economy.

Third, nominal wages are sticky and adjust over time based on country-specific labor contracting assumptions. Firms hire labor in each sector up to the points that the marginal product of labor equals the real wage defined in terms of the output price level of that sector. Any excess labor enters the unemployed pool of workers. Unemployment or the presence of excess demand for labor causes the nominal wage to adjust to clear the labor market in the long run. In the short-run, unemployment can arise due to structural supply shocks or changes in aggregate demand in the economy.

Fourth, rigidities prevent the economy from moving quickly from one equilibrium to another. These rigidities include nominal stickiness caused by wage rigidities, lack of complete foresight in the formation of expectations, cost of adjustment in investment by firms with physical capital being sector-specific in the short run, monetary and fiscal authorities following particular monetary and fiscal rules. Short term adjustment to economic shocks can be very different from the long-run equilibrium outcomes. The focus on short-run rigidities is important for assessing the impact over the initial decades of demographic change.

Fifth, we incorporate heterogeneous households and firms. Firms are modeled separately within each sector. There is a mixture of two types of consumers and two types of firms within each sector, within each country: one group which bases its decisions on forward-looking expectations and the other group which follows simpler rules of thumb which are optimal in the long run.

4. Modeling epidemiological scenarios in an economic model

We follow the approach in Lee and McKibbin (2003) and McKibbin and Sidorenko (2006) to convert different assumptions about mortality rates and morbidity rates in the country where the disease outbreak occurs (the epicenter country). Given the epidemiological assumptions based on previous experience of pandemics we create a set of filters that convert the shocks into economic shocks to: reduced labor supply in each country (mortality and morbidity); rising

cost of doing business in each sector including disruption of production networks in each country; consumption reduction due to shifts in consumer preferences over each good from each country (in addition to those changes generated by the model based on change in income and prices); rise in equity risk premia on companies in each sector in each country (based on exposure to the disease); and increases in country risk premium based on exposure to the disease as well as vulnerabilities to changing macroeconomic conditions.

In the remainder of this section, we outline how the various indicators are constructed. The approach follows McKibbin and Sidorenko (2006) with some improvements. There are, of course, many assumptions in this exercise and the results are sensitive to these assumptions. The goal of the paper is to provide policymakers with some idea of the costs of not intervening and allowing the various scenarios to unfold.

Epidemiological assumptions

The attack rates (proportion of the population who are infected) and case-fatality rates (proportion of those infected who die) and the implied mortality rate (proportion of total population who dies) assumed for China under seven different scenarios are contained in Table 2 below. Each scenario is given a name. S01 is scenario 1,

Table 2 – Epidemiological Assumptions for China

Scenario	Attack Rate for China	Case-fatality Rate for China	Mortality Rate for China
S01	1%	2.0%	0.02%
S02	10%	2.5%	0.25%
S03	30%	3.0%	0.90%
S04	10%	2.0%	0.20%
S05	20%	2.5%	0.50%
S06	30%	3.0%	0.90%
S07	10%	2.0%	0.20%

We explore seven scenarios based on the survey of historical pandemics in McKibbin and Sidorenko (2006) and the most recent data on the COVID-19 virus. Table 3 summarizes the scenarios for the disease outbreak. The scenarios vary by attack rate, mortality rate and the countries experiencing the epidemiological shocks. The attack rate is the proportion of the entire population who become infected (i.e. the frequency of morbidity). The case fatality rate is the proportion of infected people who die and the mortality rate is the proportion of the

entire population who die from the disease. Scenarios 1-3 assume the epidemiological events are isolated to China. The economic impact on China and the spillovers to other countries are through trade, capital flows and the impacts of changes in risk premia in global financial markets – as determined by the model. Scenarios 4-6 are the pandemic scenarios where the epidemiological shocks occur in all countries to differing degrees. Scenarios 1-6 assume the shocks are temporary. Scenario 7 is a case where a mild pandemic is expected to be recurring each year for the indefinite future.

Table 3 – Scenario Assumptions

Scenario	Countries Affected	Severity	Attack Rate for China	Case fatality rate China	Nature of Shocks	Shocks Activated	Shocks Activated
						China	Other countries
1	China	Low	1.0%	2.0%	Temporary	All	Risk
2	China	Mid	10.0%	2.5%	Temporary	All	Risk
3	China	High	30.0%	3.0%	Temporary	All	Risk
4	Global	Low	10.0%	2.0%	Temporary	All	All
5	Global	Mid	20.0%	2.5%	Temporary	All	All
6	Global	High	30.0%	3.0%	Temporary	All	All
7	Global	Low	10.0%	2.0%	Permanent	All	All

a) Shocks to labor supply

The shock to labor supply in each country includes three components: mortality due to infection, morbidity due to infection and morbidity arising from caregiving for affected family members. For the mortality component, a mortality rate is initially calculated using different attack rates and case-fatality rates for China. These attack rates and case-fatality rates are based on observations during SARS and following McKibbin and Sidorenko (2006) on pandemic influenza, as well as currently publicly available epidemiological data for COVID-19.

We take the Chinese epidemiological assumptions and scale these for different countries. The scaling is done by calculating an Index of Vulnerability. This index is then applied to the Chinese mortality rates to generate country specific mortality rates. Countries that are more vulnerable than China will have higher rate of mortality and morbidity and countries who are less vulnerable with lower epidemiological outcomes, The index of vulnerability is constructed by aggregating an Index of Geography and an Index of Health Policy, following McKibbin and Sidorenko (2006). The Index of Geography is the average of two indexes. The first is the urban

population density of countries divided by the share of urban in total population. This is expressed relative to China. The second sub index is an index of openness to tourism relative to China. The Index of Health Policy also consists of two components: the Global Health Security Index and Health Expenditure per Capita relative to China. The Global Health Security Index assigns scores to countries according to six criteria, which includes the ability to prevent, detect and respond to epidemics (see GHSIndex 2020). The Index of Geography and Index of Health Policy for different countries are presented in Figures 1 and 2, respectively. The **lower** the value of the Index of Health Policy, the **better** would be a given country's health standards. However, a **lower** value for the Index of Geography represents a **lower** risk to a given country.

When calculating the second component of the labor shock we need to adjust for the problem that the model is an annual model. Days lost therefore have to be annualized. The current recommended incubation period for COVID-19 is 14 days², so we assume an average employee in a country would have to be absent from work for 14 days, if infected. Absence from work indicates a loss of productive capacity for 14 days out of working days for a year. Hence, we calculate an effective attack rate for China using the attack rate assumed for a given scenario, and the proportion of days absent from work and scale them across other countries using the Index of Vulnerability.

The third component of the labor shock accounts for absenteeism from work due to caregiving family members who are infected. We assume the same effective attack rate as before and that around 70 percent of the female workers would be care givers to family members. We adjust the effective attack rate using the Index of Vulnerability and the proportion of labor force who have to care for school-aged children (70 percent of female labor force participation). This does account for school closures.

² There is evidence that this figure could be close to 21 days. This would increase the scale of the shock.

Figure 1 - Index of Geography relative to China

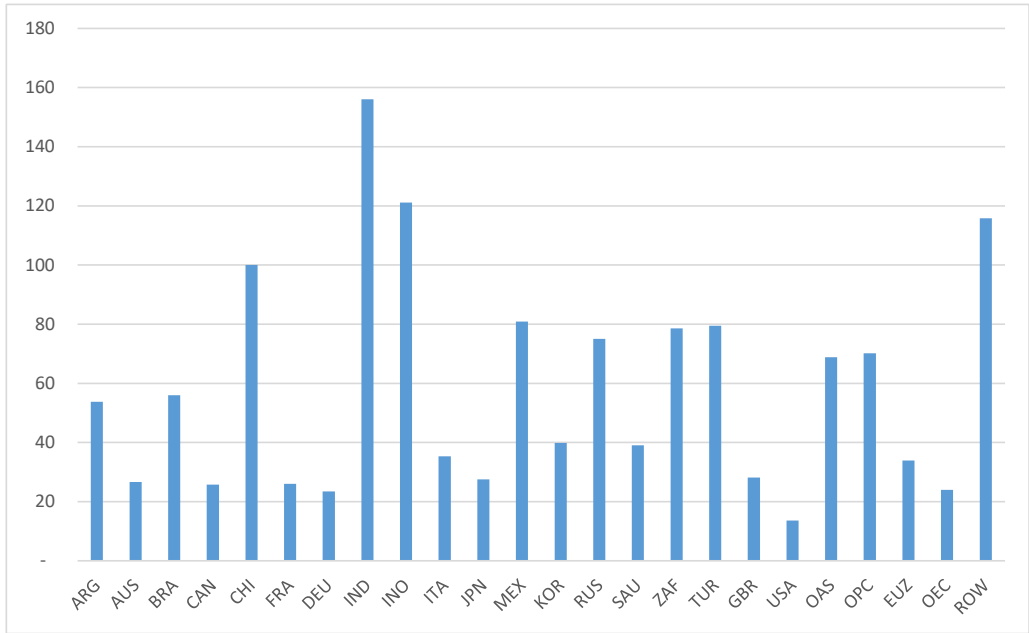


Figure 2 - Index of Health Policy relative to China

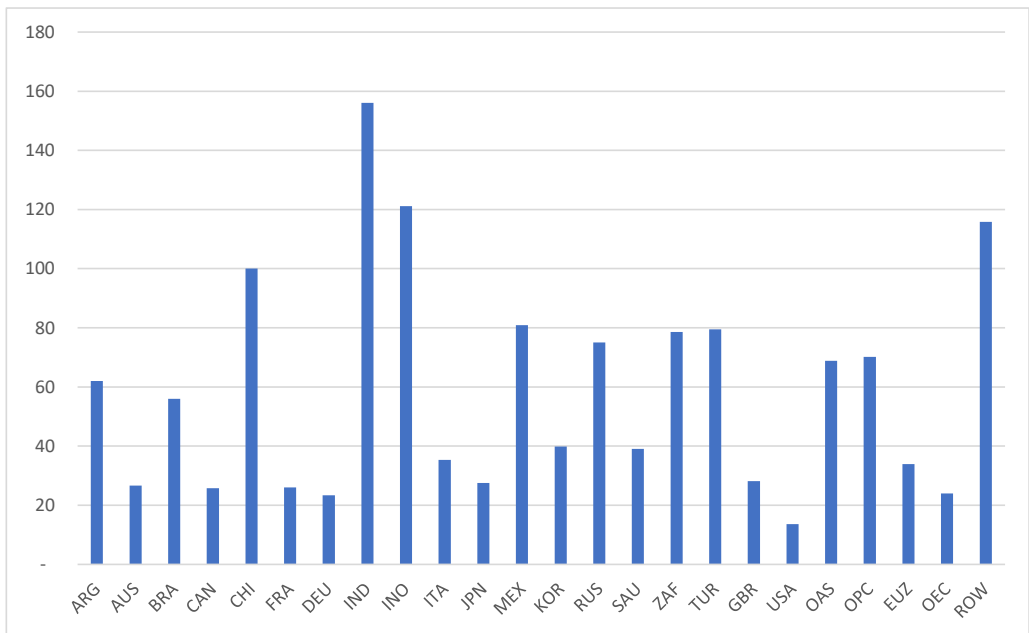


Table 4 contains the labor shocks for countries for different scenarios.

Table 4 – Shocks to labor supply

Region	S01	S02	S03	S04	S05	S06	S07
Argentina	0	0	0	-0.65	-1.37	-2.14	-0.65
Australia	0	0	0	-0.48	-1.01	-1.58	-0.48
Brazil	0	0	0	-0.66	-1.37	-2.15	-0.66
Canada	0	0	0	-0.43	-0.89	-1.40	-0.43
China	-0.10	-1.10	-3.44	-1.05	-2.19	-3.44	-1.05
France	0	0	0	-0.52	-1.08	-1.69	-0.52
Germany	0	0	0	-0.51	-1.06	-1.66	-0.51
India	0	0	0	-1.34	-2.82	-4.44	-1.34
Indonesia	0	0	0	-1.39	-2.91	-4.56	-1.39
Italy	0	0	0	-0.48	-1.02	-1.60	-0.48
Japan	0	0	0	-0.50	-1.04	-1.64	-0.50
Mexico	0	0	0	-0.78	-1.64	-2.57	-0.78
Republic of Korea	0	0	0	-0.56	-1.17	-1.85	-0.56
Russia	0	0	0	-0.71	-1.48	-2.31	-0.71
Saudi Arabia	0	0	0	-0.41	-0.87	-1.37	-0.41
South Africa	0	0	0	-0.80	-1.67	-2.61	-0.80
Turkey	0	0	0	-0.76	-1.59	-2.50	-0.76
United Kingdom	0	0	0	-0.53	-1.12	-1.75	-0.53
United States of America	0	0	0	-0.40	-0.83	-1.30	-0.40
Other Asia	0	0	0	-0.88	-1.84	-2.89	-0.88
Other oil producing countries	0	0	0	-0.97	-2.01	-3.13	-0.97
Rest of Euro Zone	0	0	0	-0.46	-0.97	-1.52	-0.46
Rest of OECD	0	0	0	-0.43	-0.89	-1.39	-0.43
Rest of the World	0	0	0	-1.29	-2.67	-4.16	-1.29

b) Shocks to the equity risk premium of economic sectors

We assume that the announcement of the virus will cause risk premia through the world to change. We create risk premia in the United States to approximate the observed initial response to scenario 1. We then adjust the equity risk shock to all countries across a given scenario by

applying indexes outline next. We also scale the shock across scenarios by applying the different mortality rate assumptions across countries.

The Equity Risk Premium shock is the aggregation of the mortality component of the labor shock and a Country Risk Index. The Country Risk Index is the average of three indices: Index of Governance Risk, Index of Financial Risk and Index of Health Policy. In developing these indices, we use the US as a benchmark due to the prevalence of well-developed financial markets there (Fisman and Love 2004).

The Index of Governance Risk is based on the International Country Risk Guide, which assigns countries scores based on performance in 22 variables across three categories: political, economic, and financial (see PRSGroup 2020). The political variables include government stability, as well as the prevalence of conflicts, corruption and the rule of law. GDP per capita, real GDP growth and inflation are some of the economic variables considered in the Index. Financial variables contained in the Index account for exchange rate stability and international liquidity among others. Figure 3 summarizes the scores for countries for the governance risk relative to the United States.

One of the most easily available indicators of the expected global economic impacts of COVID-19 has been movements in financial market indices. Since the commencement of the outbreak, financial markets continue to respond to daily developments regarding the outbreak across the world. Particularly, stock markets have been demonstrating investor awareness of industry-specific (unsystematic) impacts. Hence, when developing the Equity Risk Premium Shocks for sectors, we include an Index of Financial Risk, even though it is already partially accounted for within the Index of Governance Risk. This higher weight on financial risk enables us to reproduce the prevailing turbulence in financial markets. The Index of Financial Risk uses the current account balance of the countries as a proportion of GDP in 2015. Figure 4 contains the scores for the countries relative to the United States

Even though construction of the Index of Health Policy follows the procedure described for developing the mortality component of the labor shock, the US has been used as the base-country instead of China, when developing the shock on equity risk premium since the US is the center of the global financial system and in the model, all risks are defined relative to the US. Figure 5 contains the scores for the countries for the Index of Health Policy relative to the United States.

Figure 3 - Index of Governance relative to US

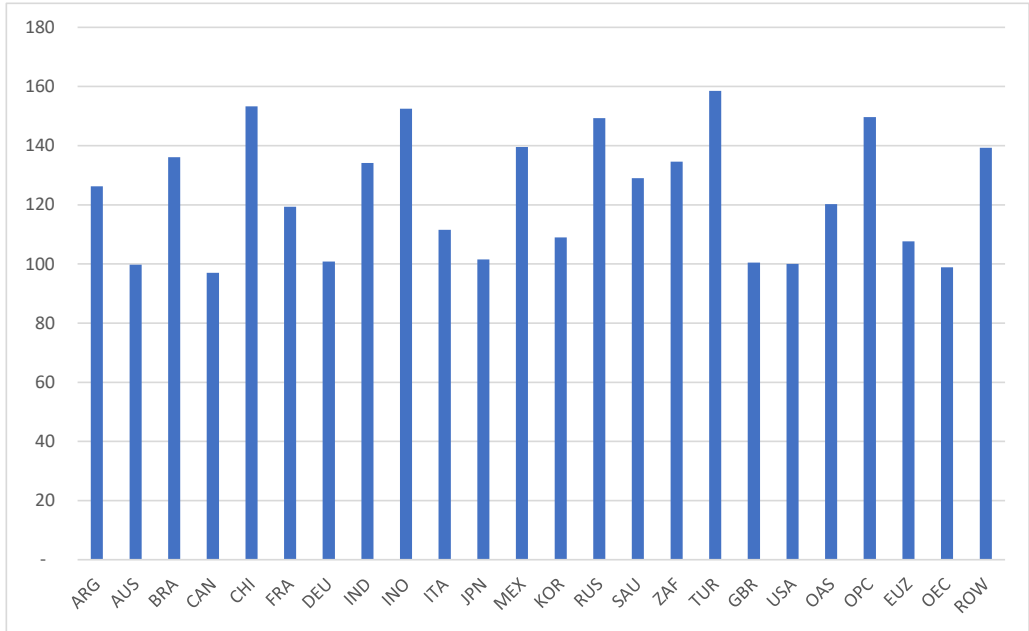


Figure 4 - Index of Financial Risk relative to US

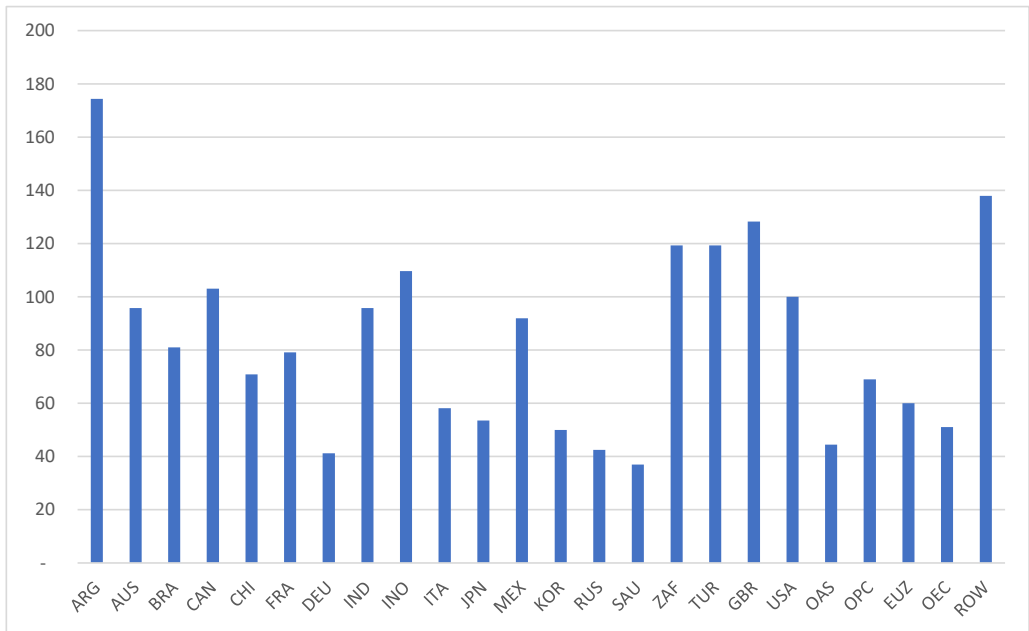
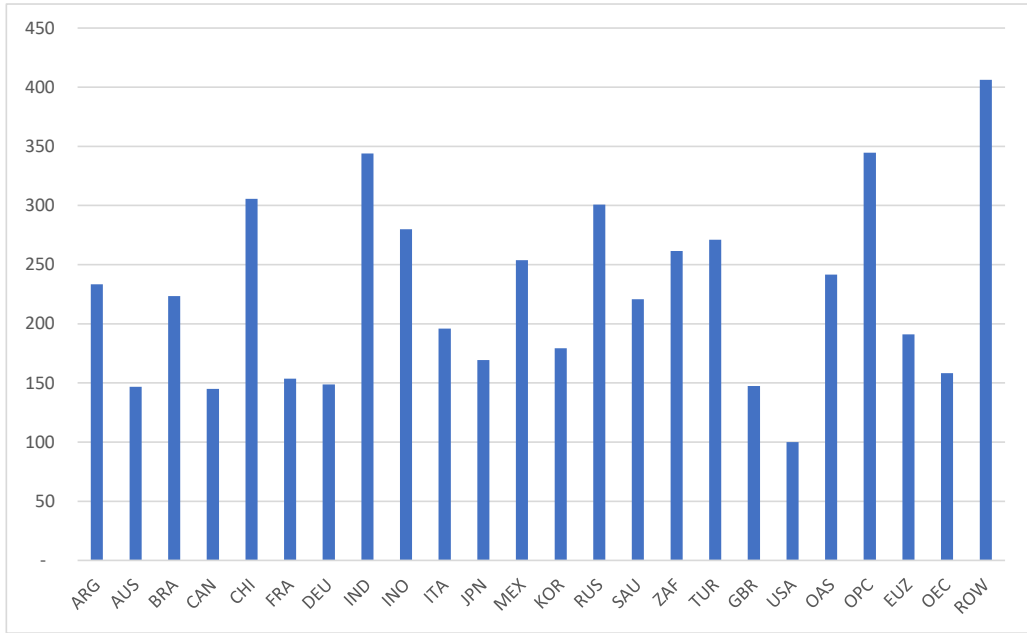


Figure 5 - Index of Health Policy relative to US



The Net Risk Index for countries is presented in Figure 6 and Shock on Equity Risk Premia for Scenario 4-7 are presented in Table 5.

Figure 6 - Net Country Risk Index

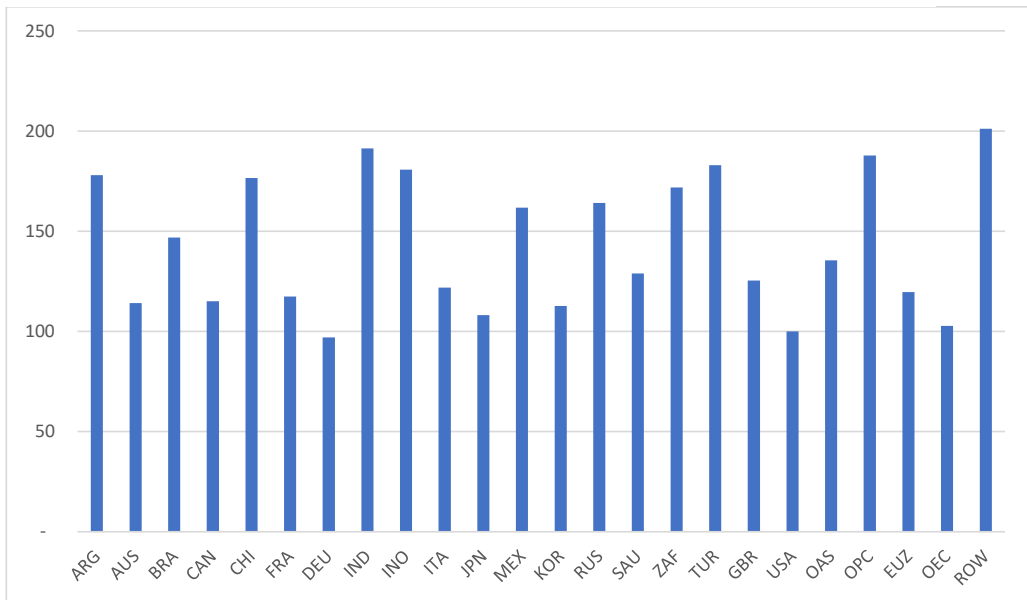


Table 5 – Shock to equity risk premium for scenario 4-7

Region	S04	S05	S06	S07
Argentina	1.90	2.07	2.30	1.90
Australia	1.23	1.37	1.54	1.23
Brazil	1.59	1.78	2.03	1.59
Canada	1.23	1.36	1.52	1.23
China	1.97	2.27	2.67	1.97
France	1.27	1.40	1.59	1.27
Germany	1.07	1.21	1.41	1.07
India	2.20	2.62	3.18	2.20
Indonesia	2.06	2.43	2.93	2.06
Italy	1.32	1.47	1.66	1.32
Japan	1.18	1.33	1.53	1.18
Mexico	1.76	1.98	2.27	1.76
Republic of Korea	1.25	1.43	1.67	1.25
Russia	1.77	1.96	2.22	1.77
Saudi Arabia	1.38	1.52	1.70	1.38
South Africa	1.85	2.06	2.33	1.85
Turkey	1.98	2.20	2.50	1.98
United Kingdom	1.35	1.50	1.70	1.35
United States of America	1.07	1.18	1.33	1.07
Other Asia	1.51	1.75	2.07	1.51
Other oil-producing countries	2.03	2.25	2.55	2.03
Rest of Euro Zone	1.29	1.42	1.60	1.29
Rest of OECD	1.11	1.22	1.38	1.11
Rest of the World	2.21	2.51	2.91	2.21

c) Shocks to the cost of production in each sector

As well as the shock to labor inputs, we identify that other inputs such as Trade, Land Transport, Air Transport and Sea Transport have been significantly affected by the outbreak. Thus, we calculate the share of inputs from these exposed sectors to the six aggregated sectors of the model and compare the contribution relative to China. We then benchmark the percentage increase in the cost of production in Chinese production sectors during SARS to the first

scenario and scale the percentage across scenarios to match the changes in the mortality component of the labor shock. Variable shares of inputs from exposed sectors to aggregated economic sectors also allow us to vary the shock across sectors in the countries. Table 6 contains the shocks to the cost of production in each sector in each country due to the share of inputs from exposed sectors.

Table 6 – Shocks to cost of production

Region	Energy	Mining	Agriculture	Durable Manufacturing	Non-durable Manufacturing	Services
Argentina	0.37	0.24	0.37	0.35	0.40	0.38
Australia	0.43	0.43	0.42	0.39	0.41	0.45
Brazil	0.44	0.46	0.44	0.42	0.45	0.44
Canada	0.44	0.37	0.42	0.40	0.41	0.44
China	0.50	0.50	0.50	0.50	0.50	0.50
France	0.38	0.31	0.36	0.40	0.42	0.46
Germany	0.43	0.37	0.40	0.45	0.45	0.47
India	0.47	0.33	0.47	0.42	0.45	0.43
Indonesia	0.37	0.33	0.31	0.36	0.40	0.38
Italy	0.36	0.33	0.38	0.42	0.44	0.46
Japan	0.45	0.40	0.45	0.47	0.47	0.49
Mexico	0.41	0.38	0.39	0.42	0.42	0.41
Other Asia	0.44	0.39	0.44	0.45	0.45	0.47
Other oil producing countries	0.49	0.41	0.47	0.40	0.43	0.45
Republic of Korea	0.39	0.30	0.37	0.43	0.42	0.43
Rest of Euro Zone	0.42	0.41	0.43	0.43	0.46	0.48
Rest of OECD	0.42	0.38	0.41	0.41	0.43	0.46
Rest of the World	0.52	0.46	0.51	0.45	0.49	0.48
Russia	0.54	0.37	0.43	0.41	0.42	0.45
Saudi Arabia	0.32	0.25	0.29	0.29	0.25	0.35
South Africa	0.40	0.35	0.39	0.41	0.43	0.38
Turkey	0.37	0.36	0.39	0.39	0.42	0.42
United Kingdom	0.39	0.37	0.39	0.39	0.42	0.46
United States of America	0.53	0.40	0.51	0.50	0.51	0.53

a) Shocks to consumption demand

The G-Cubed model endogenously changes spending patterns in response to changes in income, wealth, and relative price changes. However, independent of these variables, during an outbreak, it is likely that preferences for certain activities will change with the outbreak. Following McKibbin and Sidorenko (2006), we assume that the reduction in spending on those activities will reduce the overall spending, hence saving money for future expenditure. In modeling this behavior, we employ a Sector Exposure Index. The Index is calculated as the share of exposed sectors: Trade, Land, Air & Sea Transport and Recreation, within the GDP of a country relative to China. The reduction in consumption expenditure during the SARS outbreak in China is used as the benchmark for the first scenario. This benchmark is then scaled across other scenarios relative to the mortality component of the labor shock and adjusted across countries through the different sectoral exposure. Figure 7 contains the Sector Exposure Indices for the countries and the shock to consumption demand is presented in Table 7. Note that CBO (2005) uses a shock of 3% to US consumption from an H5N1 influenza pandemic which is between S05 and S06 in Table 7.

Figure 7 - Index of Sector Exposure to Exposed Activities

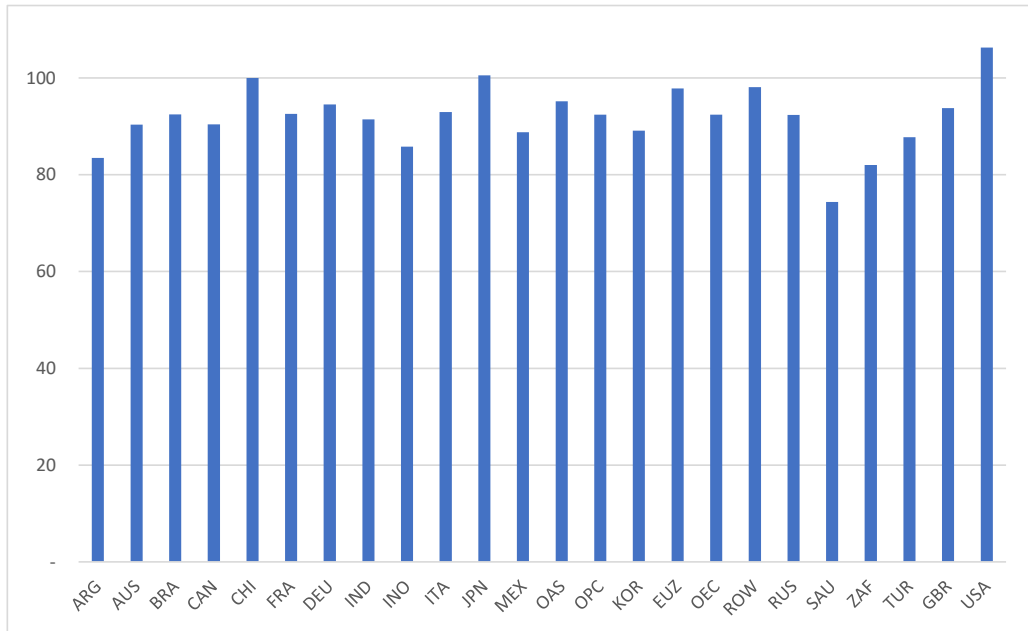


Table 7 – Shocks to consumption demand

Region	S04	S05	S06	S07
Argentina	- 0.83	- 2.09	- 3.76	- 0.83
Australia	- 0.90	- 2.26	- 4.07	- 0.90
Brazil	- 0.92	- 2.31	- 4.16	- 0.92
Canada	- 0.90	- 2.26	- 4.07	- 0.90
China	- 1.00	- 2.50	- 4.50	- 1.00
France	- 0.93	- 2.31	- 4.16	- 0.93
Germany	- 0.95	- 2.36	- 4.25	- 0.95
India	- 0.91	- 2.29	- 4.11	- 0.91
Indonesia	- 0.86	- 2.15	- 3.86	- 0.86
Italy	- 0.93	- 2.32	- 4.18	- 0.93
Japan	- 1.01	- 2.51	- 4.52	- 1.01
Mexico	- 0.89	- 2.22	- 4.00	- 0.89
Other Asia	- 0.95	- 2.38	- 4.28	- 0.95
Other oil producing countries	- 0.92	- 2.31	- 4.16	- 0.92
Republic of Korea	- 0.89	- 2.23	- 4.01	- 0.89
Rest of Euro Zone	- 0.98	- 2.45	- 4.40	- 0.98
Rest of OECD	- 0.92	- 2.31	- 4.16	- 0.92
Rest of the World	- 0.98	- 2.45	- 4.42	- 0.98
Russia	- 0.92	- 2.31	- 4.16	- 0.92
Saudi Arabia	- 0.74	- 1.86	- 3.35	- 0.74
South Africa	- 0.82	- 2.05	- 3.69	- 0.82
Turkey	- 0.88	- 2.19	- 3.95	- 0.88
United Kingdom	- 0.94	- 2.34	- 4.22	- 0.94
United States of America	- 1.06	- 2.66	- 4.78	- 1.06

b) Shocks to government expenditure

With the previous experience of pandemics, governments across the world have exercised a stronger caution towards the outbreak by taking measures, such as strengthening health screening at ports and investments in strengthening healthcare infrastructure, to prevent the outbreak reaching additional countries. They have also responded by increasing health expenditures to contain the spread. In modeling these interventions by governments, we use the change in Chinese government expenditure relative to GDP in 2003 during the SARS outbreak as a benchmark and use the average of Index of Governance and Index of Health Policy to obtain the potential increase in government expenditure by other countries. We then

scale the shock across scenarios using the mortality component of the labor shock. Table 8 demonstrates the magnitude of the government expenditure shocks for countries for Scenario 4 to 7.

Table 8 – Shocks to government expenditure

Region	S04	S05	S06	S07
Argentina	0.39	0.98	1.76	0.39
Australia	0.27	0.67	1.21	0.27
Brazil	0.39	0.98	1.76	0.39
Canada	0.26	0.66	1.19	0.26
China	0.50	1.25	2.25	0.50
France	0.30	0.74	1.34	0.30
Germany	0.27	0.68	1.22	0.27
India	0.52	1.30	2.34	0.52
Indonesia	0.47	1.18	2.12	0.47
Italy	0.34	0.84	1.51	0.34
Japan	0.30	0.74	1.33	0.30
Mexico	0.43	1.07	1.93	0.43
Republic of Korea	0.31	0.79	1.41	0.31
Russia	0.49	1.23	2.21	0.49
Saudi Arabia	0.38	0.95	1.71	0.38
South Africa	0.43	1.08	1.94	0.43
Turkey	0.47	1.17	2.11	0.47
United Kingdom	0.27	0.68	1.22	0.27
United States of America	0.22	0.54	0.98	0.22
Other Asia	0.39	0.99	1.77	0.39
Other oil producing countries	0.54	1.35	2.42	0.54
Rest of Euro Zone	0.33	0.81	1.46	0.33
Rest of OECD	0.28	0.70	1.26	0.28
Rest of the World	0.59	1.49	2.67	0.59

5. Simulation Results

(a) Baseline scenario

We first solve the model from 2016 to 2100 with 2015 as the base year. The key inputs into the baseline are the initial dynamics from 2015 to 2016 and subsequent projections from 2016 forward for labor-augmenting technological progress by sector and by country. The labor-augmenting technology projections follow the approach of Barro (1991, 2015). Over long periods, Barro estimates that the average catchup rate of individual countries to the world-wide productivity frontier is 2% per year. We use the Groningen Growth and Development database (2018) to estimate the initial level of productivity in each sector of each region in the model. Given this initial productivity, we then take the ratio of this to the equivalent sector in the US, which we assume is the frontier. Given this initial gap in sectoral productivity, we use the Barro catchup model to generate long term projections of the productivity growth rate of each sector within each country. Where we expect that regions will catch up more quickly to the frontier due to economic reforms (e.g., China) or more slowly to the frontier due to institutional rigidities (e.g., Russia), we vary the catchup rate over time. The calibration of the catchup rate attempts to replicate recent growth experiences of each country and region in the model.

The exogenous sectoral productivity growth rate, together with the economy-wide growth in labor supply, are the exogenous drivers of sector growth for each country. The growth in the capital stock in each sector in each region is determined endogenously within the model.

In the alternative COVID-19 scenarios, we incorporate the range of shocks discussed above to model the economic consequences of different epidemiological assumptions. All results below are the difference between the COVID-19 scenario and the baseline of the model.

(b) Results

Table 9 contains the impact on populations in different regions. These are the core shocks that are combined with the various indicators above to create the seven scenarios. The mortality rates for each country under each scenario are contained in Table B-1 in Appendix B.

Table 9 – Impact on populations under each scenario

Country/Region	Population (Thousands)	Mortality in First Year (Thousands)						
		S01	S02	S03	S04	S05	S06	S07
Argentina	43,418	-	-	-	50	126	226	50
Australia	23,800	-	-	-	21	53	96	21
Brazil	205,962	-	-	-	257	641	1,154	257
Canada	35,950	-	-	-	30	74	133	30
China	1,397,029	279	3,493	12,573	2,794	6,985	12,573	2,794
France	64,457	-	-	-	60	149	268	60
Germany	81,708	-	-	-	79	198	357	79
India	1,309,054	-	-	-	3,693	9,232	16,617	3,693
Indonesia	258,162	-	-	-	647	1,616	2,909	647
Italy	59,504	-	-	-	59	147	265	59
Japan	127,975	-	-	-	127	317	570	127
Mexico	125,891	-	-	-	184	460	828	184
Republic of Korea	50,594	-	-	-	61	151	272	61
Russia	143,888	-	-	-	186	465	837	186
Saudi Arabia	31,557	-	-	-	29	71	128	29
South Africa	55,291	-	-	-	75	187	337	75
Turkey	78,271	-	-	-	116	290	522	116
United Kingdom	65,397	-	-	-	64	161	290	64
United States of America	319,929	-	-	-	236	589	1,060	236
Other Asia	330,935	-	-	-	530	1,324	2,384	530
Other oil producing countries	517,452	-	-	-	774	1,936	3,485	774
Rest of Euro Zone	117,427	-	-	-	106	265	478	106
Rest of OECD	33,954	-	-	-	27	67	121	27
Rest of the World	2,505,604	-	-	-	4,986	12,464	22,435	4,986
Total	7,983,209	279	3,493	12,573	15,188	37,971	68,347	15,188

Table 9 shows that for even the lowest of the pandemic scenarios (S04), there are estimated to be around 15 million deaths. In the United States, the estimate is 236,000 deaths. These estimated deaths from COVID-19 can be compared to a regular influenza season in the United States, where around 55,000 people die each year.

Table 10 - GDP loss in 2020 (% deviation from baseline)

Country/Region	S01	S02	S03	S04	S05	S06	S07
AUS	-0.3	-0.4	-0.7	-2.1	-4.6	-7.9	-2.0
BRA	-0.3	-0.3	-0.5	-2.1	-4.7	-8.0	-1.9
CHI	-0.4	-1.9	-6.0	-1.6	-3.6	-6.2	-2.2
IND	-0.2	-0.2	-0.4	-1.4	-3.1	-5.3	-1.3
EUZ	-0.2	-0.2	-0.4	-2.1	-4.8	-8.4	-1.9
FRA	-0.2	-0.3	-0.3	-2.0	-4.6	-8.0	-1.5
DEU	-0.2	-0.3	-0.5	-2.2	-5.0	-8.7	-1.7
ZAF	-0.2	-0.2	-0.4	-1.8	-4.0	-7.0	-1.5
ITA	-0.2	-0.3	-0.4	-2.1	-4.8	-8.3	-2.2
JPN	-0.3	-0.4	-0.5	-2.5	-5.7	-9.9	-2.0
GBR	-0.2	-0.2	-0.3	-1.5	-3.5	-6.0	-1.2
ROW	-0.2	-0.2	-0.3	-1.5	-3.5	-5.9	-1.5
MEX	-0.1	-0.1	-0.1	-0.9	-2.2	-3.8	-0.9
CAN	-0.2	-0.2	-0.4	-1.8	-4.1	-7.1	-1.6
OECD	-0.3	-0.3	-0.5	-2.0	-4.4	-7.7	-1.8
OPC	-0.2	-0.2	-0.4	-1.4	-3.2	-5.5	-1.3
ARG	-0.2	-0.3	-0.5	-1.6	-3.5	-6.0	-1.2
RUS	-0.2	-0.3	-0.5	-2.0	-4.6	-8.0	-1.9
SAU	-0.2	-0.2	-0.3	-0.7	-1.4	-2.4	-1.3
TUR	-0.1	-0.2	-0.2	-1.4	-3.2	-5.5	-1.2
USA	-0.1	-0.1	-0.2	-2.0	-4.8	-8.4	-1.5
OAS	-0.1	-0.2	-0.4	-1.6	-3.6	-6.3	-1.5
INO	-0.2	-0.2	-0.3	-1.3	-2.8	-4.7	-1.3
KOR	-0.1	-0.2	-0.3	-1.4	-3.3	-5.8	-1.3

Tables 10 and 11 provide a summary of the overall GDP loss for each country/region under the seven scenarios. The results in Table 10 are the Change in GDP in 2020 expressed as a percentage change from the baseline. The results in Table 11 are the results from Table 10 converted into billions of \$2020US.

Table 11 - GDP Loss in 2020 (\$US billions)

Country/Region	S01	S02	S03	S04	S05	S06	S07
AUS	(4)	(5)	(9)	(27)	(60)	(103)	(27)
BRA	(9)	(12)	(19)	(72)	(161)	(275)	(65)
CHI	(95)	(488)	(1,564)	(426)	(946)	(1,618)	(560)
IND	(21)	(26)	(40)	(152)	(334)	(567)	(142)
EUZ	(11)	(13)	(19)	(111)	(256)	(446)	(101)
FRA	(7)	(8)	(11)	(63)	(144)	(250)	(46)
DEU	(11)	(14)	(21)	(99)	(225)	(390)	(78)
ZAF	(1)	(2)	(3)	(14)	(33)	(57)	(12)
ITA	(6)	(7)	(9)	(54)	(123)	(214)	(56)
JPN	(17)	(20)	(28)	(140)	(318)	(549)	(113)
GBR	(5)	(6)	(9)	(48)	(108)	(187)	(39)
ROW	(24)	(29)	(43)	(234)	(529)	(906)	(227)
MEX	(2)	(2)	(3)	(24)	(57)	(98)	(24)
CAN	(3)	(4)	(6)	(32)	(74)	(128)	(28)
OEC	(5)	(6)	(10)	(40)	(91)	(157)	(36)
OPC	(10)	(12)	(18)	(73)	(164)	(282)	(69)
ARG	(2)	(3)	(5)	(15)	(33)	(56)	(11)
RUS	(10)	(12)	(19)	(84)	(191)	(331)	(81)
SAU	(3)	(3)	(5)	(12)	(24)	(40)	(22)
TUR	(3)	(4)	(6)	(33)	(75)	(130)	(30)
USA	(16)	(22)	(40)	(420)	(1,004)	(1,769)	(314)
OAS	(6)	(10)	(19)	(80)	(186)	(324)	(77)
INO	(6)	(7)	(11)	(45)	(99)	(167)	(46)
KOR	(3)	(4)	(7)	(31)	(71)	(124)	(29)
Total Change (USD Billion)	(283)	(720)	(1,922)	(2,330)	(5,305)	(9,170)	(2,230)

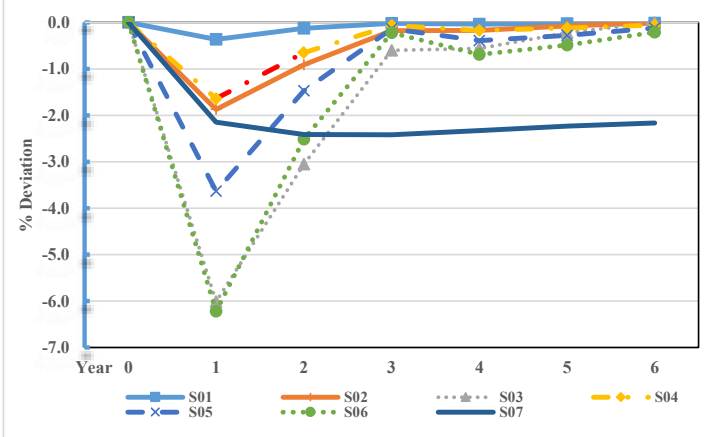
Tables 10 and 11 illustrate the scale of the various pandemic scenarios on reducing GDP in the global economy. Even a low-end pandemic modeled on the Hong Kong Flu is expected to reduce global GDP by around \$US2.4 trillion and a more serious outbreak similar to the Spanish flu reduces global GDP by over \$US9trillion in 2020.

Figures 8-10 provide the time profile of the results for several countries. The patterns in the figures represents the nature of the assumed shocks which for the first 6 scenarios are expected to disappear over time, Figure 8 contains results for China under each scenario. We present results for Real GDP, private investment, consumption, the trade balance and then the short real interest rate and the value of the equity market for sector 5 which is durable manufacturing. Figure 9 contains the results for the United States and Figure 10 for Australia.

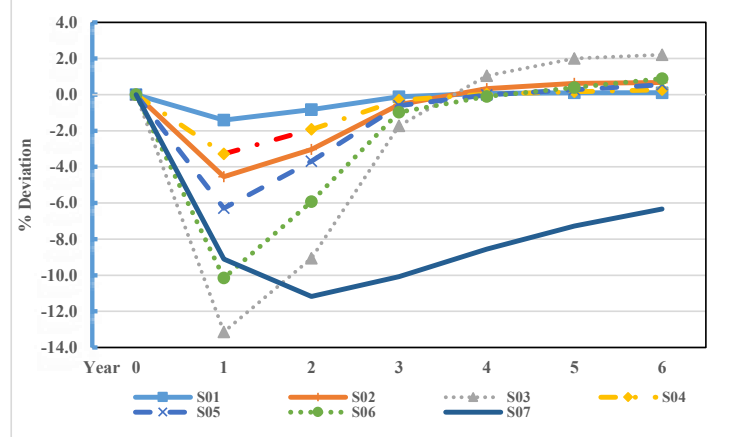
The shocks which make up the pandemic cause a sharp drop in consumption and investment. The decline in aggregate demand, together with the original risk shocks cause a sharp drop in equity markets. The funds from equity markets are partly shifted into bonds, partly into cash and partly overseas depending on which markets are most affected. Central banks respond by cutting interest rates which drive together with the increased demand for bonds from the portfolio shift drives down the real interest rate. Equity markets drop sharply both because of the rise in risk but also because of the expected economic slowdown and the fall in expected profits. For each scenario, there is a V shape recovery except for scenario 7. Recall that scenario 7 is the same as scenario 4 in year 1, but with the expectation that the pandemic will recur each year into the future.

Similar patterns can be seen in the dynamic results for the United States and Australia shown in Figures 9 and 10. The quantitative magnitudes differ across countries but the pattern of a sharp shock followed by a gradual recovery are common across countries. The improvement in the trade balance of China and deterioration in the US trade balance reflect to global reallocation of financial capital as a results for the shock. Capital flows out of severely affected economies like China and other developing and emerging economies and into safer advanced economies like the United States, Europe and Australia. This movement of capital tends to appreciate the exchange rate of countries that are receiving capital and depreciate the exchange rates of countries that are losing capital. The depreciation of the exchange rate increases exports and reduced imports in the countries losing capital and hence lead to the current account adjustment that is consistent with the capital account adjustment.

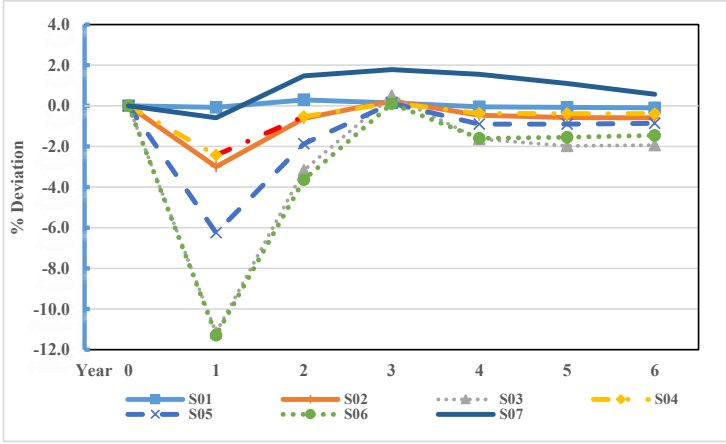
Figure 8 - Dynamic Results for China
Change in Real GDP



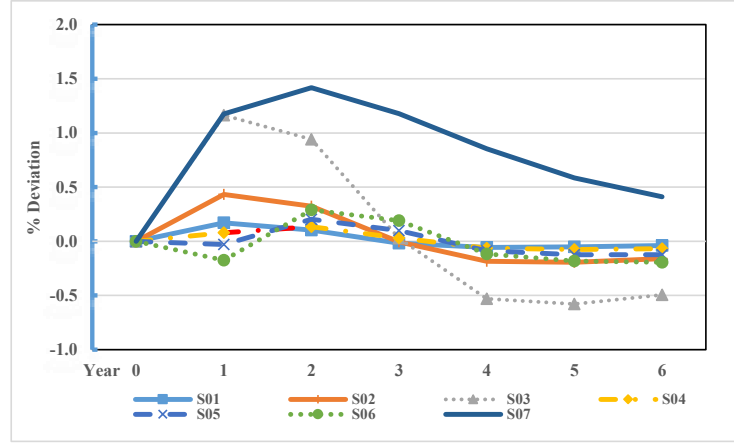
Change in Investment



Change in Consumption

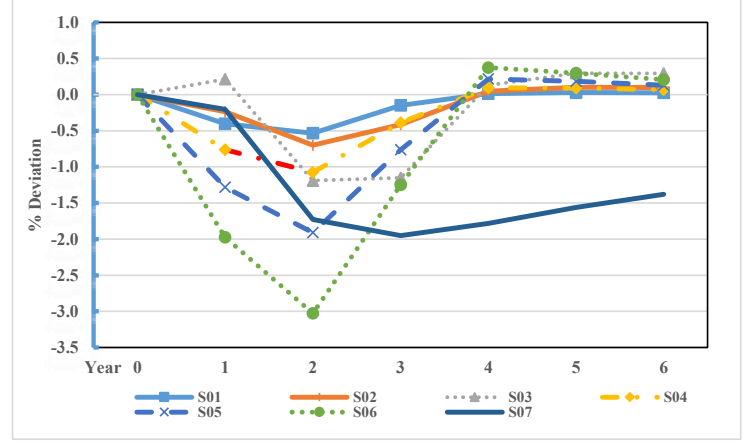


Change in Trade Balance as a proportion of GDP

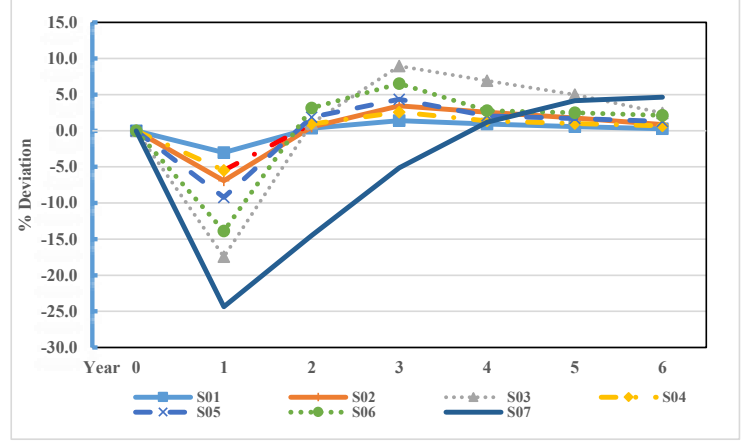


Covid Economics 10, 27 April 2020: 121-161

Figure 8 - Dynamic Results for China (Contd.)
Change in Short-term Real Interest Rates

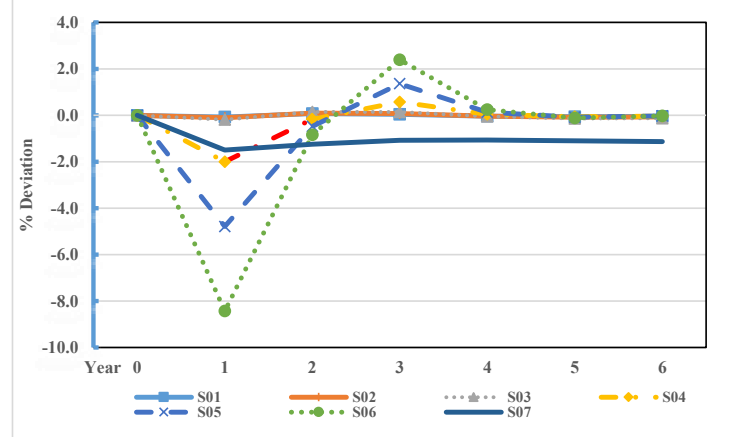


Change in Tobin's Q for Durable Manufacturing Sector

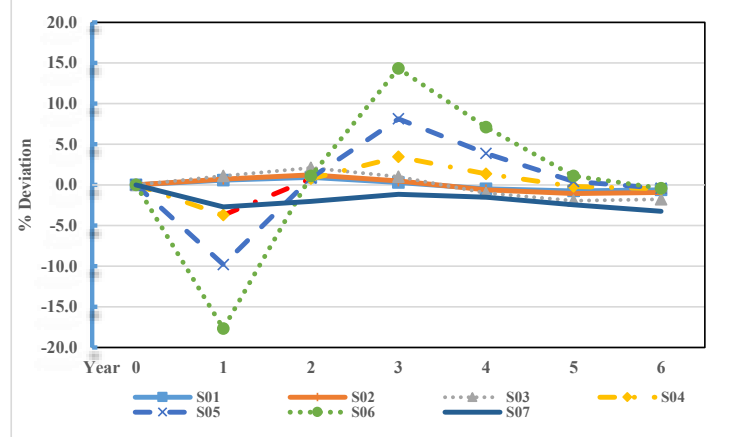


Covid Economics 10, 27 April 2020: 121-161

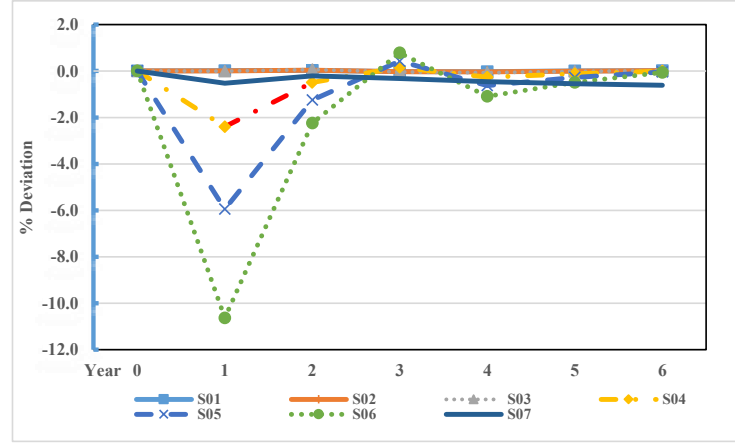
Figure 9 - Dynamic Results for United States
Change in Real GDP



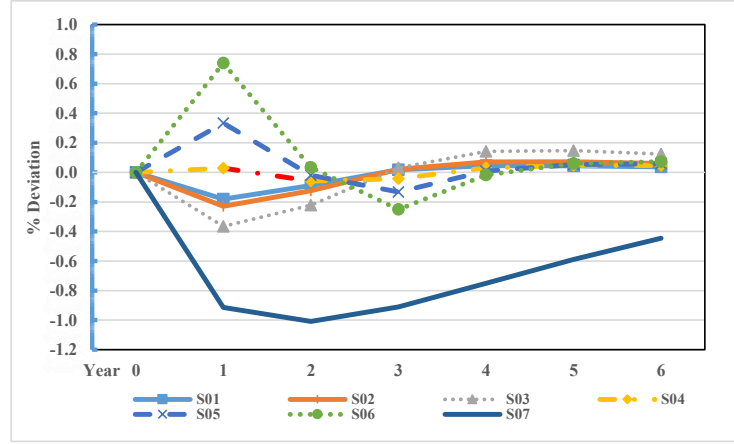
Change in Investment



Change in Consumption

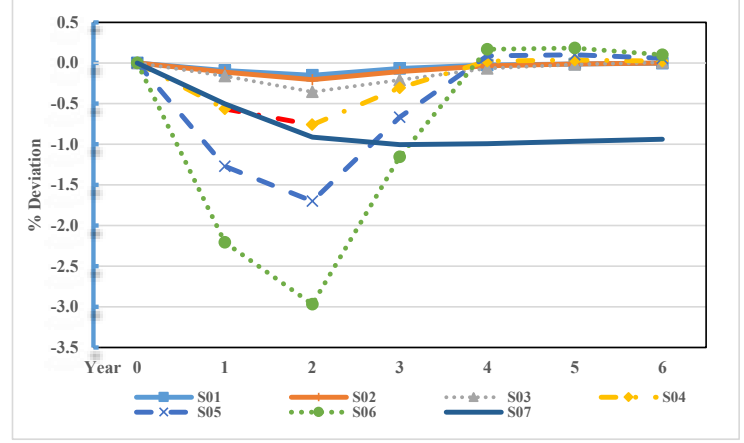


Change in Trade Balance as a proportion of GDP

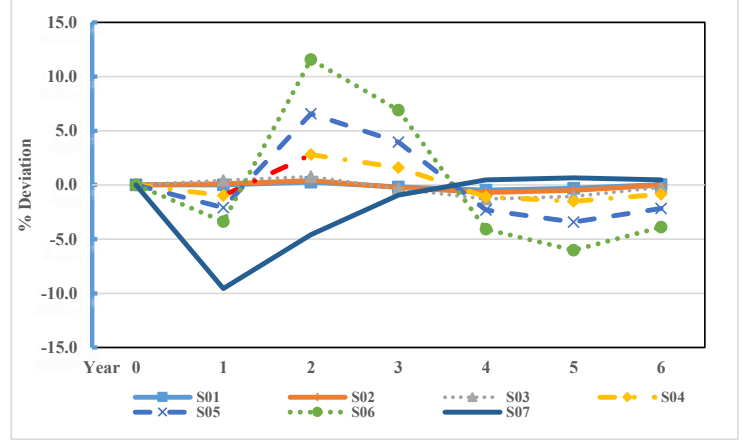


Covid Economics 10, 27 April 2020: 121-161

Figure 9 - Dynamic Results for United States (Contd.)
Change in Short-term Real Interest Rates

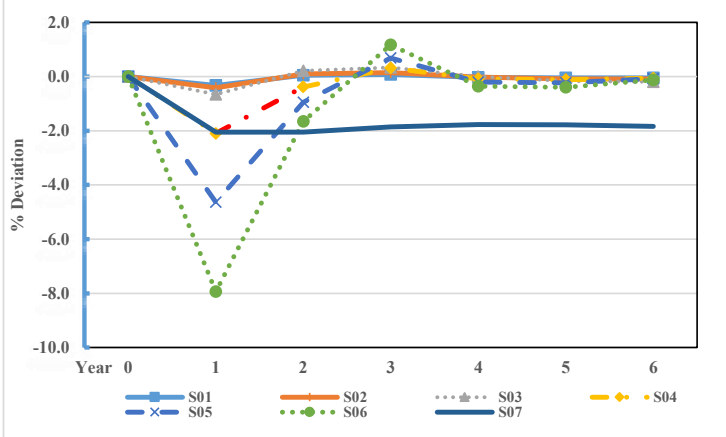


Change in Tobin's Q for Durable Manufacturing Sector

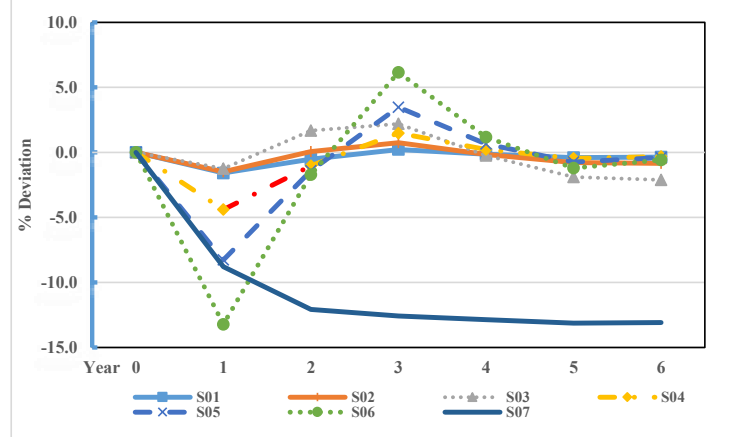


Covid Economics 10, 27 April 2020: 121-161

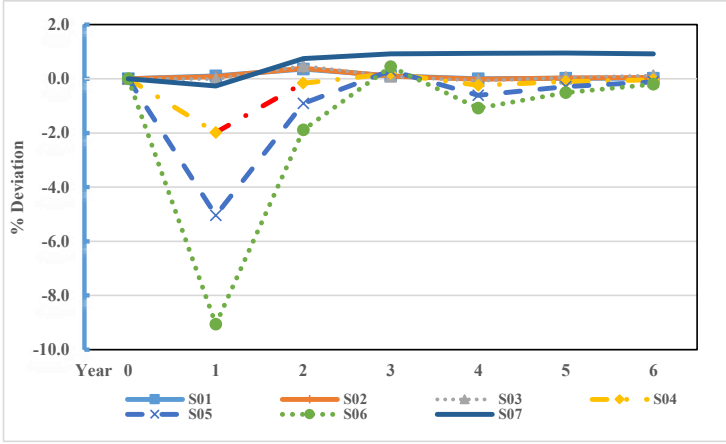
Figure 10 - Dynamic Results for Australia
Change in Real GDP



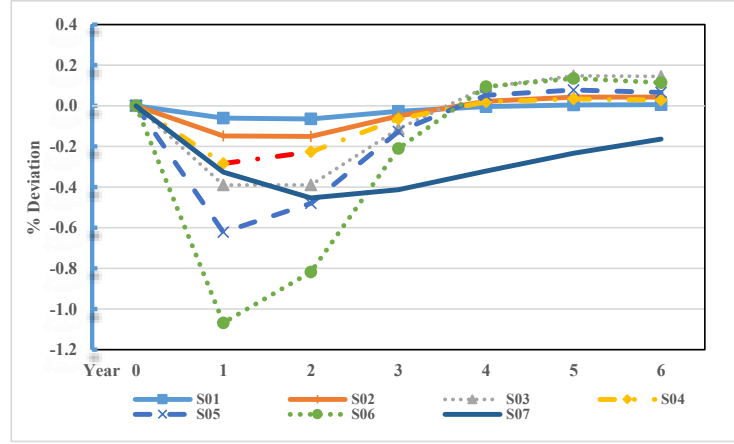
Change in Investment



Change in Consumption

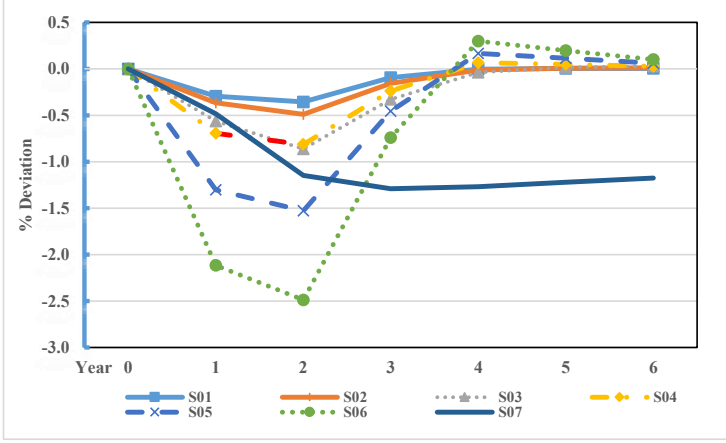


Change in Trade Balance as a proportion of GDP

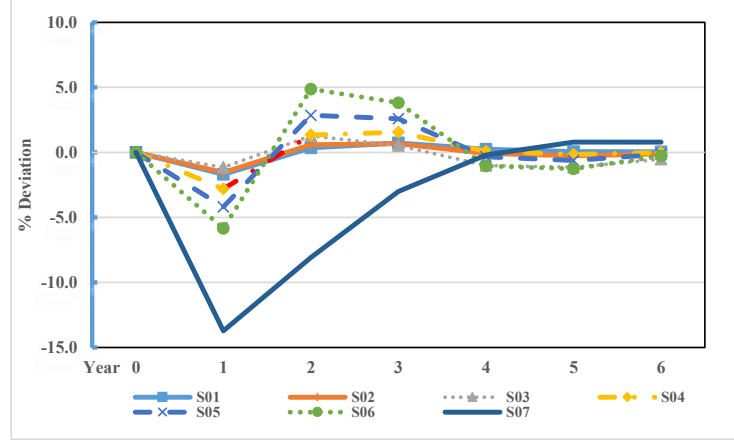


Covid Economics 10, 27 April 2020: 121-161

Figure 10 - Dynamic Results for Australia (Contd.)
Change in Short-term Real Interest Rates



Change in Tobin's Q for Durable Manufacturing Sector



Covid Economics 10, 27 April 2020: 121-161

These results are very sensitive to the assumptions in the model, to the shocks we feed in and to the assumed macroeconomic policy responses in each countries. Central banks are assumed to respond according to a Henderson-Mckibbin-Taylor rule which differs across countries (see Mckibbin and Triggs (2018)). Fiscal authorities are allowing automatic stabilizers to increase budget deficits but cover addition debt servicing costs with a lump-sum tax levied on households over time. In addition, there is the fiscal spending increase assumed in the shock design outlined above.

6. Conclusions and Policy Implications

This paper has presented some preliminary estimates of the cost of the COVID-19 outbreak under seven different scenarios of how the disease might evolve. The goal is not to be definitive about the virus outbreak but to provide important information about a range of possible economic costs of the disease. At the time of writing this paper, the probability of any of these scenarios and the range of plausible alternatives are highly uncertain. In the case where COVID-19 develops into a global pandemic, our results suggest that the cost can escalate quickly.

A range of policy responses will be required both in the short term as well as in the coming years. In the short term, central banks and Treasuries need to make sure that disrupted economies continue to function while the disease outbreak continues. In the face of real and financial stress, there is a critical role for governments. While cutting interest rates is a possible response for central banks, the shock is not only a demand management problem but a multi-faceted crisis that will require monetary, fiscal and health policy responses. Quarantining affected people and reducing large scale social interaction is an effective response. Wide dissemination of good hygiene practices as outlined in Levine and McKibbin (2020) can be a low cost and highly effective response that can reduce the extent of contagion and therefore reduce the social and economic cost.

The longer-term responses are even more important. Despite the potential loss of life and the possible large-scale disruption to a large number of people, many governments have been reluctant to invest sufficiently in their health care systems, let alone public health systems in less developed countries where many infectious diseases are likely to originate. Experts have warned and continue to warn that zoonotic diseases will continue to pose a threat to the lives of millions of people with potentially major disruption to an integrated world economy. The idea that any country can be an island in an integrated global economy is proven wrong by the

latest outbreak of COVID-19. Global cooperation, especially in the sphere of public health and economic development, is essential. All major countries need to participate actively. It is too late to act once the disease has taken hold in many other countries and attempt to close borders once a pandemic has started.

Poverty kills poor people, but the outbreak of COVID-19 shows that diseases can be generated in poor countries due to overcrowding, poor public health and the interaction with wild animal can kill people of any socioeconomic group in any society. There needs to be vastly more investment in public health and development in the richest but also, and especially, in the poorest countries. This study indicates the possible costs that can be avoided through global cooperative investment in public health in all countries. We have known this critical policy intervention for decades, yet politicians continue to ignore the scientific evidence on the role of public health in improving the quality of life and as a driver of economic growth.

References

- Aguiar, A., Chepeliev, M., Corong, E., McDougall, R., & van der Mensbrugge, D. (2019). The GTAP Data Base: Version 10. *Journal of Global Economic Analysis*, 4(1), 1-27.
- Arndt, C. and J. D. Lewis (2001). The HIV/AIDS Pandemic in South Africa: Sectoral Impacts and Unemployment. *Journal of International Development* 13(4): 427-49.
- Barker, W. H. and J. P. Mullooly (1980). Impact of epidemic type A influenza in a defined adult population. *American Journal of Epidemiology* 112(6): 798-811
- Barro, R. J. (1991). Economic Growth in a Cross-Section of Countries. *The Quarterly Journal of Economics*, Vol. 106, No. 2, pp. 407-443.
- Barro, R. J. (2015). Convergence and Modernisation. *Economic Journal*, Vol. 125, No. 585, pp. 911-942.
- Bell, C., S. Devarajan and H. Hersbach (2004). Thinking about the long-run economic costs of AIDS, in *The Macroeconomics of HIV/AIDS*, M. Haacker (eds). Washington DC, IMF: 96-144.
- Beveridge, W. I., 1991. The chronicle of influenza epidemics. *History and Philosophy of the Life Sciences* 13(2), 223-34.
- Bhargava, A. and et al., 2001. Modeling the Effects of Health on Economic Growth. *Journal of Health Economics* 20(3), 423-40.
- Bittlingmayer, G., 1998. Output, Stock Volatility, and Political Uncertainty in a Natural Experiment: Germany, 1880-1940. *Journal of Finance* 53(6), 2243-57.
- Bloom, D. E. and J. D. Sachs, 1998. Geography, Demography, and Economic Growth in Africa. *Brookings Papers on Economic Activity* 0(2), 207-73.
- Bloom, E., V. d. Wit, et al., 2005. Potential economic impact of an Avian Flu pandemic on Asia. ERD Policy Brief Series No. 42. Asian Development Bank, Manila.
http://www.adb.org/Documents/EDRC/Policy_Briefs/PB042.pdf.
- Chou, J., N.-F. Kuo, et al., 2004. Potential Impacts of the SARS Outbreak on Taiwan's Economy. *Asian Economic Papers* 3(1), 84-112.
- Congressional Budget Office (2005) *A Potential Influenza Pandemic: Possible Macroeconomic Effects and Policy Issues*, CBO Washington DC.
- Cox, N. J. and K. Fukuda (1998). Influenza. *Infectious Disease Clinics of North America* 12(1): 27-38.
- Cuddington, J. T., 1993a. Further results on the macroeconomic effects of AIDS: the dualistic, labour-surplus economy. *World Bank Economic Review* 7(3), 403-17.
- Cuddington, J. T., 1993b. Modeling the macroeconomic effects of AIDS, with an application to Tanzania. *World Bank Economic Review* 7(2), 173-89.
- Cuddington, J. T. and J. D. Hancock, 1994. Assessing the Impact of AIDS on the Growth Path of the Malawian Economy. *Journal of Development Economics* 43(2), 363-68.

- Cuddington, J. T., J. D. Hancock, et al., 1994. A Dynamic Aggregate Model of the AIDS Epidemic with Possible Policy Interventions. *Journal of Policy Modeling* 16(5), 473-96.
- Das, S. R. and R. Uppal, 2004. Systemic Risk and International Portfolio Choice. *Journal of Finance* 59(6), 2809-34.
- Feldstein, M. and C. Horioka, 1980. Domestic Saving and International Capital Flows. *Economic Journal* 90(358), 314-29.
- Figura, S. Z. (1998). The forgotten pandemic. The Spanish Flu of 1918 was gravest crisis American hospitals had ever faced. *The Volunteer Leader* 39(2): 5.
- Fisman, R. and I. Love, 2004. Financial Development and Growth in the Short and Long Run. The World Bank, Policy Research Working Paper Series 3319.
- Freire, S., 2004. Impact of HIV/AIDS on saving behaviour in South Africa. African development and poverty reduction: the macro-micro linkage, Lord Charles Hotel, Somerset West, South Africa.
- GHSIndex, 2020. Global Health Security Index 2019. Nuclear Threat Initiative, Washington D.C; Johns Hopkins Center for Health Security, Maryland; and The Economist Intelligence Unit, London. <https://www.ghsindex.org/>.
- Gordon, R. H. and A. L. Bovenberg, 1996. Why Is Capital So Immobile Internationally? Possible Explanations and Implications for Capital Income Taxation. *American Economic Review* 86(5), 1057-75.
- Grais, R. F., J. H. Ellis, et al., 2003. Assessing the impact of airline travel on the geographic spread of pandemic influenza. *European Journal of Epidemiology* 18(11), 1065-72.
- Haacker, M., 2002a. The economic consequences of HIV/AIDS in Southern Africa. IMF Working Paper W/02/38, 41-95.
- Haacker, M., 2002b. Modeling the macroeconomic impact of HIV/AIDS. IMF Working Paper W/02/195, 41-95.
- Haacker, M., Ed. 2004. *The Macroeconomics of HIV/AIDS*. IMF, Washington DC.
- Hai, W., Z. Zhao, et al., 2004. The Short-Term Impact of SARS on the Chinese Economy. *Asian Economic Papers* 3(1), 57-61.
- Henderson, D. W. and W. McKibbin (1993). A Comparison of Some Basic Monetary Policy Regimes for Open Economies: Implications of Different Degrees of Instrument Adjustment and Wage Persistence. *Carnegie-Rochester Conference Series on Public Policy* 39(1): 221-317.
- Hyams, K. C., F. M. Murphy, et al., 2002. Responding to Chemical, Biological, or Nuclear Terrorism: The Indirect and Long-Term Health Effects May Present the Greatest Challenge. *Journal of Health Politics, Policy and Law* 27(2), 273-91.
- Kaufmann, D., A. Kraay, et al., 2004. Governance Matters III: Governance Indicators for 1996, 1998, 2000, and 2002. *World Bank Economic Review* 18(2), 253-87.
- Kilbourne, E. D., 2004. Influenza pandemics: can we prepare for the unpredictable? *Viral Immunology* 17(3), 350-7.

- Kilbourne, E. D., 2006. Influenza immunity: new insights from old studies. *The Journal of Infectious Diseases* 193(1), 7-8.
- Killingray, D. and H. Phillips, 2003. *The Spanish influenza pandemic of 1918-19 : new perspectives.* Routledge, London ; New York.
- Lee J-W and W. McKibbin (2004) "Globalization and Disease: The Case of SARS" *Asian Economic Papers* Vol . 3 no 1. MIT Press Cambridge USA. pp. 113-131 (ISSN 1535-3516).
- Lee J-W and W. McKibbin (2004) "Estimating the Global Economic Costs of SARS" in S. Knobler, A. Mahmoud, S. Lemon, A. Mack, L. Sivitz, and K. Oberholtzer (Editors), *Learning from SARS: Preparing for the next Outbreak*, The National Academies Press, Washington DC (0-309-09154-3)
- Levine D.I. and W. J. McKibbin, W. (2020) "Simple steps to reduce the odds of a global catastrophe" The Brookings Institution, <https://www.brookings.edu/opinions/simple-steps-to-reduce-the-odds-of-a-global-catastrophe/>
- Lokuge, B., 2005. Patent monopolies, pandemics and antiviral stockpiles: things that developing and developed countries can do. Centre for Governance of Knowledge and Development Working Paper, ANU. mimeo
- McKibbin, W. and Sachs, J. (1991). *Global Linkages: Macroeconomic Interdependence and Cooperation in the World Economy.* Brookings Institution. Washington D.C. June. <https://www.brookings.edu/book/global-linkages/>.
- McKibbin, W. and Triggs, A. (2018). *Modelling the G20.* Centre for Applied Macroeconomic Analysis. Working paper 17/2018. Australian National University. April. <https://cama.crawford.anu.edu.au/publication/cama-working-paper-series/12470/modelling-g20>.
- McKibbin W. and A. Sidorenko (2006) "Global Macroeconomic Consequences of Pandemic Influenza" *Lowy Institute Analysis*, February. 100 pages.
- McKibbin W. and A. Sidorenko (2009) "What a Flu Pandemic Could Cost the World" , *Foreign Policy*, April. <https://foreignpolicy.com/2009/04/28/what-a-flu-pandemic-could-cost-the-world/>
- McKibbin W. and P. Wilcoxon (1999) "The Theoretical and Empirical Structure of the G-Cubed Model" *Economic Modelling* , 16, 1, pp 123-148 (ISSN 0264-9993)
- McKibbin W and Wilcoxon P (2013), *A Global Approach to Energy and the Environment: The G-cubed Model" Handbook of CGE Modeling*, Chapter 17, North Holland, pp 995-1068
- Maddison, A. and Organisation for Economic Co-operation and Development. Development Centre. (1995). *Monitoring the world economy, 1820-1992.* Paris, Development Centre of the Organisation for Economic Co-operation and Development.
- Meltzer, M. I., N. J. Cox, et al., 1999. The economic impact of pandemic influenza in the United States: priorities for intervention. *Emerging Infectious Diseases* 5(5), 659-71.
- Monto, A. S., 2005. The threat of an avian influenza pandemic. *New England Journal of Medicine* 352(4), 323-325.

- Obstfeld, M. and Rogoff, K. (2000). The six major puzzles in international macroeconomics. NBER Working Paper 7777, Cambridge, MA. National Bureau of Economic Research. <http://www.nber.org/chapters/c11059.pdf>.
- Over, M., 2002. The Macroeconomic Impact on HIV/AIDS in Sub-Saharan Africa. African Technical Working Paper No. 3 Population Health and Nutrition Division, Africa Technical Department, World Bank.
- Palese, P., 2004. Influenza: old and new threats. *Nature Medicine* 10(12 Suppl), S82-7.
- Patterson, K. D. and G. F. Pyle (1991). The geography and mortality of the 1918 influenza pandemic. *Bulletin of the History of Medicine* 65(1): 4-21.
- Peiris, J. S., Y. Guan, et al., 2004. Severe acute respiratory syndrome. *Nature Medicine* 10(12 Suppl), S88-97.
- Potter, C. W., 2001. A history of influenza. *Journal of Applied Microbiology* 91(4), 572-9.
- Pritchett, L. and L. H. Summers, 1996. Wealthier Is Healthier. *Journal of Human Resources* 31(4), 841-868.
- PRS Group, 2012. The International Country Risk Guide Methodology (ICRG). PRSGroup. <https://www.prsgroup.com/wp-content/uploads/2012/11/icrgmethodology.pdf>.
- Reid, A. H. and J. K. Taubenberger (1999). The 1918 flu and other influenza pandemics: "over there" and back again. *Laboratory Investigation: a Journal of Technical Methods and Pathology* 79(2): 95-101
- Robalino, D. A., C. Jenkins, et al., 2002a. The Risks and Macroeconomic Impact of HIV/AIDS in the Middle East and North Africa: Why Waiting to Intervene Can Be Costly. Policy Research Working Paper Series: 2874, 2002. The World Bank. [URL:http://econ.worldbank.org/files/16774_wps2874.pdf] URL.
- Robalino, D. A., A. Voetberg, et al., 2002b. The Macroeconomic Impacts of AIDS in Kenya Estimating Optimal Reduction Targets for the HIV/AIDS Incidence Rate. *Journal of Policy Modeling* 24(2), 195-218.
- Ruef, C., 2004. A new influenza pandemic-unprepared for a big threat? *Infection* 32(6), 313-4.
- Sanford, J. P. (1969). Influenza: consideration of pandemics. *Advances in Internal Medicine* 15: 419-53.
- Schoenbaum, S. C., 1987. Economic impact of influenza. The individual's perspective. *American Journal of Medicine* 82(6A), 26-30.
- Scholtissek, C., 1994. Source for influenza pandemics. *Eur J Epidemiol* 10(4), 455-8.
- Shannon, G. W. and J. Willoughby, 2004. Severe Acute Respiratory Syndrome (SARS) in Asia: A Medical Geographic Perspective. *Eurasian Geography and Economics* 45(5), 359-81.
- Shortridge, K. F., J. S. Peiris, et al., 2003. The next influenza pandemic: lessons from Hong Kong. *Journal of Applied Microbiology* 94 Suppl, 70S-79S.
- Simonsen, L., M. J. Clarke, L. B. Schonberger, N. H. Arden, N. J. Cox and K. Fukuda (1998). Pandemic versus epidemic influenza mortality: a pattern of changing age distribution. *Journal of*

Infectious Diseases 178(1): 53-60.

- Simonsen, L., D. R. Olsen, et al., 2005. Pandemic influenza and mortality: past evidence and projections for the future. The threat of pandemic influenza: Are we ready? Workshop Summary. S. L. Knobler, A. Mack, A. Mahmoud and S. M. Lemon. The National Academies Press, Washington, D.C., 89-106.
- Smith, R. D., M. Yaho, et al., 2005. Assessing the macroeconomic impact of a healthcare problem: The application of computable general equilibrium analysis to antimicrobial resistance. *Journal of Health Economics* 24(5), 1055-75.
- Sui, A. and Y. C. R. Wong, 2004. Economic Impact of SARS: The Case of Hong-Kong. *Asian Economic Papers* 3(1), 62-83.
- Sunstein, C. R., 1997. Bad Deaths. *Journal of Risk and Uncertainty* 14(3), 259-82.
- The World Bank, 2006. Socioeconomic Impact of HIV/AIDS in Ukraine. The World Bank and The International HIV/AIDS Alliance in Ukraine, Washington D.C. .
http://siteresources.worldbank.org/INTUKRAINE/Resources/328335-1147812406770/ukr_aids_eng.pdf.
- Viscusi, W. K., J. K. Hakes, et al., 1997. Measures of Mortality Risks. *Journal of Risk and Uncertainty* 14(3), 213-33.
- WHO Commission on Macroeconomics and Health, Ed. 2001. *Macroeconomics and Health: Investing in Health for Economic Development*. World Health Organization.
- Wilton, P. (1993). "Spanish flu outdid WWI in number of lives claimed." *Canadian Medical Association Journal* 148(11): 2036-7.

Appendix A. G-Cubed Regions

Version G20 (6)

United States
 Japan
 Germany
 United Kingdom
 France
 Italy
 Rest of Euro Zone
 Canada
 Australia
 Rest of Advanced Economies
 Korea
 Turkey
 China
 India
 Indonesia
 Other Asia
 Mexico
 Argentina
 Brazil
 Russia
 Saudi Arabia
 South Africa
 Oil-exporting and the Middle East
 Rest of World

Rest of Euro Zone:

Spain, Netherlands, Belgium, Luxemburg, Ireland, Greece, Portugal, Finland, Cyprus, Malta, Slovakia, Slovenia, Estonia

Rest of Advanced Economies:

New Zealand, Norway, Sweden, Switzerland, Iceland, Denmark, Iceland, Liechtenstein

Oil-exporting and the Middle East:

Ecuador, Nigeria, Angola, Congo, Iran, Venezuela, Algeria, Libya, Bahrain, Iraq, Israel, Jordan, Kuwait, Lebanon, Palestinian Territory, Oman, Qatar, Syrian Arab Republic, United Arab Emirates, Yemen

Other Asia:

Singapore, Taiwan, Hong Kong, Indonesia, Malaysia, Philippines, Thailand, Vietnam

Rest of World:

All countries not included in other groups.

Appendix B: Additional results

Table B-1 - Mortality Rates for each Country under each Scenario

Country/Region	Mortality Rate						
	S01	S02	S03	S04	S05	S06	S07
Argentina	-	-	-	0.12%	0.29%	0.52%	0.12%
Australia	-	-	-	0.09%	0.22%	0.40%	0.09%
Brazil	-	-	-	0.12%	0.31%	0.56%	0.12%
Canada	-	-	-	0.08%	0.21%	0.37%	0.08%
China	0.02%	0.25%	0.90%	0.20%	0.50%	0.90%	0.20%
France	-	-	-	0.09%	0.23%	0.42%	0.09%
Germany	-	-	-	0.10%	0.24%	0.44%	0.10%
India	-	-	-	0.28%	0.71%	1.27%	0.28%
Indonesia	-	-	-	0.25%	0.63%	1.13%	0.25%
Italy	-	-	-	0.10%	0.25%	0.45%	0.10%
Japan	-	-	-	0.10%	0.25%	0.45%	0.10%
Mexico	-	-	-	0.15%	0.37%	0.66%	0.15%
Republic of Korea	-	-	-	0.12%	0.30%	0.54%	0.12%
Russia	-	-	-	0.13%	0.32%	0.58%	0.13%
Saudi Arabia	-	-	-	0.09%	0.23%	0.41%	0.09%
South Africa	-	-	-	0.14%	0.34%	0.61%	0.14%
Turkey	-	-	-	0.15%	0.37%	0.67%	0.15%
United Kingdom	-	-	-	0.10%	0.25%	0.44%	0.10%
United States of America	-	-	-	0.07%	0.18%	0.33%	0.07%
Other Asia	-	-	-	0.16%	0.40%	0.72%	0.16%
Other oil producing countries	-	-	-	0.15%	0.37%	0.67%	0.15%
Rest of Euro Zone	-	-	-	0.09%	0.23%	0.41%	0.09%
Rest of OECD	-	-	-	0.08%	0.20%	0.36%	0.08%
Rest of the World	-	-	-	0.20%	0.50%	0.90%	0.20%